Regulation of innate liver injury by TLR9

Alyse Douglass

A thesis

submitted in partial fulfillment of the

requirements for the degree of

Master of Science

University of Washington

2022

Committee:

Ian N. Crispe

Alexis Kaushansky

Steve Polyak

Program Authorized to Offer Degree:

Global Health Pathobiology

University of Washington

Abstract

Regulation of innate liver injury by TLR9

Alyse Douglass

Chair of the Supervisory Committee:

Ian N Crispe

Department of Pathology

The inflammatory response to hepatocyte death is mediated by TIR-domain containing adapters, which are involved in pattern recognition receptor (PRR) signaling. We study this mechanism during acute liver injury in mice, induced by Diphtheria Toxin (DT) in cells that have been transduced with the human DT receptor. Dying cells promote a local innate immune response in several different ways, including chemokine production, inflammasome activation, and PRR stimulation. Toll-like receptor 9 (TLR9), a PRR that interacts with the TIR-domain containing adapter MyD88, has been implicated in models of both acute liver failure and chronic liver disease. However, the role of TLR9 in DT-induced acute liver injury has not yet been determined. TLR9 deletion exacerbated liver injury compared to WT mice by 48 hours post-DT treatment. TLR9 deletion also had cell type specific effects in steady state liver, most notably in hepatocyte programmed cell death gene expression. *Fas* gene expression was increased in TLR9-deficient mice, while inhibition of TLR9 *in vitro* caused elevated Fas and FasL expression in a hepatocyte-derived cell line. In this thesis, we argue that TLR9 is hepatoprotective during acute liver inflammation by controlling Fas hepatotoxicity. In addition, we briefly discuss the impact of TLR9 deletion on chemokine gene expression in purified hepatocytes and Kupffer cells, and the impact of Silymarin treatment on the inflammatory response to DT-induced hepatocyte death.

Table of Contents

Acknowledgements

It is difficult to know how to begin recognition of everyone who made it possible for me to go on this journey in the Pathobiology program. Everyone has been absolutely essential for getting my research this far, and I am eternally grateful to you all. However, since I must start somewhere, I want to first recognize the unique academic opportunities and wonderful student and faculty community promoted by the Pathobiology program. While I did not often participate in the winter seminar happy hours, the interactions I had with my fellow students during the program retreats and the Current Literature in Pathobiology and Critical Thinking courses have been immeasurably valuable in shaping me as a scientist.

I also want to thank my committee members for their insight and troubleshooting expertise that helped propel my project beyond the rough spots. Alexis has had an especially significant impact on my scientific career even before starting the Pathobiology program. In addition to her brilliant mind, her enthusiasm for research continuously inspires my own passion for science. She also fostered my unique sense of humor during my time as her technician – Bruce Wayne/Batman will forever be in the acknowledgment section of one of our papers.

To the Liver Crew – each and every one of you contributed to such a wonderful lab family over the past 7 years. Katie, we only overlapped for a few short months, but I really appreciate the friendship that we developed and your ongoing technical support after you progressed to your next position. Sarah, not only do you have magic liver perfusion hands, but the conversations we have had over the years, both hilarious and emotional, are so important to me. I am incredibly honored to be taking the reins from you going forward and am deeply sad that we will not be working together regularly anymore. Radika, you

have been such an amazing friend and colleague and I feel so lucky that we shared that little office for as long as we did. Not only did you provide expertise, emotional support, and laughter, but you also made sure that I remembered people's names at the Immunology retreats. And Nick, I can't thank you enough for taking a chance on me 7 years ago when I couldn't find a lab. Your mentorship helped grow my critical thinking skills and progress as a (*slightly* more cultured) scientist in general regardless of the final degree I am awarded. You have also been incredibly supportive during the challenges I have faced over the years, both in and out of the lab.

To my friends – if I were to acknowledge each of you here in the way that you deserve, this thesis would be twice as long. You have helped me laugh so hard I cry and made sure I never lost sight of the other important parts of life outside of science. And over the years you have all generously let me drone on about my research projects into the wee hours. It means so much to me that you have always been my cheerleaders, and I am so lucky that each of you are part of my life. I am so excited for us to raise the next generation together and for our many adventures (with and without the kids).

To my family – I would not be the person I am today without you. Again, were I to detail the degree to which you have loved and supported me over the years, this document would be ridiculously long. Mom and Dad, you are both exceptional parents and have given me the intellectual and emotional tools that I needed to pursue research. And this past year especially, you have both been so generous with your time caring for Isabelle so that I could focus on my research. Mom, you have taught me how to be brave when choosing between different paths in life and how to be resilient when encountering life's challenges. Dad, you have been a great sounding board to discuss both big decisions and the small mundane bits of life, as well as encouraging an appreciation for the art of the running joke. Pamela, you have shown me how to be effectively proactive, a skill that has been immeasurably valuable in all parts

of my life. Valerie, I am so lucky to have grown up with you for my sister. From our shared sense of humor and cynicism to you introducing me to the world of Dungeons and Dragons and the delight of creating those stories together, no one sees the world quite as similarly to me as you do.

To my husband Charlie's family – I could not have imagined a better family to have married into. Not only have you welcomed me into the Nystrom family with open arms, but you have also been such a support for Charlie and me since the beginning. We have had some amazing family adventures over the years, and you have broadened my photography and gardening horizons exponentially. And to Peggy specifically, your help this past year caring for Isabelle has been a critical component of me being able to finish my degree.

To Charlie – we had been living together less than a year before I started this program, and for the past 7 years you have unconditionally supported me every single day. Your love and belief that there was no question I would succeed in this endeavor means more to me than you will ever know. I do not know how I got so lucky to have you as my teammate and co-parent, but I treasure every moment we have had together so far and am so excited for our future adventures, big and small.

And lastly, to my ION – as I am writing this, you are just 10 months old and learning to stand on your own. Your laughter is the best sound I have ever heard, and I feel so privileged to be your mother. You already have such determination and curiosity that I hope to foster as you grow up. It is such a pleasure to share each new experience with you and I look forward to sharing the science part of me with you one day.

Abbreviations

AAV – Adeno-associated Virus

AIH – Autoimmune Hepatitis

AIM2 – Absent in Melanoma 2

Alb – Albumin

ALT – Alanine Aminotransferase

AM404 – *N*-arachidonoylainophenol

AMPK – AMP-activated Kinase, aka Prkaa1

ANA – Anti-nuclear Autoantibodies

AP-1 – Activator Protein 1

APAP – *N*-acetyl-para-aminophenol, or Acetaminophen

Arg – Arginase 1

ASC – Apoptosis-associated Speck-like Protein Containing a CARD

ASGR-2 – Asialoglycoprotein Receptor Protein 2

AST – Aspartate Transaminase

ATG5 – Autophagy Related 5

ATG7 – Autophagy Related 7

ATP – Adenosine Triphosphate

BAK – BCL2 Antagonist/Killer

BAX – BCL2-like Protein 4

BCL2 – B-cell Lymphoma-2

BID – BH3 interacting-domain Death Agonist

C3 – Complement Component 3

C4-B – Complement Component 4

CCL2 – C-C Motif Chemokine Ligand 2, aka MCP-1

CCL25 – C-C Motif Chemokine Ligand 25, aka TEK

CCL3 – C-C Motif Chemokine Ligand 3, aka MIP-1α

CCl_4 – Carbon Tetrachloride

CCL5 – C-C Motif Chemokine Ligand 5, aka RANTES

CCL7 – C-C Motif Chemokine Ligand 7, aka MCP3

CCL8 – C-C Motif Chemokine Ligand 8, aka MCP2

CD11b – Cluster of Differentiation Molecule 11B, aka ITGAM or CR3

CD14 – Cluster of Differentiation Molecule 14

CD45.2 – Cluster of Differentiation Molecule 45.2, aka Leukocyte Common Antigen (LCA)

CFH – Complement Factor H

CMC – Carboxymethyl Cellulose

Con A – Concanavalin A

CpG – Refers to the presence of methylation of DNA island cytosines followed by guanines

Cre – Cre-recombinase

CTLA-4 – Cytotoxic T-lymphocyte-associated Protein 4, aka CD152

CXCL1 – C-X-C Motif Chemokine Ligand 1, aka KC

CXCL10 – C-X-C Motif Chemokine Ligand 10, aka IP-10

CXCL2 – C-X-C Motif Chemokine Ligand 2, aka MIP-2α

CXCL9 – C-X-C Motif Chemokine Ligand 9, aka Monokine Induced by Gamma Interferon (MIG)

CYP2E1 – Cytochrome P450 2E1

DAMPs – Danger-associated Molecular Patterns

DC – Dendritic cell

DMEM – Dulbecco's Modified Eagle Medium

DNase – Deoxyribonuclease

DRB1 – MHC Class II DR Beta 1

DT – Diphtheria Toxin

DTR – Diphtheria Toxin Receptor

EBV – Epstein-Barr Virus

EDTA – Ethylenediaminetetraacetic Acid

eEF2α – Eukaryotic Elongation Factor 2

eNOS – Endothelial Nitric Oxide Synthase

ERK1 – Extracellular Signal-regulated Kinase 1, aka MAPK3

ERK2 – Extracellular Signal-regulated Kinase 2, aka MAPK1

ET – Endotoxin

ET-1 – Endothelin-1

F4/80 – aka EMR1, ADGRE1

Fas – aka Fas receptor, CD95

FasL – Fas ligand, aka CD178

FBS – Fetal Bovine Serum

GalN – *D*-galactosamine

GAPDH – Glyceraldehyde-3 Phosphate Dehydrogenase

H&E – Hematoxylin and Eosin

HAV – Hepatitis A virus

HB-EGF – Heparin-binding EGF-like Growth Factor

HBSS – Hank's Balanced Salt Solution

HCC – Hepatocellular Carcinoma

HCV – Hepatitis C Virus

$Hep^{\Delta TLR9}$ – Hepatocyte-specific TLR9 Knockout

HLA – Human Leukocyte Antigen

HMGB1 – High Mobility Group Box 1

HPRT – Hypoxanthine-guanine Phosphoribosyltransferase

HSC – Hepatic Stellate cell

HSPs – Heat Shock Proteins

HSV-1 – Herpes-simplex Virus-1

ICP – Ischemic Pre-conditioning

IFNα – Interferon Alpha, Type I Interferon

IFNβ – Interferon Beta, Type I Interferon

IFNγ – Interferon Gamma, Type II Interferon

IgG – Immunoglobulin G

IL-1R – Interleukin 1 Receptor

IL1β – Interleukin 1 Beta

IL10 – Interleukin 10

IL12 – Interleukin 12

IL17 – Interleukin 17

IL18 – Interleukin 18

IL22 – Interleukin 22

IL6 – Interleukin 6

IRF1 – Interferon Regulatory Factor 1

IRF3 – Interferon Regulatory Factor 3

IRF7 – Interferon Regulatory Factor 7

IRI – Ischemia Reperfusion Injury

ISG15 – Interferon-stimulated Gene 15

JAK – Janus Kinase

JNK – c-Jun N-terminal Kinase

KC – Kupffer cell

LC1 – Liver Cytosol Type 1 Antibody

LDH – Lactate Dehydrogenase

LKM-1 – Liver Kidney Microsomal 1 Antibody

LKM-3 – Liver Kidney Microsomal 3 Antibody

LPS – Lipopolysaccharide

LRR – Leucine-rich Repeats

LSEC – Liver Sinusoidal Endothelial cell

Ly6G – Lymphocyte Antigen 6 Complex Locus G6D

MAMPs – Microbe-associated Molecular Patterns

MAPK – Mitogen-activated Protein Kinase

miRNA – micro RNA

MMP8 – Matrix Metallopeptidase 8

mRNA – messenger RNA

mtDNA – mitochondrial DNA

MX1 – MX Dynamin Like GTPase 1

MyD88 – Myeloid Differentiation Primary Response 88

NAPQI – *N*-acetyl-*p*-benzoquinone Imine

NASH – Non-alcoholic Steatohepatitis

NFκB – Nuclear Factor Kappa-light-chain-enhancer of Activated B cells

NLRP3 – NOD-, LRR- and Pyrin Domain-containing Protein 3

ODN – Oligodeoxynucleotides

PAMPs – Pathogen-associated Molecular Patterns

PBS – Phosphate-buffered Saline

PD-L1 – Programmed Death-ligand 1, aka B7-H1

PosCl – Ischemic Post-conditioning

PRRs – Pattern Recognition Receptors

RAGE – Receptor for Advanced Glycation Endproducts, aka AGER

RIPK1 – Receptor-interacting Serine/Threonine-protein Kinase 1

RIPK3 – Receptor-interacting Serine/Threonine-protein Kinase 3

ROS – Reactive Oxygen Species

RSAD2 – Radical S-Adenosyl Methionine Domain Containing 2

SGOT – Serum Glutamic Oxaloacetic Transaminase

SMA – Smooth-muscle Antigen Antibodies

SNPs – Single Nucleotide Polymorphisms

STAT1 – Signal Transducer and Activator of Transcription 1

STAT3 – Signal Transducer and Activator of Transcription 3

TGFβ – Transforming Growth Factor Beta

T_H1 – T Helper Type 1 cell

TIR – Toll/interleukin-1 Receptor/Resistance Protein Domain

TLR1 – Toll-like Receptor 1

TLR2 – Toll-like Receptor 2

TLR3 – Toll-like Receptor 3

TLR4 – Toll-like Receptor 4

TLR5 – Toll-like Receptor 5

TLR6 – Toll-like Receptor 6

TLR7 – Toll-like Receptor 7

TLR9 – Toll-like Receptor 9

$TLR9^{-/-}$ – TLR9 Knockout

TNFα – Tumor Necrosis Factor Alpha

TNFAIP3 – Tumor Necrosis Factor, Alpha-induced Protein 3

TNFR1 – Tumor Necrosis Factor Receptor 1, aka TNFRSF1A

TNFR2 – Tumor Necrosis Factor Receptor 2, aka TNFRSF1B

T_{reg} – Regulatory T cell

TRIF – TIR-domain-containing Adapter-inducing Interferon-β

tRNA – transfer RNA

Unc93b1 – Unc-93 Homolog B1

VCAM1 – Vascular Cell Adhesion Protein 1

WT – Wild-type

List of Figures

Chapter 1

Chapter 3

List of Tables

Chapter 1 – Introduction

The Liver

Liver Function

The liver performs many essential functions including macronutrient metabolism, blood volume regulation, immune system support, endocrine control of growth signaling pathways, lipid and cholesterol homeostasis, and breakdown of xenobiotic compounds such as medication(1, 2). Glucose secretion by the liver responds to the energy needs from other parts of the body, such as the brain and the immune system(1, 2). Upon feeding, the liver shifts from a mode of net glucose output to net uptake, requiring a decline in glucagon and increase in insulin to facilitate glucose uptake and glycogen storage(1, 2). Macronutrient processing in the liver also involves protein synthesis and breakdown. 80-90% of proteins (by volume) secreted into the blood are produced by the liver(2). The most abundant of those proteins is albumin, which helps to maintain blood volume and transport molecules such as lipids and hormones(1, 2). The liver also performs uptake, synthesis, packaging, and secretion of lipids and lipoproteins(1, 2). Cholesterol, which is required for assembly of cellular membranes and maintenance of membrane fluidity, can be absorbed from the intestines, or synthesized in the liver. Fatty acids provide an internal energy source via oxidative pathways but can also provide energy to other organs from ketogenic products during times of extreme fasting or extreme deprivation of carbohydrates(2).

The liver is made up of parenchymal cells (hepatocytes and cholangiocytes) and non-parenchymal cells (sinusoidal endothelial cells, stellate cells, and Kupffer cells). Hepatocytes are the most abundant cell population and are responsible for most of the glucose, protein, and lipid metabolism in the liver(3). Cholangiocytes line the bile ducts and are responsible for producing and transporting bile(4). Liver sinusoidal endothelial cells (LSECs) are specialized endothelial cells that form fenestrated sieve plates in

the sinusoids, creating pores for protein exchange between hepatocytes and the sinusoid (Fig. 1)(5). In the quiescent form, hepatic stellate cells (HSC) store vitamin A in lipid droplets(6). HSC activation results in loss of vitamin A stores, induces proliferation, and the primary function switches to collagen deposition and organization(6). Kupffer cells (KC) are sentinels for enteric pathogens entering the liver via the portal vein(7). Depending on their microenvironment, KC can contribute to pro- or anti-inflammatory responses during liver injury(7).

The structural unit of the liver is the lobule. Hepatocytes are organized in a loosely hexagonal shape around the central vein, and portal triads are located at each of the vertices. Portal triads are closely grouped branches of the portal vein, hepatic artery, and bile duct. Oxygenated blood from the hepatic artery mixes with nutrient-rich blood directly from the intestines via the portal vein and then flows across the sinusoidal network before draining into the central vein (Fig. 1). While this creates gradients of oxygen, nutrients, and waste products that dictate different “zones” of metabolic processes in hepatocytes especially, these are not terminally differentiated functions and hepatocyte metabolic processes can adapt to changes in the surrounding microenvironment, such as injury(2, 3).

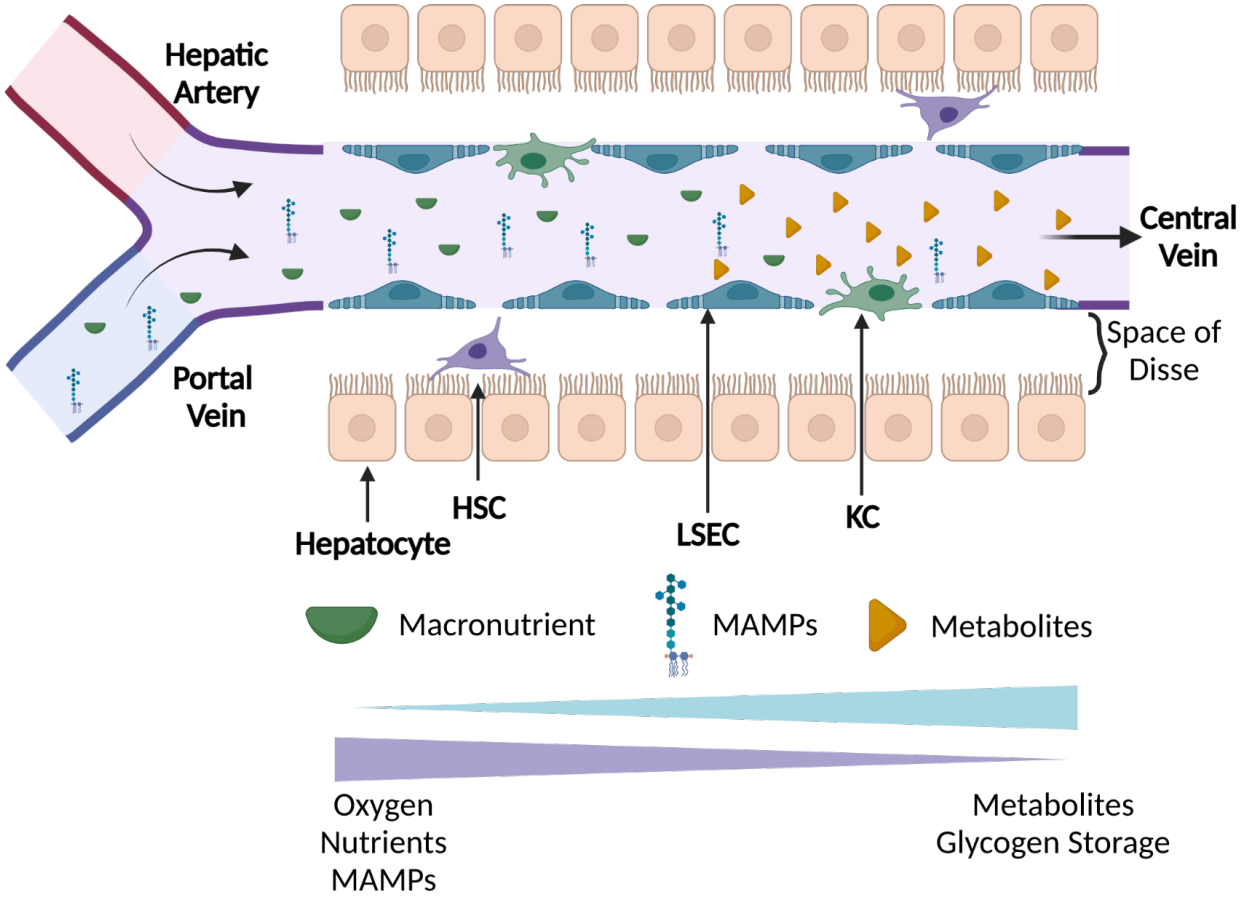

Fig. 1 The liver sinusoidal microenvironment. The sinusoids are lined with liver sinusoidal endothelial cells (LSECs) that form small pores for direct interaction between hepatocytes and the blood. Kupffer cells (KCs) also have direct contact with the blood, and hepatic stellate cells (HSC) have direct contact with hepatocytes within the Space of Disse. As blood flows from the hepatic artery (red) and portal vein (blue) towards the central vein (purple), the components switch from highly oxygenated blood containing high levels of macronutrients to less oxygenated blood containing high levels of metabolites to be sent off to other areas of the body. Blood from the portal vein is sourced directly from the intestines and contains microbe-associated molecular patterns (MAMPs). Figure generated with BioRender.

Liver Immunology

In the liver sinusoids, there is constant exposure to non-self proteins from nutrients or resident microbe-associated molecular patterns (MAMPs) in the portal-vein blood supply directly from the intestines (Fig. 1). To prevent accidental immune activation against harmless antigens there are specialized mechanisms in place to promote an immunologically tolerant environment. One such mechanism is endotoxin tolerance, where constant low levels of endotoxin makes cells resistant to canonical pro-inflammatory toll-like receptor 4 (TLR4) signaling and instead promotes an immunosuppressive environment through KC production of IL10 and TGFβ(7-9). This cytokine microenvironment, in addition to PD-L1 expression by KC, HSC, LSECs, and hepatocytes, promotes T cell anergy, deletion, or T_{reg} priming and expansion(8). However, the liver must be capable of mounting an effective inflammatory response - it is the first line of defense for any enteric pathogens that breach the gut epithelial barrier. Hepatocytes, KC, HSC, and LSECs act as sensors for and triggers of immune responses and inflammatory injury in the liver(8, 10).

Danger signals secreted by stressed cells (active release) or cell death (passive release) trigger liver inflammation by binding to their cognate pattern recognition receptor(s) (PRRs)(11). PRRs are evolutionarily conserved among most eukaryotes and play a crucial role in activating the innate immune response. The earliest identified PRRs were Toll receptors in Drosophila that activated the NFκB-dependent anti-fungal response(12). Mammalian orthologues are called toll-like receptors (TLRs), and they recognize a wide range of pathogen-, symbiotic microbe-, and host danger-associated molecular patterns (PAMPs, MAMPs, and DAMPs respectively). TLRs are transmembrane proteins located either on the cell surface or in endosomes to detect extracellular and endocytosed molecular patterns, respectively. The ligand-binding domain of the TLR family possesses tandem short motifs of Leucine-rich repeats (LRRs), and the cytosolic Toll/IL-1R (TIR) domain induces signaling cascades via interactions with

multiple different TIR adapters such as MyD88 and TRIF (13). Canonical TLR signaling induces inflammatory gene expression via NFkB, AP-1, and IRF signaling pathways(13, 14).

With this wide range of signaling pathways induced by TLR stimulation, it is no surprise that there are cell type-specific responses to TLR activation(14, 15). For the purposes of this chapter, we will focus on TLR2, TLR3, TLR4, TLR5, TLR7, and TLR9 cell-specific signaling in the liver. As previously mentioned, constant low-level endotoxin (e.g. lipopolysaccharide, LPS) stimulation of TLR4 in KC induces anti-inflammatory gene expression to promote immune tolerance in the liver. However, high levels of TLR4 stimulation in KC trigger production of IL6, IL12, TNFα, and inflammasome activation resulting in secretion of IL1β and IL18(16). Additional KC-specific TLR signaling includes (but is not limited to) TLR3- and TLR4-dependent IFNβ production, TLR1/2-, TLR2/6-, and TLR4-dependent IFNγ production, and TLR9-dependent inflammasome activation(8, 15, 17). Upon HSC activation TLR2, TLR4, and TLR9 stimulation triggers VCAM-1 expression and secretion of IL6, TGFβ, and CCL2(16). LSECs respond to stimulation of the TLR2/6 heterodimer, TLR4, and TLR9 by producing TNFα, whereas TLR3 stimulation by induces TNFα, IL6, and IFNγ(14). While hepatocytes are relatively unresponsive to TLR2 activation in the absence of injury, liver inflammation increases sensitivity to TLR2 ligands leading to inflammasome activation(15, 18). Other TLR signaling effects observed in hepatocytes include TLR3-dependent IFNβ, TLR5-dependent CXCL1 and IL6 and TLR9-dependent PD-L1(19-21).

TLR2, TLR4, and TLR5 are located on the plasma membrane and sense DAMPs released into the extracellular microenvironment. TLR2 and TLR4 each recognize multiple DAMPs involved in liver inflammation (Fig. 2)(15, 18, 22). This may be due, in part, to TLR2 and TLR4 interactions with the co-receptor CD14, a LRR glycoprotein that can bind to a wide range of molecular patterns with similar structures to Poly(I:C), peptidoglycan, LPS, lipoteichoic acid, and DNA(13).

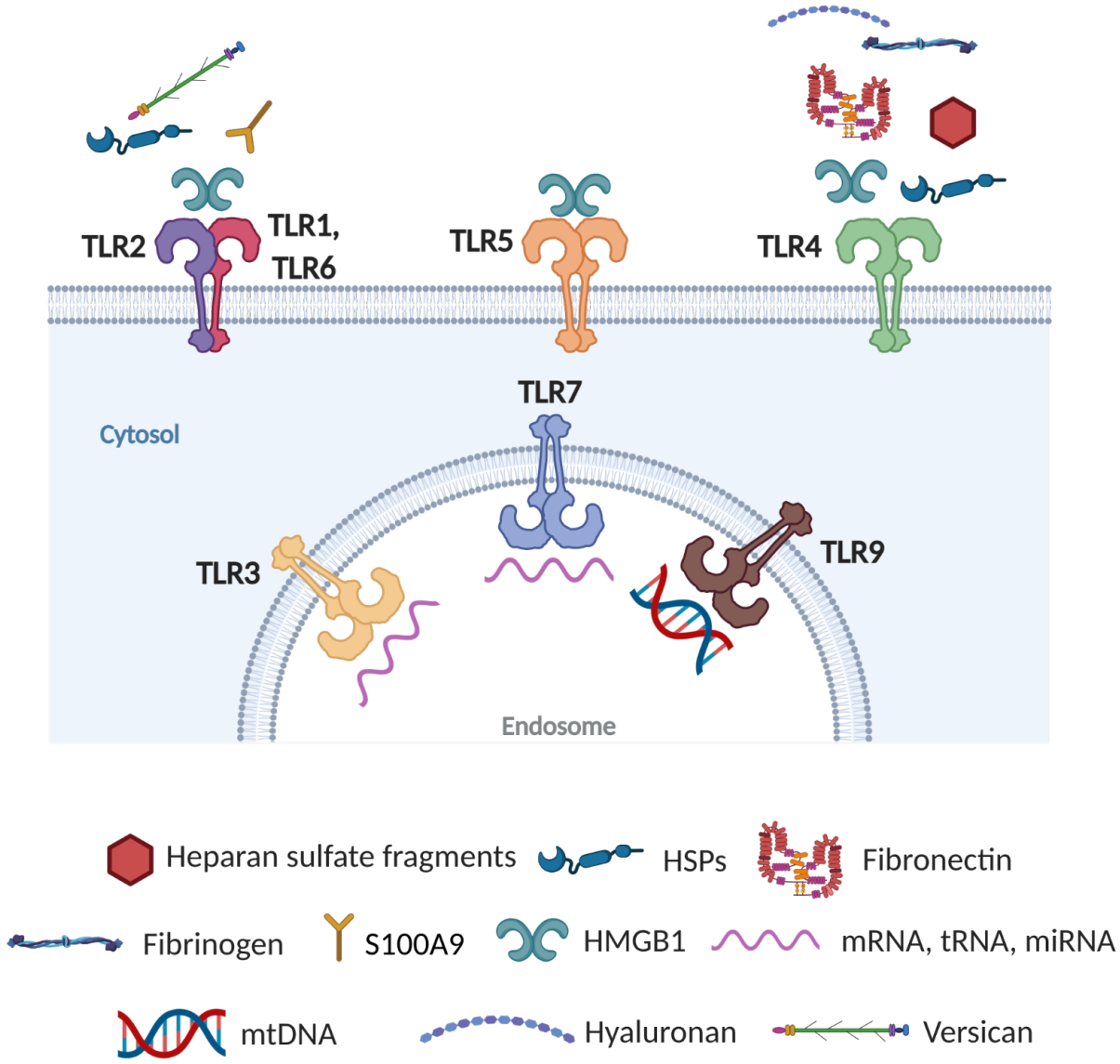

Fig. 2 Danger Associated Molecular Patterns recognized by TLRs that contribute to liver inflammation. TLR2 forms heterodimers with either TLR1 or TLR6, while all other TLRs shown mainly form homodimers. TLR2, TLR4, and TLR5 are located on the plasma membrane. TLR2 and TLR4 bind a wide range of DAMPS, whereas TLR5 is only stimulated by HMGB1. TLR3, TLR7, and TLR9 are located in endosomes and bind molecular patterns associated with nucleic acid structures such as RNA (TLR3 and TLR7) and mtDNA (TLR9). Figure generated with BioRender.

TLR3, TLR7, and TLR9 are located in endosomes and recognize endocytosed nucleic acid DAMPs. All three endosomal TLRs also interact with CD14, however their range of DAMP ligands is more restricted with TLR3 and TLR7 binding different self RNA structures and TLR9 binding mitochondrial DNA (Fig. 2)(15, 19, 23).

Sterile Acute Liver Injury

Acute hepatitis is defined by liver cell death, cellular disarray, and immune cell infiltration. The pathophysiology of acute liver injury is orchestrated by immune cells, cytokines, and parenchymal cells. For example, neutrophils that infiltrate into the liver can aggravate tissue damage by activating KC and LSEC adhesion molecule expression, triggering further leukocyte recruitment to the liver, and secretion of reactive nitrogen and oxygen species, IL1β, and TNFα(8). The immune responses to DAMPs released by cell death causes liver inflammation(24). In mice, the liver can regenerate from extreme cell loss, such as a 70% hepatectomy recovering almost the original organ mass within a few days(25). However, after a certain threshold, hepatic proliferation is insufficient to regenerate liver function, leading to acute liver failure and death without interventions(25). Acute liver failure presents as acute disorder in liver coagulopathy (impairments in clotting, and reduced platelet number and function), high ALT and AST, and hepatic encephalopathy (cognitive impairment due to increased circulation of toxic metabolism byproducts). There is rapid progression to multiorgan failure with unpredictable complications(26). This part of the chapter will review common causes of acute sterile liver injury in humans and the mouse models used to study them, particularly in the context of TLR-mediated inflammatory liver injury.

Acetaminophen Overdose

Human Disease

APAP overdose accounts for 50% of acute liver failure cases in humans(27-29). *N*-acetyl-para-aminophenol (acetaminophen, or APAP) is a readily available anti-inflammatory oral drug that is used to treat common aches and pains and is often paired with opioid analgesics for post-surgery pain management. To generate the active metabolite, AM404, APAP processing occurs predominantly via the glucuronidation and sulfation metabolic pathways in hepatocytes(28, 29). When therapeutic doses of APAP are ingested, a minor amount is oxidized by cytochrome P450 and generates the reactive metabolite *N*-acetyl-*p*-benzoquinone imine (NAPQI). In hepatocytes, NAPQI is neutralized by the ROS scavenger glutathione. Increasing concentrations of APAP saturates the sulfation pathway, shifting towards cytochrome P450 processing and increased generation of NAPQI, which results in glutathione depletion and hepatotoxicity(28). NAPQI forms protein adducts, which are covalent modifications created by electrophile and nucleophilic amino acid residues. These modifications disrupt protein structure and function, damaging metabolic pathways, cytological processes, and submembrane organelles(30). NAPQI-induced protein adducts are significantly produced on the mitochondria, enhancing free radical production, loss of membrane potential, and Bax-dependent membrane permeability that culminates in massive hepatocyte death(28, 29).

There is controversy over whether therapeutic doses of APAP (325-1000mg every 6 hours) can cause liver injury in certain people. This phenomenon may be due to pre-existing effects on the liver at the time of APAP ingestion. Some medications and supplements can induce cytochrome P450 activity and enhance oxidative metabolism, and malnutrition has been shown to deplete glutathione in hepatocytes(28, 29). Chronic alcohol consumption is a predicted risk factor for decreased tolerance to APAP-induced liver injury because it increases cytochrome P450 activity in rats, however studies with

human alcoholics receiving 1000mg per day do not support this hypothesis(31-33). Conversely, acute alcohol consumption may increase tolerance to APAP overdose because ethanol directly inhibits NAPQI production by cytochrome P450(34, 35).

Clinical biomarkers that predict outcome of APAP-induced liver injury in large patient cohorts (but not individuals) are serum or plasma levels of protein adducts, mitochondrial DNA, glutamate dehydrogenase, and nuclear DNA fragments – ALT and AST do not predict whether a patient will progress to acute liver failure(28). Currently, the glutathione synthesis inducer N-acetylcysteine (NAC) is the only clinically approved treatment for APAP overdose(36). It is generally effective if given early after overdose but has limited effect in late-presenting patients of acute overdose and can lead to issues if given as a treatment for prolonged periods(28, 36).

APAP Mouse Model

APAP overdose is the most common model of drug-induced liver injury (DILI) because the progression of disease in humans and mice are relatively similar. CYP2E1 is the only human cytochrome P450 that is functionally conserved across mammals, with mice and humans having the most similar activity levels(29, 37). Mice and humans experience liver injury at doses >150mg/kg, and the main hepatotoxic mechanisms appear to be the same, although peak for mice is 12-24 hours while for humans it is 24-72 hours(37). Overnight fasting is required in the mouse model for doses of 200-300mg/kg to ensure that all mice have the same baseline levels of glutathione and Cyp2E1(28, 29, 37). Higher doses of 400-600mg/kg generate consistent toxicity between mice regardless of food intake variation(37).

Necrosis is currently the hypothesized mechanism of APAP-induced hepatocyte death even though some components of the intrinsic apoptosis mechanism, such as Bax, are activated. Hepatocytes exhibit

cell and organelle swelling, cell content release, and there is no evidence of caspase involvement(28, 38). Investigations into whether necroptosis is the mechanism of hepatotoxicity are conflicting. Necrostatin-1, a RIPK1 inhibitor, provided protection however hepatocyte-specific RIPK1 deletion was not protective(27). RIPK3 deletion provided partial protection from APAP injury in one study, but did not protect against liver injury in another(28). APAP hepatotoxicity mechanisms are difficult to study *in vivo* because many solvents used to dissolve compounds that are intended to interrupt APAP metabolism are themselves capable of competing with APAP for cytochrome P450(34, 38-40).

The mouse model has yielded some crucial information about the immune response in human APAP-induced liver injury, such as discovering that infiltrating monocytes and neutrophils do not contribute to liver injury but are crucial for recovery(29). However, there are aspects of this model that misrepresent human disease, either through experimental design or inherent differences between mouse and human liver biology. While fasting is used to equalize baseline glutathione and Cyp2E1 between mice prior to APAP treatment, fasting induces autophagy and may mask potential effects of pharmacological interventions(37). Additionally, most APAP studies use male mice because female mice are less susceptible to APAP induced liver injury(37, 41, 42). Female mice exhibit less necrosis due to faster glutathione recovery, which results in less ROS and mitochondrial damage(41, 42). Estrogen treatment of male mice prior to APAP overdose provided moderate protection from injury and ROS production but did not increase glutathione recovery(41). In humans however, more females than males are admitted to hospitals in the US for APAP-induced liver injury or acute liver failure(43). This disparity of sex differences between mice and humans is a confounding factor that contributes to the high rate of failure that pre-clinical drug candidates experience in human trials(29, 37).

While defining therapeutic candidates with the APAP mouse model has been challenging, genetically modified mice revealed the role of different TLRs in promoting the aggravated immune response during

APAP overdose without impacting metabolic production of NAPQI. TLR4 activation by HMGB1 in macrophages promotes IL17+ γδ T cell-dependent recruitment of neutrophils(44). Neutrophil and pro-inflammatory macrophage inflammasome activation is a crucial step in the APAP aggravated immune response and is induced by TLR9 recognition of mtDNA released by NAPQI-killed hepatocytes(45, 46). TLR3 activation promotes KC and DC TNFα production which contributes to hepatotoxicity(47). Cavassani, et al showed that TLR3 deletion protected mice from APAP-induced liver injury by suppressing TNFα production(47). The effect on TNFα was still present when TLR3 was blocked with an antibody 3 hours after APAP treatment, suggesting that this pathway may be a useful clinical intervention target for humans after APAP liver injury has been initiated(47).

Ischemia Reperfusion Injury

Human Disease

During liver surgery, blood flow from both the portal vein and hepatic artery is interrupted either continuously or intermittently to prevent the need for blood transfusion and the accompanying potential short-term and long-term consequences(48). However, prolonged interruption (ischemia) and subsequent reestablishment (reperfusion) of blood flow causes injury that can significantly impair liver function(48, 49). Prolonged tissue deoxygenation causes ATP depletion and a switch to anaerobic metabolism, which cannot be maintained for long periods before resulting in cell death. Reperfusion leads to injury because the return of oxygen exceeds the rate at which cells can transition from anaerobic to aerobic metabolism, and this leads to ROS-dependent cell death. Ischemic reperfusion injury (IRI) is classically described as having early (<6 hours) or late (>12 hours) phases of reperfusion injury(49). Kupffer cells are the primary producers of ROS in the very early phase, transitioning to NKT cells later in the early phase (>1 hour), and finally neutrophils in the late phase(49, 50).

IRI is measured by circulating ALT, AST, LDH, SGOT (serum glutamic oxaloacetic transaminase), and by histology using the Suzuki classification which grades on sinusoidal congestion, hepatocyte necrosis, and ballooning degeneration of the injured lesions(49). LSECs and hepatocytes are the main targets of reperfusion injury, initially due to stimulation with high levels of endothelin-1 (ET-1), a vasoconstrictor, which constricts sinusoids and reduces liver perfusion. ET-1 signaling also increases expression of protective IL6, and endothelial nitric oxide synthase (eNOS), and injurious TNFα(51-53). Additionally, hepatocytes are more susceptible to warm ischemic injury (37°C), while LSECs are more sensitive to the cold ischemic injury (4°C)(48, 49). Warm ischemic injury is caused by the mechanical injury of the surgery itself, whereas cold ischemic injury occurs in preserved liver donor grafts during storage prior to transplantation(48).

Nakazato, et al discuss surgical efforts to mitigate IRI damage and lesion formation and highlight the most promising strategies: ischemic pre- and post-conditioning(48). Ischemic pre-conditioning (ICP) involves short periods of interruption and resumption of blood flow prior to the prolonged interruption during the surgical procedure and has been shown in both the heart and kidneys to increase resistance to IRI. ICP is associate with an increase in adenosine monophosphate kinase, which would increase ATP availability during prolonged ischemia and reduce the need for anaerobic metabolism. Ischemic post-conditioning (PosCI) employs a similar strategy as ICP however the short periods alternating between flow interruption and resumption occur at the end of the main surgical procedure but prior to the final full reperfusion. This method appears to promote a gentle switch back to aerobic metabolism, which reduces the toxic levels of ROS production associated with the reperfusion phase of IRI. Studies comparing the two strategies showed that both ICP and PosCI are protective against injury from warm ischemia, however PosCI greatly reduced injury due to hypothermic ischemia(48). When considered with cell-specific sensitivity to warm and cold ischemia, these data suggest that LSECs are more sensitive

to ROS-mediated injury during reperfusion, whereas increased ATP or decreased ROS are hepatoprotective.

Mouse Model – Partial Hepatic Ischemia Reperfusion (IR)

To mimic human liver injury during surgery, the mouse model employs a specific clamping strategy during surgery to restrict blood flow to 70% of the liver for varying times(54). Mice are fasted overnight prior to surgery, where the hepatic artery and portal vein are cross clamped above the quadrate and right lateral lobes to induce ischemia in the median and left lateral lobes of the liver(54). Platelets and leukocytes start to adhere to LSECs within 5 minutes of reperfusion, and neutrophil oxidative burst in the later stages of IR directly causes additional hepatocyte injury after the initial ischemic insult(49). While ATP depletion during blood flow interruption would indicate hepatocytes are initially dying via necrosis, $Bax^{-/-}$ mice have moderate protection from IR injury suggesting intrinsic apoptosis may also be activated during ischemia(49, 55).

During hypothermic IR liver injury TRIF-mediated TLR4 signaling in hepatocytes induces IRF1-dependent cell death and subsequent HMGB1 release(15, 56). When HMGB1 is recognized by TLR4 in KC, the results are TNFα, IL6, and CXCL10 secretion and a feed-forward loop increasing TLR4 expression(15, 57). Additionally, KC-specific TLR2 activation is an important source of TNFα during warm IR(15, 57, 58). Neutrophil activation during the reperfusion phase is due, in part, to TLR9 stimulation with mtDNA released by the dead cells from the ischemic phase(15, 49, 57).

Autoimmune hepatitis

Human Disease

Autoimmune hepatitis (AIH) occurs when immune tolerance in the liver breaks down and causes severe immune-mediated tissue injury. The exact mechanism responsible for escaping immune tolerance in AIH is unknown, although an increase in T_{reg} homing to the liver and hepatic CXCL10 expression suggest that liver injury is T cell-mediated(59, 60). As with most autoimmune diseases, a combination of genetic predisposition and viral molecular mimicry are suspected causes. Genetic risk factors include allelic variants of DRB1 within the HLA region of chromosome 6, tumor necrosis factor, alpha-induced protein 3 (TNFAIP3) SNPs, and CTLA-4 SNPs(60). Viral candidates that may trigger molecular mimicry include hepatitis A virus (HAV), Hepatitis C virus (HCV), hepatitis E virus (HEV), measles, Epstein-Barr virus (EBV), and herpes-simplex virus-1 (HSV-1)(60).

Positive diagnosis of AIH occurs with the combination of high ALT and AST, increased gamma-globulin or IgG, the presence of autoantibodies, and biopsy evidence of hepatitis(60). The milieu of autoantibodies further divides AIH diagnosis into two subtypes. In the most common subtype, Type 1, smooth-muscle antigen antibodies (SMA) with or without anti-nuclear autoantibodies (ANA) are present. Type 2 AIH, representing 5-10% of AIH cases, is characterized by liver kidney microsomal 1 and 3 antibodies (LKM-1 and LKM-3) or liver cytosol type 1 antibody (LC1), with or without ANA and SMA(59, 60). The female to male ratio is 4:1 for Type 1 and 10:1 for Type 2(59). Mortality is highest during the first year after diagnosis, potentially because at least 1/3 have evidence of cirrhosis at the time of diagnosis. When treated with immunosuppressive therapeutics the 10 year mortality rate is 6-10%, however the mortality rate without treatment is 50% in 5 years(59, 61). While immunosuppressive therapeutics are effective, some patients will still progress to acute liver failure or end-stage cirrhosis and require a liver transplant. Additionally, up to 20% of patients present with acute onset of disease associated with the

development of acute liver failure(59). Autoimmune hepatitis can also occur in patients who receive a liver transplant for other reasons, termed *de novo* AIH(59, 60).

Mouse Model – Concanavalin A

Concanavalin A (Con A), a jack bean-derived lectin, induces immune-mediated liver injury in mice to model T cell-mediated damage during acute-onset severe autoimmune hepatitis(27, 62). Following i.v. injection, Con A binds to LSECs within 15 minutes and induces membrane breakdown and detachment from the sinusoid(61). By 4 hours, KC cross-present Con A to CD4+ T cells resulting in high levels of TNFα and IFNγ production and intrasinusoidal thrombosis(61, 63). IFNγ also promotes KC-dependent prothrombotic liver injury via STAT1 induced procoagulant pathway activation(63). Unlike other models of acute sterile liver injury discussed in this chapter, Con A is not directly hepatotoxic. However, hepatocytes are susceptible to stress and death due to high levels of TNFα and IFNγ produce by the activated CD4 +T cells(27, 64).

While TLR2 inhibition prevents T cell infiltration into the liver and results in decreased TNFα, IFNγ, and IL6(65), Con A itself binds to the TLR2/6 heterodimer(66). The decreased liver injury observed with TLR2 inhibition may therefore be due to inhibiting the initial effect of ConA on LSECs and/or KC. TLR9 activation with mtDNA promotes neutrophil recruitment and p38-mediated activation(67). TLR5 signaling moderates liver injury in Con A hepatitis; TLR5 deletion leads to increased pathology and mouse mortality(68). Treatment with a TLR5 agonist further ameliorates Con A-induced liver injury in an IL22-dependent manner, which may promote hepatocyte tolerance to pro-inflammatory cytokines produced by activated CD4+ T cells(69).

Other Animal Models of Sterile Acute Liver Injury

Carbon Tetrachloride (CCl_4)

High doses (>1mg/kg) of carbon tetrachloride (CCl_4) cause reproducible acute liver injury that resembles the drug-induced liver injury disease course in humans(37). Toxicity is dependent on cytochrome P450 metabolism to the reactive metabolite trichloromethyl radical, which induces lipid peroxidation and can alkylate proteins, nucleic acids, and lipids causing reduced protein synthesis, steatosis and altered calcium homeostasis(37). CCl_4-induced hepatotoxicity induces mitochondrial damage and DNA depletion in addition to alkylation reactions and lipid peroxidation(37).

The CCl_4 model of liver injury uncovered the role of TLR2 in promoting CXCL2-dependent neutrophil recruitment to the liver via hepatocyte stimulation with the DAMP S100A9(22). While this mechanism did not alter CCl_4-induced acute liver injury, it did provide insight into hepatocyte-specific TLR-dependent chemokine production which can be applied to other liver injury models with neutrophil-mediated pathogenesis such as IR(22, 49).

Fas-mediated Liver Injury

This model of Fas signaling evaluates the impact of primary apoptosis followed by secondary necrosis on the acute liver injury immune response(27). The monoclonal anti-Fas antibody clone Jo2 activates Fas and induces apoptosis in both hepatocytes and LSECs(27, 70). Fas activation induces cleavage of the pro-caspases 3, 8, and 9, as well as Bid-dependent cytochrome c release from mitochondria to induce apoptosis(27). Apoptosis is induced less than 1 hour post-Jo2 administration, as observed by cell morphology and no ALT release. However, the massive amount of cell death induced directly by Fas activation deteriorates into secondary necrosis with high ALT and hemorrhage(71). Animal death occurs within several hours of Jo2 injection and is due to hemorrhage caused by LSEC death rather than

hepatotoxicity(71). The distinction between primary necrosis (APAP) and secondary necrosis is that in secondary necrosis there is still high levels of caspase activation, and secondary necrosis can be prevented with a pan-caspase inhibitor(70). The immune response to Fas-mediated liver injury is characterized by CXCL1- and CXCL2-dependent neutrophil infiltration and activation, as well as non-canonical IL1β and TNFα production(72, 73). Based on several extensive literature searches, the role of TLR signaling in Fas-mediated liver injury has not been reported on – this may be due to the extremely quick progression of liver failure and death after Jo2 treatment(71).

GalN/ET (*D*-galactosamine/endotoxin (LPS))

The GalN/ET model of acute sterile injury is used to study TNFα-mediated apoptotic signaling mechanisms and inflammatory-mediated liver injury(27). Rodent livers are relatively resistant to LPS – lethal doses generally cause death due to hypotensive shock and do not induce liver injury on their own. However, co-administration of LPS and *D*-galactosamine (GalN) causes severe liver injury via a two-hit mechanism. First, a high dose of LPS stimulates KC to produce TNFα and recruit and activate neutrophils(74). GalN then depletes uridine triphosphate and inhibits mRNA synthesis in hepatocytes, resulting in DNA fragmentation and TNFα-induced apoptosis(27). After mice are injected with LPS and GalN, TNFα production by KC occurs after 60-90 minutes, neutrophils accumulate at 4 hours, hepatocyte death occurs at 5-6 hours, and neutrophil aggravation of liver injury occurs from 6-8 hours post-treatment(27, 74). Mouse death is caused by hypovolemic shock due to severe hemorrhage after development of gaps in LSECs, not due to hepatotoxicity(75). Hepatocyte apoptosis, rather than CXC chemokine production, is required for neutrophil extravasation into the parenchyma, where they exert ROS-dependent cytotoxic effects(76, 77). While there is some argument for DAMP-mediated aggravation of TNF-induced hepatocyte death, this is confounded by studies focusing on small molecule interruption of TLR4-RAGE interactions(78, 79). TLR4 stimulation by LPS is required for liver injury in

GalN/ET, and any pre-treatment that impacts TLR4 may be preventing the initial TNFα production required to initiate hepatocyte death.

DT-induced Hepatocyte Death

To study the innate immune response to hepatotoxicity in a hepatocyte metabolism-independent manner, we utilize the extremely specific interactions of Diphtheria Toxin (DT) and its receptor(80). DT binds to human HB-EGF (hDTR) and induces irreversible ribosylation of eEF2α, which inhibits translation and leads to cell death (Fig. 3)(81-83). DT cannot induce cell death in the mouse without expression of the human DTR – this strategy has been used to deplete specific cell populations in mice for years(84-86). To induce acute liver injury due to hepatocyte-specific death, our lab injects mice with a hepatocyte-tropic AAV vector containing the human DTR sequence which leads to human DTR expression in 10-20% of the hepatocytes(80). The immune response to AAV is generally mild and very short-lived, however we wait a full 2 weeks before inducing hepatocyte-specific death by DT administration to ensure any immune response to AAV has completely resolved(87). In this model, peak liver injury, evaluated by serum ALT activity, occurs at 48 hours and is resolved by 96 hours post-DT administration(80). Peak inflammatory gene expression begins at 24 hours post-DT and begins to decrease by 72 hours(80). The DTR mouse model does not specifically emulate any one form of acute sterile liver injury in humans, however it does allow us to specifically characterize mechanisms of neighboring hepatocyte contributions to the innate immune response in the liver. Hepatocyte responses from our model can then be compared to other models of acute liver injury, such as APAP, to discern common mechanisms by which hepatocytes contribute to the innate immune response in the liver.

Thus far, we know that DT-induced liver injury, neutrophil recruitment, and hepatocyte chemokine gene expression are mediated by both TRIF- and MyD88, while monocyte recruitment is exclusively TRIF-

dependent(80). This suggests a crucial role for DAMP-TLR signaling, although previous work indicates this signaling is independent of TLR3 or TLR4(80). TLR signaling promotes neutrophil-mediated aggravation of liver injury in the APAP, IRI, and CCl_4 mouse models(15, 22, 44-47, 49, 51, 56-58). In models of neutrophil-independent inflammatory liver injury (Con A and binge alcohol) TLR signaling is more nuanced and can promote protection or inflammation(68, 88, 89). Unlike the other the liver injury models discussed earlier, there is no centralized protocol for ethanol administration in the alcohol-dependent liver injury mouse model and was therefore beyond the scope of this review. However, to fully demonstrate the duality of TLR9 signaling in the liver in particular, we will discuss the chronic-then-binge ethanol-induced liver injury model used by Hao, et al where mice received a liquid diet containing ethanol for 8 weeks followed by one "binge" dose via oral gavage. TLR9 knockout mice exhibited increased liver injury and hepatocyte death despite decreased neutrophil infiltration compared to WT mice(88). Conversely, TLR9 activation in macrophages promotes neutrophil-dependent inflammation in APAP and IRI models of liver injury(15, 45, 46, 49, 57). Neutrophil infiltration, while mediated by TLR signaling, does not contribute to inflammatory liver injury in the DTR model(80). Taken together with the dichotomy of TLR9 signaling during of other liver inflammation models makes it an attractive candidate to study in the context of DT-induced liver injury. Therefore, the purpose of this thesis is to define whether TLR9 is involved in DT-induced inflammatory liver injury and contribute to the greater body of knowledge about innate immunology in the liver.

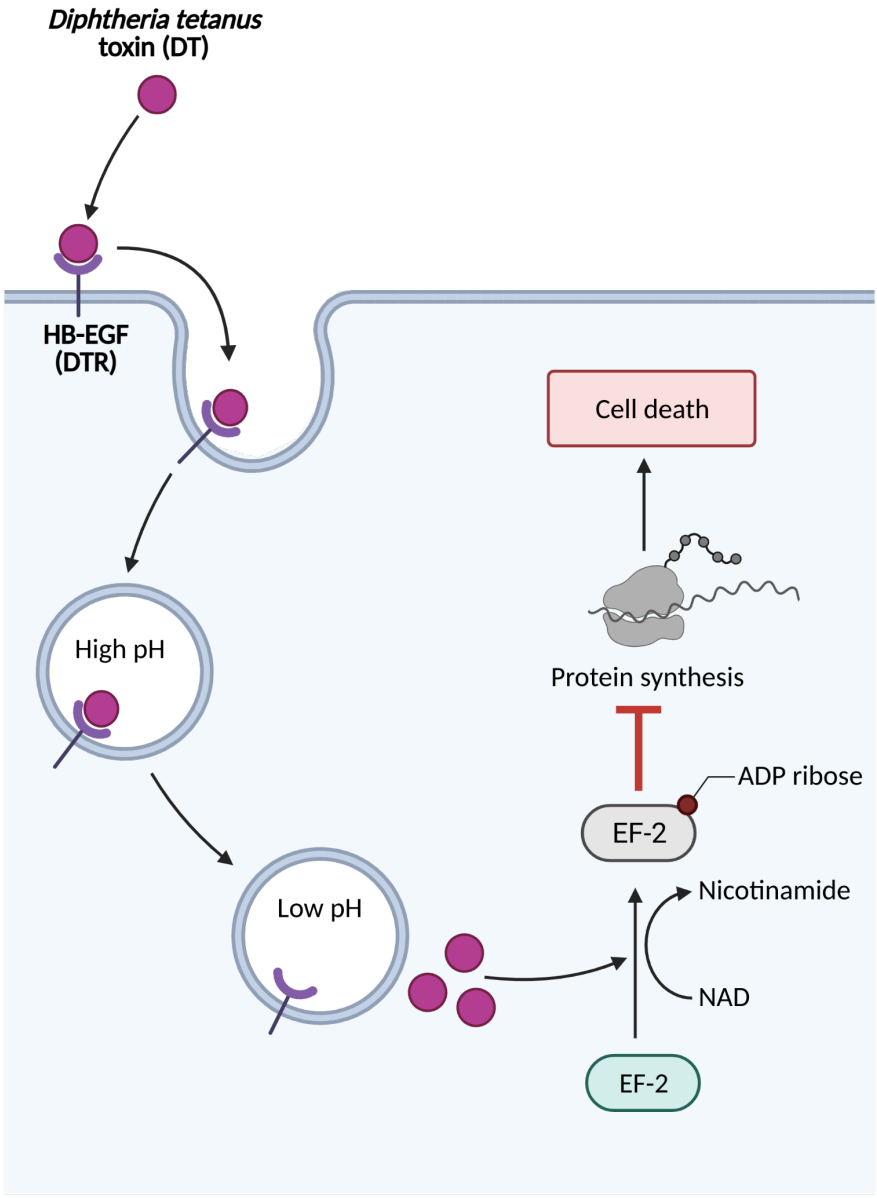

Fig. 3 Diphtheria toxin induces cell death. DT binds human HB-EGF, inducing endocytosis. A decrease in pH within the endolysosome releases DT from HB-EGF and into the cytosol. The toxin then ribosylates eEF2, causing irreversible protein synthesis inhibition which eventually results in cell death. Figure generated with BioRender.

Chapter 1 References

1. Corless JK, Middleton HM, 3rd. Normal liver function. A basis for understanding hepatic disease. Arch Intern Med. 1983;143(12):2291-4.
2. Trefts E, Gannon M, Wasserman DH. The liver. Curr Biol. 2017;27(21):R1147-r51.
3. Gissen P, Arias IM. Structural and functional hepatocyte polarity and liver disease. J Hepatol. 2015;63(4):1023-37.
4. Banales JM, Huebert RC, Karlsen T, Strazzabosco M, LaRusso NF, Gores GJ. Cholangiocyte pathobiology. Nat Rev Gastroenterol Hepatol. 2019;16(5):269-81.
5. DeLeve LD, Maretti-Mira AC. Liver Sinusoidal Endothelial Cell: An Update. Semin Liver Dis. 2017;37(4):377-87.
6. Tsuchida T, Friedman SL. Mechanisms of hepatic stellate cell activation. Nat Rev Gastroenterol Hepatol. 2017;14(7):397-411.
7. Dixon LJ, Barnes M, Tang H, Pritchard MT, Nagy LE. Kupffer cells in the liver. Compr Physiol. 2013;3(2):785-97.
8. Heymann F, Tacke F. Immunology in the liver--from homeostasis to disease. Nat Rev Gastroenterol Hepatol. 2016;13(2):88-110.
9. Kubes P, Jenne C. Immune Responses in the Liver. Annu Rev Immunol. 2018;36:247-77.
10. Crispe IN. Hepatocytes as Immunological Agents. J Immunol. 2016;196(1):17-21.
11. Murao A, Aziz M, Wang H, Brenner M, Wang P. Release mechanisms of major DAMPs. Apoptosis. 2021;26(3-4):152-62.
12. Lemaitre B, Nicolas E, Michaut L, Reichhart JM, Hoffmann JA. The dorsoventral regulatory gene cassette spätzle/Toll/cactus controls the potent antifungal response in Drosophila adults. Cell. 86. United States1996. p. 973-83.
13. Behzadi P, García-Perdomo HA, Karpiński TM. Toll-Like Receptors: General Molecular and Structural Biology. J Immunol Res. 2021;2021:9914854.
14. Żeromski J, Kierepa A, Brzezicha B, Kowala-Piaskowska A, Mozer-Lisewska I. Pattern Recognition Receptors: Significance of Expression in the Liver. Arch Immunol Ther Exp (Warsz). 2020;68(5):29.
15. Kiziltas S. Toll-like receptors in pathophysiology of liver diseases. World J Hepatol. 2016;8(32):1354-69.
16. Nakamoto N, Kanai T. Role of toll-like receptors in immune activation and tolerance in the liver. Front Immunol. 2014;5:221.
17. Wu J, Meng Z, Jiang M, Zhang E, Trippler M, Broering R, et al. Toll-like receptor-induced innate immune responses in non-parenchymal liver cells are cell type-specific. Immunology. 2010;129(3):363-74.
18. Getachew A, Hussain M, Huang X, Li Y. Toll-like receptor 2 signaling in liver pathophysiology. Life Sci. 2021;284:119941.
19. Zhang E, Lu M. Toll-like receptor (TLR)-mediated innate immune responses in the control of hepatitis B virus (HBV) infection. Med Microbiol Immunol. 2015;204(1):11-20.
20. Etienne-Mesmin L, Vijay-Kumar M, Gewirtz AT, Chassaing B. Hepatocyte Toll-Like Receptor 5 Promotes Bacterial Clearance and Protects Mice Against High-Fat Diet-Induced Liver Disease. Cell Mol Gastroenterol Hepatol. 2016;2(5):584-604.

Chapter 1 References, continued

21. Zhou B, Yan J, Guo L, Zhang B, Liu S, Yu M, et al. Hepatoma cell-intrinsic TLR9 activation induces immune escape through PD-L1 upregulation in hepatocellular carcinoma. Theranostics. 2020;10(14):6530-43.
22. Moles A, Murphy L, Wilson CL, Chakraborty JB, Fox C, Park EJ, et al. A TLR2/S100A9/CXCL-2 signaling network is necessary for neutrophil recruitment in acute and chronic liver injury in the mouse. J Hepatol. 2014;60(4):782-91.
23. Garcia-Martinez I, Santoro N, Chen Y, Hoque R, Ouyang X, Caprio S, et al. Hepatocyte mitochondrial DNA drives nonalcoholic steatohepatitis by activation of TLR9. J Clin Invest. 2016;126(3):859-64.
24. Khan HA, Ahmad MZ, Khan JA, Arshad MI. Crosstalk of liver immune cells and cell death mechanisms in different murine models of liver injury and its clinical relevance. Hepatobiliary Pancreat Dis Int. 2017;16(3):245-56.
25. Malhi H, Gores GJ, Lemasters JJ. Apoptosis and necrosis in the liver: a tale of two deaths? Hepatology. 2006;43(2 Suppl 1):S31-44.
26. Munoz SJ, Stravitz RT, Gabriel DA. Coagulopathy of acute liver failure. Clin Liver Dis. 2009;13(1):95-107.
27. Maes M, Vinken M, Jaeschke H. Experimental models of hepatotoxicity related to acute liver failure. Toxicol Appl Pharmacol. 2016;290:86-97.
28. Ramachandran A, Jaeschke H. Acetaminophen Hepatotoxicity. Semin Liver Dis. 2019;39(2):221-34.
29. McGill MR, Jaeschke H. Mechanistic biomarkers in acetaminophen-induced hepatotoxicity and acute liver failure: from preclinical models to patients. Expert Opin Drug Metab Toxicol. 2014;10(7):1005-17.
30. Lopachin RM, Decaprio AP. Protein adduct formation as a molecular mechanism in neurotoxicity. Toxicol Sci. 2005;86(2):214-25.
31. Sato C, Matsuda Y, Lieber CS. Increased hepatotoxicity of acetaminophen after chronic ethanol consumption in the rat. Gastroenterology. 1981;80(1):140-8.
32. Kuffner EK, Dart RC, Bogdan GM, Hill RE, Casper E, Darton L. Effect of maximal daily doses of acetaminophen on the liver of alcoholic patients: a randomized, double-blind, placebo-controlled trial. Arch Intern Med. 2001;161(18):2247-52.
33. Kuffner EK, Green JL, Bogdan GM, Knox PC, Palmer RB, Heard K, et al. The effect of acetaminophen (four grams a day for three consecutive days) on hepatic tests in alcoholic patients--a multicenter randomized study. BMC Med. 2007;5:13.
34. Sato C, Lieber CS. Mechanism of the preventive effect of ethanol on acetaminophen-induced hepatoxicity. J Pharmacol Exp Ther. 1981;218(3):811-5.
35. Sato C, Nakano M, Lieber CS. Prevention of acetaminophen-induced hepatotoxicity by acute ethanol administration in the rat: comparison with carbon tetrachloride-induced hepatoxicity. J Pharmacol Exp Ther. 1981;218(3):805-10.
36. Rumack BH, Bateman DN. Acetaminophen and acetylcysteine dose and duration: past, present and future. Clin Toxicol (Phila). 2012;50(2):91-8.
37. McGill MR, Jaeschke H. Animal models of drug-induced liver injury. Biochim Biophys Acta Mol Basis Dis. 2019;1865(5):1031-9.

Chapter 1 References, continued

38. Jaeschke H, Cover C, Bajt ML. Role of caspases in acetaminophen-induced liver injury. Life Sci. 2006;78(15):1670-6.
39. Park Y, Smith RD, Combs AB, Kehrer JP. Prevention of acetaminophen-induced hepatotoxicity by dimethyl sulfoxide. Toxicology. 1988;52(1-2):165-75.
40. Yoon MY, Kim SJ, Lee BH, Chung JH, Kim YC. Effects of dimethylsulfoxide on metabolism and toxicity of acetaminophen in mice. Biol Pharm Bull. 2006;29(8):1618-24.
41. Du K, Williams CD, McGill MR, Jaeschke H. Lower susceptibility of female mice to acetaminophen hepatotoxicity: Role of mitochondrial glutathione, oxidant stress and c-jun N-terminal kinase. Toxicol Appl Pharmacol. 2014;281(1):58-66.
42. Masubuchi Y, Nakayama J, Watanabe Y. Sex difference in susceptibility to acetaminophen hepatotoxicity is reversed by buthionine sulfoximine. Toxicology. 2011;287(1-3):54-60.
43. Rubin JB, Hameed B, Gottfried M, Lee WM, Sarkar M. Acetaminophen-induced Acute Liver Failure Is More Common and More Severe in Women. Clin Gastroenterol Hepatol. 2018;16(6):936-46.
44. Wang X, Sun R, Wei H, Tian Z. High-mobility group box 1 (HMGB1)-Toll-like receptor (TLR)4-interleukin (IL)-23-IL-17A axis in drug-induced damage-associated lethal hepatitis: Interaction of γδ T cells with macrophages. Hepatology. 2013;57(1):373-84.
45. Imaeda AB, Watanabe A, Sohail MA, Mahmood S, Mohamadnejad M, Sutterwala FS, et al. Acetaminophen-induced hepatotoxicity in mice is dependent on Tlr9 and the Nalp3 inflammasome. J Clin Invest. 2009;119(2):305-14.
46. He Y, Feng D, Li M, Gao Y, Ramirez T, Cao H, et al. Hepatic mitochondrial DNA/Toll-like receptor 9/MicroRNA-223 forms a negative feedback loop to limit neutrophil overactivation and acetaminophen hepatotoxicity in mice. Hepatology. 2017;66(1):220-34.
47. Cavassani KA, Moreira AP, Habiel D, Ito T, Coelho AL, Allen RM, et al. Toll like receptor 3 plays a critical role in the progression and severity of acetaminophen-induced hepatotoxicity. PLoS One. 2013;8(6):e65899.
48. Nakazato PCG, Victorino JP, Fina CF, Mendes KDS, Gomes MCJ, Evora PRB, et al. Liver ischemia and reperfusion injury. Pathophysiology and new horizons in preconditioning and therapy. Acta Cir Bras. 2018;33(8):723-35.
49. Datta G, Fuller BJ, Davidson BR. Molecular mechanisms of liver ischemia reperfusion injury: insights from transgenic knockout models. World J Gastroenterol. 2013;19(11):1683-98.
50. Chung KY, Park JJ, Han KH. Pig to canine auxiliary hepatic xenotransplantation model: prevention of hyperacute rejection via Kupffer cell blockade and complement regulation. Transplant Proc. 2008;40(8):2755-9.
51. Hines IN, Kawachi S, Harada H, Pavlick KP, Hoffman JM, Bharwani S, et al. Role of nitric oxide in liver ischemia and reperfusion injury. Mol Cell Biochem. 2002;234-235(1-2):229-37.
52. Theruvath TP, Zhong Z, Currin RT, Ramshesh VK, Lemasters JJ. Endothelial nitric oxide synthase protects transplanted mouse livers against storage/reperfusion injury: Role of vasodilatory and innate immunity pathways. Transplant Proc. 2006;38(10):3351-7.

Chapter 1 References, continued

53. Camargo CA, Jr., Madden JF, Gao W, Selvan RS, Clavien PA. Interleukin-6 protects liver against warm ischemia/reperfusion injury and promotes hepatocyte proliferation in the rodent. Hepatology. 1997;26(6):1513-20.
54. Abe Y, Hines IN, Zibari G, Pavlick K, Gray L, Kitagawa Y, et al. Mouse model of liver ischemia and reperfusion injury: method for studying reactive oxygen and nitrogen metabolites in vivo. Free Radic Biol Med. 2009;46(1):1-7.
55. Ben-Ari Z, Pappo O, Cheporko Y, Yasovich N, Offen D, Shainberg A, et al. Bax ablation protects against hepatic ischemia/reperfusion injury in transgenic mice. Liver Transpl. 2007;13(8):1181-8.
56. Ueki S, Dhupar R, Cardinal J, Tsung A, Yoshida J, Ozaki KS, et al. Critical role of interferon regulatory factor-1 in murine liver transplant ischemia reperfusion injury. Hepatology. 2010;51(5):1692-701.
57. Chang WJ, Toledo-Pereyra LH. Toll-like receptor signaling in liver ischemia and reperfusion. J Invest Surg. 2012;25(4):271-7.
58. Zhang JX, Wu HS, Wang H, Zhang JH, Wang Y, Zheng QC. Protection against hepatic ischemia/reperfusion injury via downregulation of toll-like receptor 2 expression by inhibition of Kupffer cell function. World J Gastroenterol. 2005;11(28):4423-6.
59. Sucher E, Sucher R, Gradistanac T, Brandacher G, Schneeberger S, Berg T. Autoimmune Hepatitis-Immunologically Triggered Liver Pathogenesis-Diagnostic and Therapeutic Strategies. J Immunol Res. 2019;2019:9437043.
60. Sahebjam F, Vierling JM. Autoimmune hepatitis. Front Med. 2015;9(2):187-219.
61. Wang HX, Liu M, Weng SY, Li JJ, Xie C, He HL, et al. Immune mechanisms of Concanavalin A model of autoimmune hepatitis. World J Gastroenterol. 2012;18(2):119-25.
62. Tiegs G, Hentschel J, Wendel A. A T cell-dependent experimental liver injury in mice inducible by concanavalin A. J Clin Invest. 1992;90(1):196-203.
63. Tsutsui H, Nishiguchi S. Importance of Kupffer cells in the development of acute liver injuries in mice. Int J Mol Sci. 2014;15(5):7711-30.
64. Kusters S, Gantner F, Kunstle G, Tiegs G. Interferon gamma plays a critical role in T cell-dependent liver injury in mice initiated by concanavalin A. Gastroenterology. 1996;111(2):462-71.
65. Zhou M, Zhu X, Ye S, Zhou B. Blocking TLR2 in vivo attenuates experimental hepatitis induced by concanavalin A in mice. International Immunopharmacology. 2014;21(1):241-6.
66. Unitt J, Hornigold D. Plant lectins are novel Toll-like receptor agonists. Biochem Pharmacol. 2011;81(11):1324-8.
67. Liu X, Yu T, Hu Y, Zhang L, Zheng J, Wei X. The molecular mechanism of acute liver injury and inflammatory response induced by Concanavalin A. Mol Biomed. 2021;2(1):24.
68. Wang L, Zhang W, Ge CH, Yin RH, Xiao Y, Zhan YQ, et al. Toll-like receptor 5 signaling restrains T-cell/natural killer T-cell activation and protects against concanavalin A-induced hepatic injury. Hepatology. 2017;65(6):2059-73.
69. Melin N, Sánchez-Taltavull D, Fahrner R, Keogh A, Dosch M, Büchi I, et al. Synergistic effect of the TLR5 agonist CBLB502 and its downstream effector IL-22 against liver injury. Cell Death Dis. 2021;12(4):366.

Chapter 1 References, continued

70. Jaeschke H, Gujral JS, Bajt ML. Apoptosis and necrosis in liver disease. Liver Int. 2004;24(2):85-9.
71. Bajt ML, Lawson JA, Vonderfecht SL, Gujral JS, Jaeschke H. Protection against Fas receptor-mediated apoptosis in hepatocytes and nonparenchymal cells by a caspase-8 inhibitor in vivo: evidence for a postmitochondrial processing of caspase-8. Toxicol Sci. 2000;58(1):109-17.
72. Faouzi S, Burckhardt BE, Hanson JC, Campe CB, Schrum LW, Rippe RA, et al. Anti-Fas induces hepatic chemokines and promotes inflammation by an NF-kappa B-independent, caspase-3-dependent pathway. J Biol Chem. 2001;276(52):49077-82.
73. Lazic M, Eguchi A, Berk MP, Povero D, Papouchado B, Mulya A, et al. Differential regulation of inflammation and apoptosis in Fas-resistant hepatocyte-specific Bid-deficient mice. J Hepatol. 2014;61(1):107-15.
74. Stachlewitz RF, Seabra V, Bradford B, Bradham CA, Rusyn I, Germolec D, et al. Glycine and uridine prevent D-galactosamine hepatotoxicity in the rat: role of Kupffer cells. Hepatology. 1999;29(3):737-45.
75. Ito Y, Abril ER, Bethea NW, McCuskey MK, Cover C, Jaeschke H, et al. Mechanisms and pathophysiological implications of sinusoidal endothelial cell gap formation following treatment with galactosamine/endotoxin in mice. Am J Physiol Gastrointest Liver Physiol. 2006;291(2):G211-8.
76. Jaeschke H, Fisher MA, Lawson JA, Simmons CA, Farhood A, Jones DA. Activation of caspase 3 (CPP32)-like proteases is essential for TNF-alpha-induced hepatic parenchymal cell apoptosis and neutrophil-mediated necrosis in a murine endotoxin shock model. J Immunol. 1998;160(7):3480-6.
77. Dorman RB, Gujral JS, Bajt ML, Farhood A, Jaeschke H. Generation and functional significance of CXC chemokines for neutrophil-induced liver injury during endotoxemia. Am J Physiol Gastrointest Liver Physiol. 2005;288(5):G880-6.
78. Cho HI, Hong JM, Choi JW, Choi HS, Hwan Kwak J, Lee DU, et al. β-Caryophyllene alleviates D-galactosamine and lipopolysaccharide-induced hepatic injury through suppression of the TLR4 and RAGE signaling pathways. Eur J Pharmacol. 2015;764:613-21.
79. Kim SJ, Lee SM. Necrostatin-1 Protects Against D-Galactosamine and Lipopolysaccharide-Induced Hepatic Injury by Preventing TLR4 and RAGE Signaling. Inflammation. 2017;40(6):1912-23.
80. Brempelis KJ, Yuen SY, Schwarz N, Mohar I, Crispe IN. Central role of the TIR-domain-containing adaptor-inducing interferon-β (TRIF) adaptor protein in murine sterile liver injury. Hepatology. 2017;65(4):1336-51.
81. Mateyak MK, Kinzy TG. ADP-ribosylation of translation elongation factor 2 by diphtheria toxin in yeast inhibits translation and cell separation. J Biol Chem. 2013;288(34):24647-55.
82. Murphy JR. Mechanism of diphtheria toxin catalytic domain delivery to the eukaryotic cell cytosol and the cellular factors that directly participate in the process. Toxins (Basel). 2011;3(3):294-308.

Chapter 1 References, continued

83. Morimoto H, Bonavida B. Diphtheria toxin- and Pseudomonas A toxin-mediated apoptosis. ADP ribosylation of elongation factor-2 is required for DNA fragmentation and cell lysis and synergy with tumor necrosis factor-alpha. J Immunol. 1992;149(6):2089-94.
84. Wang H, Zhang H, Wang Y, Brown ZJ, Xia Y, Huang Z, et al. Regulatory T-cell and neutrophil extracellular trap interaction contributes to carcinogenesis in non-alcoholic steatohepatitis. J Hepatol. 2021;75(6):1271-83.
85. Yellon SM, Greaves E, Heuerman AC, Dobyns AE, Norman JE. Effects of macrophage depletion on characteristics of cervix remodeling and pregnancy in CD11b-dtr mice. Biol Reprod. 2019;100(5):1386-94.
86. Männ L, Kochupurakkal N, Martin C, Verjans E, Klingberg A, Sody S, et al. CD11c.DTR mice develop a fatal fulminant myocarditis after local or systemic treatment with diphtheria toxin. Eur J Immunol. 2016;46(8):2028-42.
87. Asokan A, Schaffer DV, Samulski RJ. The AAV vector toolkit: poised at the clinical crossroads. Mol Ther. 2012;20(4):699-708.
88. Hao L, Zhong W, Sun X, Zhou Z. TLR9 Signaling Protects Alcohol-Induced Hepatic Oxidative Stress but Worsens Liver Inflammation in Mice. Front Pharmacol. 2021;12:709002.
89. Byun JS, Suh YG, Yi HS, Lee YS, Jeong WI. Activation of toll-like receptor 3 attenuates alcoholic liver injury by stimulating Kupffer cells and stellate cells to produce interleukin-10 in mice. J Hepatol. 2013;58(2):342-9.

Chapter 2 – Methods

Mice and *in vivo* experiments

Male mice aged 8-12 weeks were used for all *in vivo* experiments. C57Bl/6J (WT), TLR9-deficient ($TLR9^{-/-}$), and hepatocyte-specific Cre-recombinase (Alb-Cre) mice were purchased from the Jackson Laboratory (Bar Harbor, ME). TLR9-flox mice were generously gifted from Mark Shlomchik (University of Pittsburgh, PA). Hepatocyte-specific TLR9 knockout ($Hep^{\Delta TLR9}$) mice were generated by breeding Alb-cre with TLR9-flox mice. "Wildtype" TLR9 mice were litter mates of $Hep^{\Delta TLR9}$ that possessed floxed TLR9 but lacked Alb-Cre. All mouse experiments described in this study were performed under Institutional Animal Care and Use Committee approval (University of Washington, protocol #4308-01). Mice were housed in a specific pathogen-free environment, provided with *ad libitum* food and water, and monitored daily.

To induce hepatocyte-specific death, mice were retro-orbitally injected with $5x10^9$ viral genomes of rAAV8.mCherry.T2A.hDTR (rAAV – recombinant adeno-associated vector; hDTR – human Diphtheria toxin receptor, or HB-EGF), or 1X PBS. Two weeks were allowed for hDTR and mCherry expression, and then 20 ng diphtheria toxin (DT, Sigma-Aldrich, St. Louis, MO) in 200 μL 1X PBS was injected intra-peritoneally. Experiment end points were 16 and 48 hours post-DT administration.

Silymarin Treatment (Appendix 2)

The Silymarin compound was provided by Steve Polyak, University of Washington. The hepatocyte-specific death model, as described above, was initiated in C57Bl/6J male mice aged 8-12 weeks with retro-orbital injection of rAAV.hDTR.mCherry vector or 1X sterile PBS. On the day of DT administration two weeks later, mice were also given a 200uL oral gavage treatment of one of the following: 1) Vehicle Only (0.5% w/v carboxymethyl cellulose (CMC) 0.0025% Tween20 in sterile water), 2) 100mg/kg

Silymarin in vehicle, or 3) 300mg/kg Silymarin in vehicle. Oral gavage treatments were repeated 24 hours later. Blood was collected for ALT activity quantification and liver tissue was preserved in TRIzol for RNA extraction 48 hours post-DT administration.

AAV Production

The replication-defective rAAV, rAAV8.pAlb.mCherry.hDTR, was produced with a two-plasmid calcium phosphate transfection system. Human epithelial kidney 293 cells (clone H, ATCC, Manassas, VA) were cultured in Growth Media (DMEM high glucose, +L-glutamine (Gibco/Thermo Fisher Scientific) + 1% Penicillin and Streptomycin (Gibco) + 10% Cosmic Calf Serum (Hyclone Laboratories, Inc., Logan, UT)) at 37°C, 5% CO_2, and transfected with pLIVE.pAlb.mCherry.T2A.hDTR and the helper plasmid pDG82/8 at a ratio of 2.36 μg:10 μg. The following day, Growth Media was replaced with Post-Transfection Media (DMEM high glucose, +L-glutamine (Gibco/Thermo Fisher Scientific) + 1% Penicillin, Streptomycin, and Glutamine (Gibco)). After 72 hours, the cells were lysed by three freeze-thaw cycles, incubated with 10 U/μL DNAse, and cell debris was pelleted. The AAV-containing supernatant was purified by iodixonal gradient (Optiprep, Sigma-Aldrich) and desalted using an Amicon Ultra-15 100K centrifugal filter device (EMD Millipore, Bedford, MA) with 1X PBS. Purified AAV was stored in 5% glycerol at -80°C. Viral genomes were quantified with the QuickTiter AAV Quantification Kit, according to the manufacturer's instructions (Cell Biolabs, San Diego, CA).

Detailed information about construction of the rAAV8.pAlb.mCherry.hDTR is available in Brempelis, et. al(1).

Serum ALT activity

Blood collected from the portal vein was allowed to clot at 4°C overnight and then centrifuged at 6000 rpm for 10 minutes at room temperature. The serum supernatant was collected, and levels of ALT

activity was quantified using the Alanine Aminotransferase-SL kit (Sekisui Diagnostics LLC, Lexington, MA) according to manufacturer instruction.

Liver perfusion and hepatocyte separation

Prior to liver perfusion, mice were anesthetized with Avertin, blood was collected from the portal vein for ALT analysis, liver samples were placed in TRIzol for RNA extraction, and liver samples were placed in 10% neutral-buffered formalin for histology. Perfusion Buffer (1X HBSS + 5mM Hepes (pH 7.25) + 0.5mM EDTA (pH 8.0)) followed by approximately 8 mL of 1 mg/mL Collagenase Buffer (1X HBSS (with phenol red) + 5mM Hepes (pH 7.25) + 0.5mM $CaCl_2$ + 1 mg/mL Collagenase IV) was pumped through the liver. The perfused liver was removed from the mouse, and the gall bladder was removed prior to gently mashing in Processing Buffer (1X PBS + 4% heat-inactivated FBS (Corning, Corning, NY)) to form a single cell suspension. Hepatocytes were separated from non-parenchymal cells by low-density centrifugation (500 x g, 3 minutes, 4°C), followed by two washes with Processing Buffer, before transferring 50 μL of the hepatocyte pellet into TRIzol and storing at -80°C. The non-parenchymal cells contained in the supernatant after the first low-density centrifugation were further isolated on a 40% iodixanol layer and resuspended in Flow Buffer (1X PBS + 2% FBS + 1mM EDTA) for staining. For a more detailed liver perfusion protocol, see Mohar, et. al(2).

Flow cytometry and cell sorting

Isolated non-parenchymal cells were stained with the following mouse antibodies at 1:300 dilutions: BV605-CD11b (Clone M1/70, BD Biosciences, Franklin Lakes, NJ), PE-Tie2 (Clone TEK4, BioLegend, San Diego, CA), Pacific Blue-CD45.2 (Clone 104, BioLegend), APC-Cy7-Ly6G (Clone IA8, BioLegend), and PE-Cy7-F4/80 (clone BM8, BioLegend)). Cells were also stained with LIVE/DEAD Fixable Far Red Cell Stain Kit

(1:1000, Molecular Probes/Thermo Fisher Scientific, Waltham, MA). Kupffer cells were isolated by fluorescence-activated cell sorting with a BD Aria III (BD Biosciences) and stored in TRIzol at -80°C. Hepa1-6 cells were stained with the mouse antibodies BV605-Fas (1:50, Clone SA367H8, BioLegend) and APC-FasL (1:50, Clone MFL3, BioLegend), or LIVE/DEAD Fixable Far Red Cell Stain Kit (1:100, Molecular Probes), then fixed with BD Cytofix/Cytoperm™ (BD Biosciences) prior to data collection with a BD LSR II (BD Biosciences). All cell population analysis was performed with FlowJo software (FlowJo, LLC, Ashland, OR).

Quantitative RT-PCR gene expression analysis

Liver tissue, hepatocytes, and Kupffer cells were store in TRIzol at -80°C until processing. Liver tissue was then homogenized, and hepatocyte samples were sheared by passage through a 27G1/2 needle 3-5 times. RNA was extracted using Direct-zol RNA Miniprep Kit (Zymo Research Corporation, Irvine, CA). Complementary DNA was generated using the QuantiTect Reverse Transcription Kit (Qiagen, Hilden, Germany), preamplified with the TaqMan assays of interest (Supporting Table 1) (Applied Biosciences/Thermo Fisher Scientific) and MyFiMix 2X (Meridian Bioscience, previously Bioline, Cincinnati, OH), then diluted 1:5 for analysis. Microfluidic quantitative RT-PCR was performed on a BioMark HD microfluidics system (Fluidigm, South San Francisco, CA). The Fluidigm Gene Expression software was used to calculate Ct thresholds and Excel used to calculate relative expression levels using the $2^{-\Delta Ct}$ method. Relative Transcript Abundance was calculated relative to the average abundance of *Hprt* and *Gapdh* in Microsoft Excel (Microsoft, Redmond, WA). TaqMan Assay information is listed in Table 1 (Chapter 3) and Table 2 (Appendix 2).

Histology

Liver lobes were fixed in 10% neutral-buffered formalin prior to storage in 1X PBS. Fixed tissue was paraffin-embedded, sectioned, stained with hematoxylin and eosin, and images were scanned by the University of Washington Histology Imaging Core.

Hepa1-6 cells and *in vitro* experiments

The mouse hepatocyte-derived cell line, Hepa1-6, was purchased from ATCC (Lot #70031235) and cultured in media containing DMEM (high glucose +L-glutamine (Gibco/Thermo Fisher Scientific)) + 1% Penicillin and Streptomycin (Gibco) + 10% FBS (heat inactivated, Corning) and incubated at 37°C and 5% CO_2. Cells were split 2-3 times per week to maintain fitness.

24-well plates were seeded with 300,000 Hepa1-6 cells per well to achieve 100% confluence at the start of each experiment. The following day, cells were treated with either 10 μM of the TLR9 inhibitor ODN 2088 (Invivogen, San Diego, CA) or 10 μM of the 2088 Negative Control ODN (Invivogen). Experiment endpoints were at 24, 48, and 72 hours post-treatment, where the cells were removed from the plates with trypsin + EDTA (Gibco) before staining (see the Flow Cytometry and Cell Sorting methods for further details).

Statistical Analysis

Graphs represent data from single experiments or aggregate data from 2-3 independent experiments as noted in the figure legends. For all gene expression data, samples were eliminated from the analysis if they did not pass a multi-step quality control check: RNA quality, raw Ct values present, and raw Ct consistency between 3 technical replicates.

For ALT, neutrophil, and myeloid cell data, statistical comparisons were between WT and TLR9$^{-/-}$ mice within the control, 16 hour, and 48 hour post-DT groups. For the hepatocyte-specific TLR9 deletion pilot experiment, statistical comparison of ALT was between HepTLR9+/+ and HepΔTLR9 48 hours post-DT. Significance was determined by multiple unpaired t-tests with Welch correction and corrected for false discovery rate within multiple comparisons using the two-stage step-up Benjamini, Krieger, and Yekutieli method. For data comparing gene expression between control, 16 hour, and 48 hour post-DT in WT and TLR9$^{-/-}$ purified hepatocytes, significance was determined between six groups (WT control vs WT 16 hour post-DT; WT control vs 48 hour post-DT; WT 16 hour post-DT vs WT 48 hour post-DT; TLR9$^{-/-}$ control vs TLR9$^{-/-}$ 16 hour post-DT; TLR9$^{-/-}$ control vs TLR9$^{-/-}$ 48 hour post-DT; and TLR9$^{-/-}$ 16 hour post-DT vs TLR9$^{-/-}$ 48 hour post-DT) multiple unpaired t-tests with Welch correction were performed followed by correction for false discovery rate within multiple comparisons using the two-stage step-up Benjamini, Krieger, and Yekutieli method.

For data comparing gene expression between uninjured WT and TLR9$^{-/-}$ liver tissue, hepatocytes, and Kupffer cells, multiple unpaired t-tests with Welch correction were performed followed by correction for false discovery rate within multiple comparisons using the two-stage step-up Benjamini, Krieger, and Yekutieli method. For these data, all statistical testing was performed within each sample type and then displayed as Relative Transcript Abundance from total liver, hepatocytes, and Kupffer cells for each gene in graph form.

For Hepa1-6 data, comparisons were made between ODN 2088 and Negative Control ODN at each time, multiple unpaired t-tests with Welch correction were performed followed by correction for false discovery rate within multiple comparisons using the two-stage step-up Benjamini, Krieger, and Yekutieli method. Significant p-values are represented by asterisks at the following levels: * $p < 0.05$, ** $p < 0.01$,

*** $p < 0.001$, and ns (not significant) $p > 0.05$. In general, if a test was non-significant, it is not represented by ns in the figures. All statistical analysis was performed in GraphPad Prism 6 (La Jolla, CA) or Microsoft Excel (Microsoft, Redmond, WA).

Table 1 – Chapter 3 TaqMan Assays

Gene	Assay ID	Species
Aim2	Mm01295719_m1	Mouse
Pycard (Asc)	Mm00445747_g1	Mouse
Atf2	Mm01276552_m1	Mouse
Bak1	Mm00432045_m1	Mouse
Bax	Mm00432051_m1	Mouse
Bcl2	Mm00477631_m1	Mouse
Bid	Mm00432073_m1	Mouse
Caspase 1	Mm00438023_m1	Mouse
Caspase 3	Mm01195085_m1	Mouse
Caspase 7	Mm00432322_m1	Mouse
Caspase 8	Mm01255716_m1	Mouse
Scaf11 (Caspase 11)	Mm01297328_m1	Mouse
Ccl2	Mm00441242_m1	Mouse
Ccl5	Mm01302427_m1	Mouse

Table 1 (continued)

Gene	Assay ID	Species
Ccl7	Mm00443113_m1	Mouse
Cxcl1	Mm04207460_m1	Mouse
Cxcl2	Mm00436450_m1	Mouse
Cxcl10	Mm00445235_m1	Mouse
Mapk3 (Erk1)	Mm01278702_gH	Mouse
Mapk1 (Erk2)	Mm00442479_m1	Mouse
Fas	Mm01204974_m1	Mouse
Fos	Mm00487425_m1	Mouse
HB-EGF (hDTR)	Hs00181813_m1	Mouse
Il1alpha	Mm00439620_m1	Mouse
Il1beta	Mm00434228_m1	Mouse
Il18	Mm00434226_m1	Mouse
Jak2	Mm01208489_m1	Mouse
Prkaa1	Mm01296700_m1	Mouse

Table 1 (continued)

Gene	Assay ID	Species
Ripk1	Mm00436354_m1	Mouse
Ripk3	Mm00444947_m1	Mouse
Stat3	Mm01219775_m1	Mouse
Tnfrsf1a (Tnfr1)	Mm00441883_g1	Mouse
Tnfrsf1b (Tnfr2)	Mm00441889_m1	Mouse
Unc93b1	Mm00457643_m1	Mouse
Gapdh	Mm99999915_g1	Mouse
Hprt	Mm03024075_m1	Mouse

Table 2 – Appendix 2 TaqMan Assays

Gene	Assay ID	Species
Atg5	Mm01187303_m1	Mouse
Atg7	Mm00512209_m1	Mouse
Arg1	Mm00475988_m1	Mouse
Bcl2	Mm00477631_m1	Mouse
Bid	Mm00432073_m1	Mouse
Caspase 1	Mm00438023_m1	Mouse
Scaf11 (Caspase 11)	Mm01297328_m1	Mouse
Ccl2	Mm00441242_m1	Mouse
Ccl3	Mm00441259_g1	Mouse
Ccl5	Mm01302427_m1	Mouse
Ccl7	Mm00443113_m1	Mouse
Ccl8	Mm01297183_m1	Mouse
Ccl25	Mm0043644_m1	Mouse
Cxcl1	Mm04207460_m1	Mouse

Table 2 (continued)

Gene	Assay ID	Species
Cxcl2	Mm00436450_m1	Mouse
Cxcl9	Mm00434946_m1	Mouse
Cxcl10	Mm00445235_m1	Mouse
Icam1	Mm00516023_m1	Mouse
Ifna1	Mm03030145_gH	Mouse
Ifnb1	Mm00439552_s1	Mouse
Il1beta	Mm00434228_m1	Mouse
Il6	Mm00446190_m1	Mouse
Il10	Mm01288386_m1	Mouse
Il18	Mm00434226_m1	Mouse
Irf3	Mm00516784_m1	Mouse
Irf7	Mm00516793_g1	Mouse
Isg15	Mm017052338_s1	Mouse
Mx1	Mm00487796_m1	Mouse

Table 2 (continued)

Gene	Assay ID	Species
Nfkb1	Mm00476361_m1	Mouse
Rsad2	Mm00491265_m1	Mouse
Socs2	Mm00850544_g1	Mouse
Tgfb3	Mm00436960_m1	Mouse
Tlr2	Mm01213946_g1	Mouse
Tlr3	Mm01207404_m1	Mouse
Tlr4	Mm00445273_m1	Mouse
Tlr7	Mm04933178_g1	Mouse
Tlr9	Mm00446193_m1	Mouse
Tlr11	Mm01701924_s1	Mouse
Tnfa	Mm00443258_m1	Mouse
Vcam1	Mm01320970_m1	Mouse

Chapter 2 References

1. Brempelis KJ, Yuen SY, Schwarz N, Mohar I, Crispe IN. Central role of the TIR-domain-containing adaptor-inducing interferon-β (TRIF) adaptor protein in murine sterile liver injury. Hepatology. 2017;65(4):1336-51.
2. Mohar I, Brempelis KJ, Murray SA, Ebrahimkhani MR, Crispe IN. Isolation of Non-parenchymal Cells from the Mouse Liver. Methods Mol Biol. 2015;1325:3-17.

Chapter 3 – Regulation of innate liver injury by TLR9 in hepatocytes

Introduction

Pattern recognition receptors (PRRs) recognize conserved molecular patterns in proteins, lipids, and nucleic acids and are essential for activating the innate immune response to both pathogens and damage within the host. Canonical PRR signaling induces pro-inflammatory cytokines and chemokines to recruit and activate circulating and resident innate immune cells. The liver is constantly exposed to microbe-associated molecular patterns (MAMPs) as nutrients and gut microbe components are transferred from the intestine via the portal vein(1-3). These harmless MAMPs are continuously binding to their respective PRRs, yet the liver is not in a constant pro-inflammatory state(1, 4-6). Conversely, the liver is a sentinel for gut-acquired pathogens and is able to mount a rapid and robust innate response to pathogen-associated molecular patterns (PAMPs) during an infection(3). PRRs in the liver must therefore strike a delicate balance between preventing pro-inflammatory signaling due to constant MAMP-PRR interactions but still effectively activating canonical signaling in the presence of PAMPs. This balance enables both rapid initiation and rapid resolution of liver inflammation caused by both pathogenic and non-pathogenic insults.

Hepatocyte death is a major cause of non-pathogenic, or sterile, liver inflammation. Hepatocytes can also play an active role in the innate immune response during liver injury(2, 7-9). Dying cells can stimulate the innate immune response in different ways depending on the mechanism of cell death, including the release of damage-associated molecular patterns (DAMPs), and the transcription of pro-inflammatory genes(9, 10). DAMPs, which have a variety of functions in healthy cells, are thought to be recognized by the same PRRs as MAMPs and PAMPs because they are concealed from the steady-state

microenvironment and are only released when cells are damaged or dying(9). Cell death of 10-20% of the hepatocytes is sufficient to initiate acute, self-limiting inflammation and tissue injury(7). This indicates that hepatocytes may have dual roles in the liver immune response: 1) the release of DAMPs and inflammatory stimuli from dying hepatocytes, and 2) PRR signaling in neighboring hepatocytes triggered by dying hepatocytes.

One of the main functions of hepatocytes is to produce many of the immune components found in the circulation that are essential for defense against bacterial and viral infections, such as complement and transferrin(2). During sterile liver injury, hepatocytes produce chemokines such as CCL2 and CXCL1 to initiate monocyte and neutrophil infiltration and activation(2, 7, 11). We have also previously described hepatocyte transcription of cytokine-encoding genes (*Ill6*, *Ifna1*, *Ifnb1*, *Il1beta*, *Il18*, and *Il10*) and chemokine-encoding genes (*Ccl2*, *Ccl3*, *Ccl5*, *Cxcl1*, *Cxcl2*, and *Cxcl10*) in response to acute liver injury(7). Despite these reports, the hepatocyte immune response to cell death within the liver remains largely uncharacterized. Hepatocytes play a large role in dead cell removal; DAMP-PRR interactions could therefore heavily influence the hepatocyte immune response during sterile liver injury (7, 12, 13).

DAMP recognition by PRRs, such as Toll-like receptors, produces inflammatory signals to recruit and activate both tissue-resident and circulating immune cells similarly to PAMP-PRR interactions(9, 14-16). For example, TLR9 is an intracellular PRR that is activated by unmethylated CpG DNA in the endo-lysosome(17-19). While unmethylated CpG sites are rare in vertebrate DNA, mitochondrial DNA is hypomethylated in comparison and can be recognized by TLR9 when released from dying cells(17, 19). TLR9 signaling promotes T_H1 inflammation, especially CXCL1-mediated recruitment of neutrophils and inflammasome activation(20, 21). Despite the inflammatory responses activated by canonical TLR9

signaling, TLR9 exhibits protective effects in certain situations, such as: protecting cardiomyocytes and neurons from stress(22, 23); preventing lung damage due to allergy(24); and regulating disease pathogenesis in systemic lupus erythematosus(25). In the context of the liver, TLR9 drives injury due to a high-fat diet(26-28) and acetaminophen (N-acetyl-para-aminophenol, or APAP) overdose(29), but protective in a mouse model of chronic alcohol exposure(30). These studies suggest that the role of TLR9 signaling in the liver differs depending on the type of insult and may even be cell-type specific. In this study, we examined whether TLR9 signaling was injurious or protective in the liver during inflammation caused by hepatocyte death.

Results

To determine the impact of TLR9 deletion during sterile, self-limiting hepatitis caused by moderate hepatocyte-specific death, C57Bl/6 (WT) and TLR9$^{-/-}$ mice were transduced with hepatocyte-specific rAAV.hDTR.mCherry (or vehicle) to induce DTR expression in 10-20% of the hepatocytes. After two weeks, mice were injected with DT and sacrificed either 16 hours or 48 hours later. Liver injury was then assessed in these mice via serum ALT activity and liver lobes were fixed for H&E histology. TLR9 deletion resulted in significantly increased serum ALT activity compared to WT mice 48 hours post-DT (Fig. 5A). In WT mice there were pockets of dead hepatocytes surrounded by large areas of normal hepatocytes, as we have observed previously (Fig. 5B)(7). In TLR9$^{-/-}$ mice however, there was massive hepatocyte death, evidence of hemorrhage, and very few remaining healthy hepatocytes by 48 hours post-DT (Fig. 5B). Additionally, TLR9$^{-/-}$ livers exhibited increased steatosis, hepatocyte ballooning, and hepatocyte injury 48 hours post-DT (Fig. 6A and B). There was no difference in DTR expression levels between WT and TLR9$^{-/-}$ livers to account for the increased liver injury observed in TLR9$^{-/-}$ mice (Fig. 7). Taken together, these

data indicate that TLR9 deletion results in more liver injury 48 hours following hepatocyte-specific killing with DT.

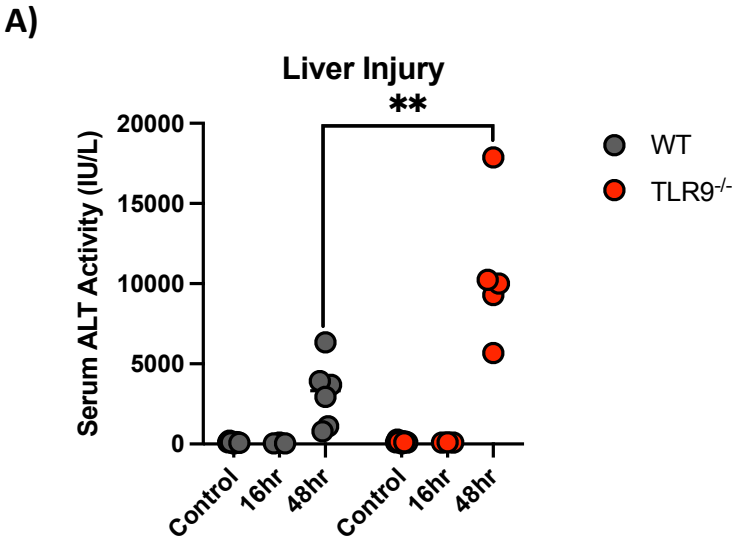

Fig 5. TLR9$^{-/-}$ mice experience greater liver injury in the DTR model. WT and TLR9$^{-/-}$ mice were injected (r.o.) with 5 x 10^{9} viral genomes of rAAV.mCherry.hDTR or PBS (control mice). After two weeks, mice were injected (i.p.) with 20ng DT and were sacrificed 16 hours or 48 hours later. A) Blood was extracted from the portal vein and ALT activity was assessed in the serum. N = 3-6 per group. Significance was determined with unpaired Welch t-test, ** = $p < 0.01$. B) *Next Page* Sections from fixed liver lobes were stained with H&E from control (No Injury) and 48 hours post-DT (48hr Injury) groups in WT and TLR9$^{-/-}$ mice. Representative images were chosen from one mouse per group.

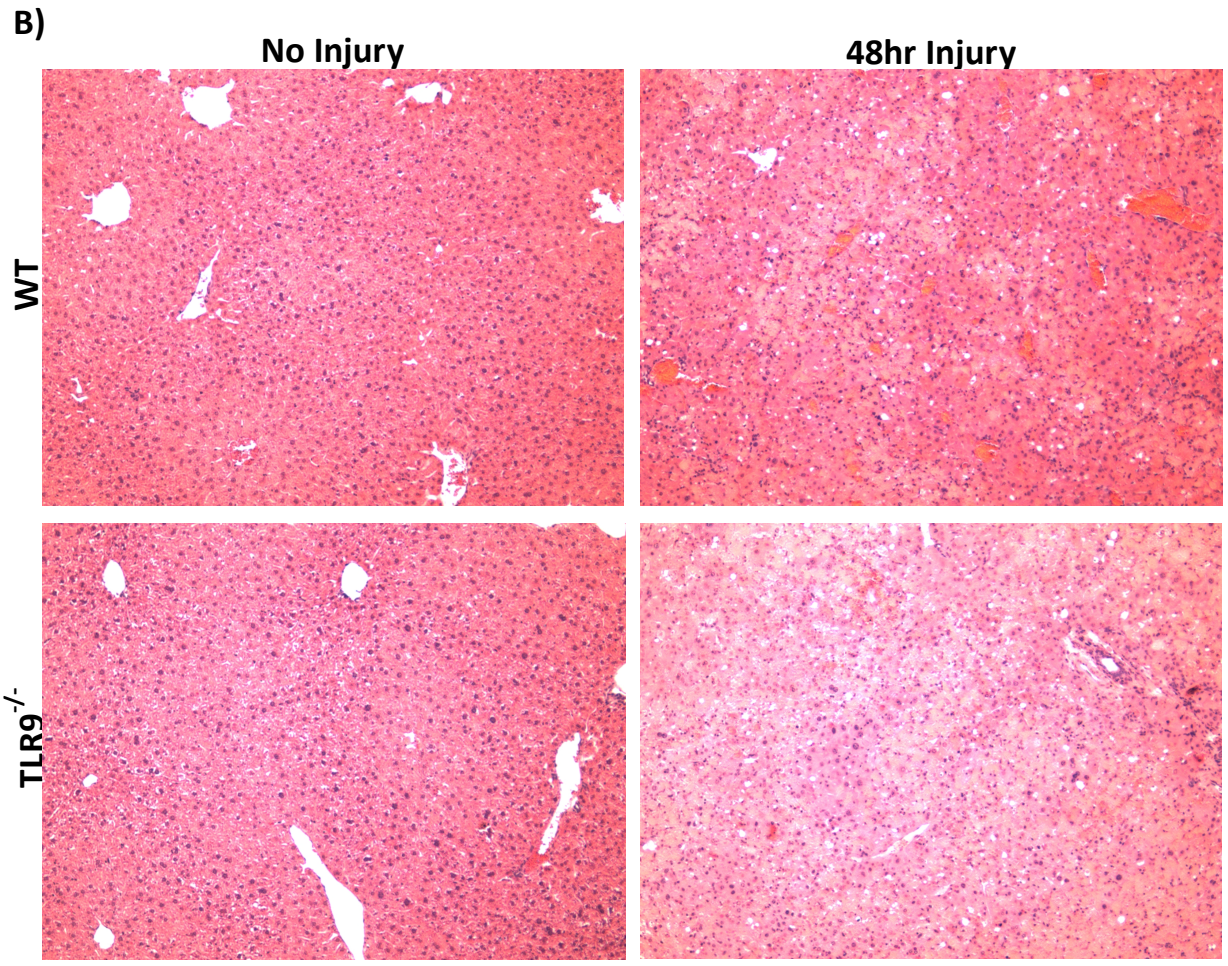
B)
No Injury
48hr Injury
WT
TLR9-/-

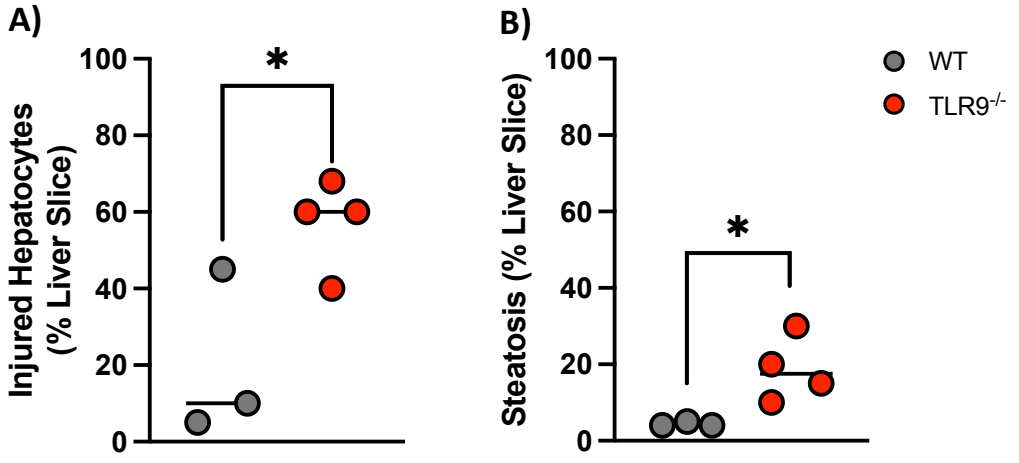

Fig 6. Steatosis and hepatocyte injury are increased in TLR9$^{-/-}$ livers 48 hours post-DT. WT and TLR9$^{-/-}$ mice were injected (r.o.) with 5 x 10^{9} viral genomes of rAAV.mCherry.hDTR. After two weeks, mice were injected (i.p.) with 20ng DT and sacrificed 48 hours later. Sections from fixed liver lobes from WT (n = 3) and TLR9$^{-/-}$ (n = 4) mice were stained with H&E and A) hepatocyte injury and B) steatosis was scored blind. Significance was determined with unpaired, Welch t-test, * = $p < 0.05$.

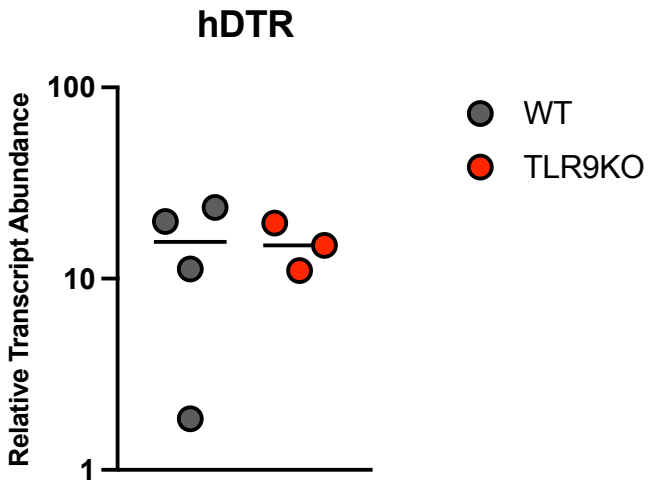

Fig 7. AAV transduction in the liver is not affected by TLR9 deletion. WT (n = 4) and TLR9$^{-/-}$ (n = 3) mice were injected (r.o.) with 5 x 10^{9} viral genomes of rAAV.mCherry.hDTR. Mice were sacrificed after two weeks, and RNA was extracted from whole liver tissue. Human *HB-EGF* (DTR) gene expression was calculated relative to *Hprt* and *Gapdh*. Significance was determined by unpaired, Welch t-test, NS = not significant.

The increased steatosis and hepatocyte ballooning observed in $TLR9^{-/-}$ livers at 48 hours post-DT indicates that lack of TLR9 increases hepatocyte injury (Fig. 5B and Fig. 6). We hypothesized that hepatocyte-specific TLR9 signaling prevents the increased hepatocyte injury observed in $TLR9^{-/-}$ livers 48 hours post-DT. To test this, we generated mice with TLR9 deleted exclusively in hepatocytes ($Hep^{\Delta TLR9}$) and compared liver injury to littermates expressing WT levels of TLR9 ($Hep^{TLR9+/+}$) in a pilot experiment. Serum ALT activity quantified 48 hours post-DT administration showed a clear biological trend for increased injury in $Hep^{\Delta TLR9}$ mice, however it was not statistically significant due to low n (Fig. 8A, $p = 0.057$). In a second pilot experiment, we tested whether TLR9 inhibition would increase hepatocyte death *in vitro*. Hepa1-6 hepatoma cells were treated with either ODN 2088 to inhibit TLR9, or a control ODN (ODN 2088 Negative Control), for 72 hours and then assessed for cell permeability as the indicator of cells death. TLR9 inhibition with ODN 2088 significantly increased permeabilized cells compared to Hepa1-6 cells treated with the control ODN (Fig. 8B). This suggested that the trend for increased liver injury observed in $Hep^{\Delta TLR9}$ mice could be because TLR9 inhibition increased hepatocyte sensitivity to death.

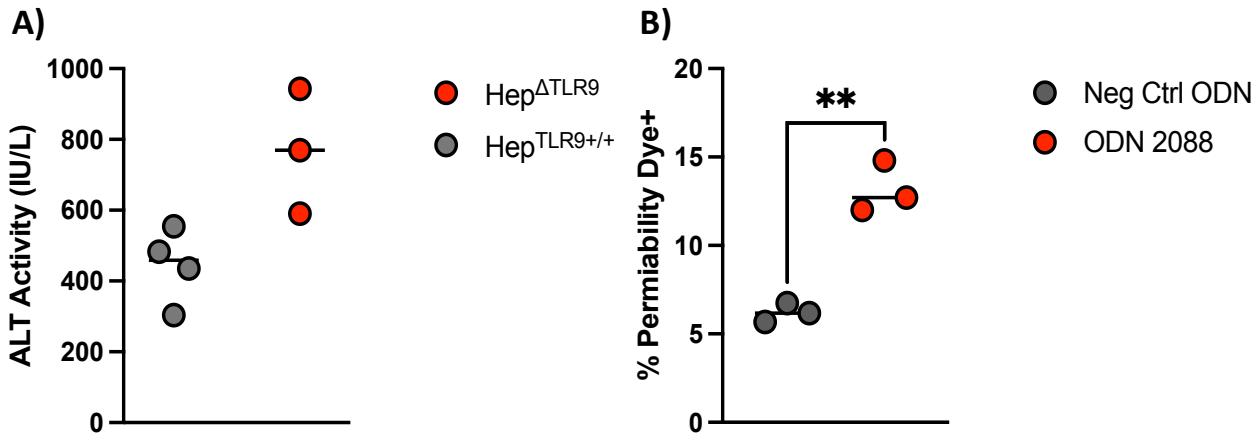

Fig 8. TLR9 deletion from hepatocytes trends towards increased liver injury and TLR9 inhibition increases susceptibility to cell death. A) TLR9-flox$^{+/+}$ (Hep$^{TLR9+/+}$) and TLR9-flox$^{+/+}$:: Alb-Cre+ (Hep$^{\Delta TLR9}$) mice were injected (r.o.) with 5 x 10^{9} viral genomes of rAAV.mCherry.hDTR or PBS (control mice). After two weeks, mice were injected (i.p.) with 20ng DT. ALT activity from portal vein blood was quantified 48 hours post-DT. Data is from a pilot study with n = 4 (Hep$^{TLR9+/+}$) and n = 3 (Hep$^{\Delta TLR9}$). B) 24-well plates were seeded with Hepa1-6 cells and then treated with 10uM TLR9 inhibitor (ODN 2088) or negative control (ODN 2088 negative control) the next day. Cells were trypsonized and incubated with a cell permeability dye 72 hours post-treatment and analyzed by flow cytometry. Cell death was determined by identifying dye-positive populations. Cells that stained positive for the permeability dye are considered dead or dying. Data is from a pilot study with n = 3 for both conditions. Significance for both experiments was determined by unpaired Welch t-test. Non-significant = not indicated, * = $p < 0.05$, ** = $p < 0.01$, *** = $p < 0.001$.

To determine if the increased injury in the absence of TLR9 also increased recruitment of innate immune cells into the liver, we perfused the livers of WT and TLR9$^{-/-}$ mice 16 hours or 48 hours post-DT and quantified infiltrating myeloid and neutrophil populations. There was no difference in either myeloid (Fig. 9A) or neutrophil (Fig. 9B) infiltration between WT and TLR9$^{-/-}$ mice. Previous work showed that hepatocytes were the major producers of chemokines during the first 48 hours of DT-induced liver injury(7). We hypothesized that, in addition to sensitizing hepatocytes to death, TLR9 deletion would also perturb hepatocyte chemokine production and influence innate immune cell infiltration into the liver. We therefore assessed the gene expression of *Ccl2* (Fig. 9C), *Ccl5* (Fig. 9D), *Ccl7* (Fig. 9E), *Cxcl1* (Fig. 9F), *Cxcl2* (Fig. 9G), and *Cxcl10* (Fig. 9H) in hepatocytes isolated from WT and TLR9$^{-/-}$ livers perfused at 16 hours or 48 hours post-DT. We observed only one difference between WT and TLR9$^{-/-}$ hepatocyte chemokine gene expression – *Cxcl10* expression was increased in TLR9$^{-/-}$ hepatocytes 16 hours post-DT ~1.5 fold, but that difference disappeared by 48 hours post-DT (Fig. 9H). These results did not support our hypothesis and instead indicate that recruitment and infiltration of innate immune cells into the liver during DT-induced injury is independent of TLR9 signaling.

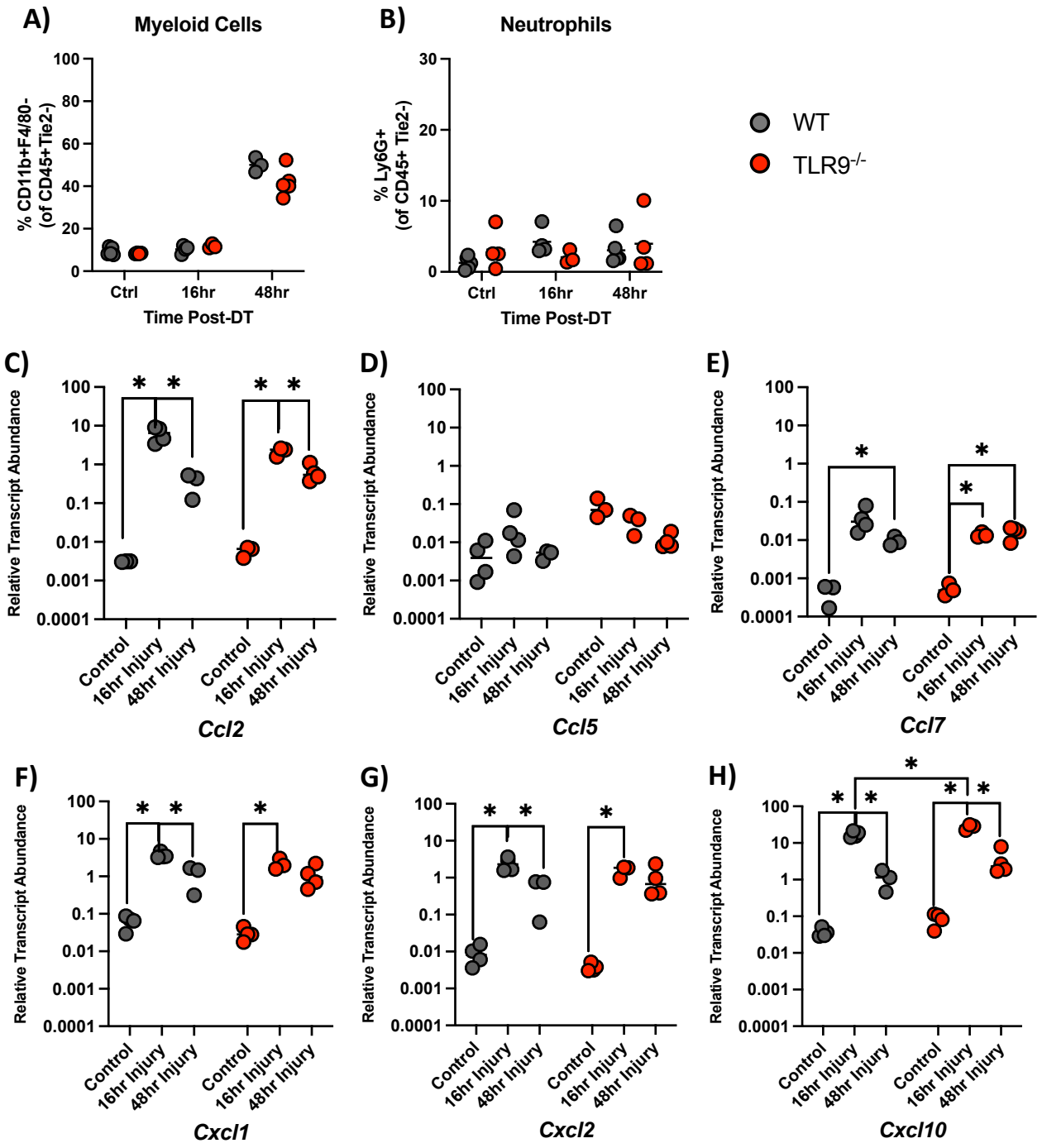
A)
Myeloid Cells
% CD11b+F4/80- (of CD45+Tie2-)
Ctrl
16hr
48hr
Time Post-DT
B)
Neutrophils
% Ly6G+ (of CD45+ Tie2-)
Time Post-DT
WT
TLR9-/-
C)
Ccl2
D)
Ccl5
E)
Ccl7
F)
Cxcl1
G)
Cxcl2
H)
Cxcl10
Relative Transcript Abundance
Control
16hr Injury
48hr Injury

Fig 9 TLR9$^{-/-}$ mice have similar myeloid cell infiltration, neutrophil infiltration, and chemokine gene expression as WT mice. WT and TLR9$^{-/-}$ mice were injected (r.o.) with 5 x 10^9 viral genomes of rAAV.mCherry.hDTR or PBS (control mice). After two weeks, mice were injected (i.p.) with 20ng DT and were sacrificed 16 hours or 48 hours later. Non-parenchymal cells were isolated from perfused livers and assessed via flow cytometry for A) myeloid cell (CD11b+F4/80-CD45+Tie2-) and B) neutrophil (Ly6G+CD11b-F4/80-CD45+Tie2-) populations (n = 3-5 per group). RNA was extracted from purified hepatocytes and gene expression of C) *Ccl2*, D) *Ccl5,* E) *Ccl7,* F) *Cxcl1*, G) *Cxcl2*, and H) *Cxcl10* relative to *Hprt* and *Gapdh* was assessed for each group. The data is representative of two experiments (n = 3-5 per group in each experiment). Significance was determined by unpaired Welch t-test. Non-significant = not indicated, * = $p < 0.05$, ** = $p < 0.01$, *** = $p < 0.001$.

During liver injury, JAK/STAT and MAPK signaling is induced in hepatocytes and is required for regeneration after inflammation is resolved(31-34). We hypothesized that the TLR9-dependent increased liver injury is in part be due to dysregulation of one or multiple JAK/STAT and MAPK signaling pathways in hepatocytes. To test this, we quantified *Erk1* (aka *Mapk3*), *Erk2* (aka *Mapk1*), and *Stat3* gene expression in purified hepatocytes from WT and TLR9$^{-/-}$ mice at 16 hours and 48 hours post-DT administration. We found that TLR9$^{-/-}$ hepatocytes had decreased Erk1 gene expression at 16 hours post-DT administration, whereas WT hepatocytes did not decrease Erk1 expression until 48 hours post-DT administration (Fig. 10A). Additionally, there was a small but significant increase of *Erk1* gene expression in TLR9$^{-/-}$ hepatocytes compared to WT hepatocytes in control mice (Fig. 10A). Conversely, *Erk2* and *Stat3* gene expression did not differ between WT and TLR9$^{-/-}$ hepatocytes during DT-induced liver injury, with the exception of a small but significant increase of *Erk2* in TLR9$^{-/-}$ hepatocytes 16 hours post-DT administration (Fig. 10B and C). While there were no significant differences in *Erk2* or *Stat3* gene expression between WT and TLR9$^{-/-}$ hepatocytes, a decrease in *Erk1* gene expression suggests that TLR9 deletion may impact hepatocyte regeneration during the resolution phase.

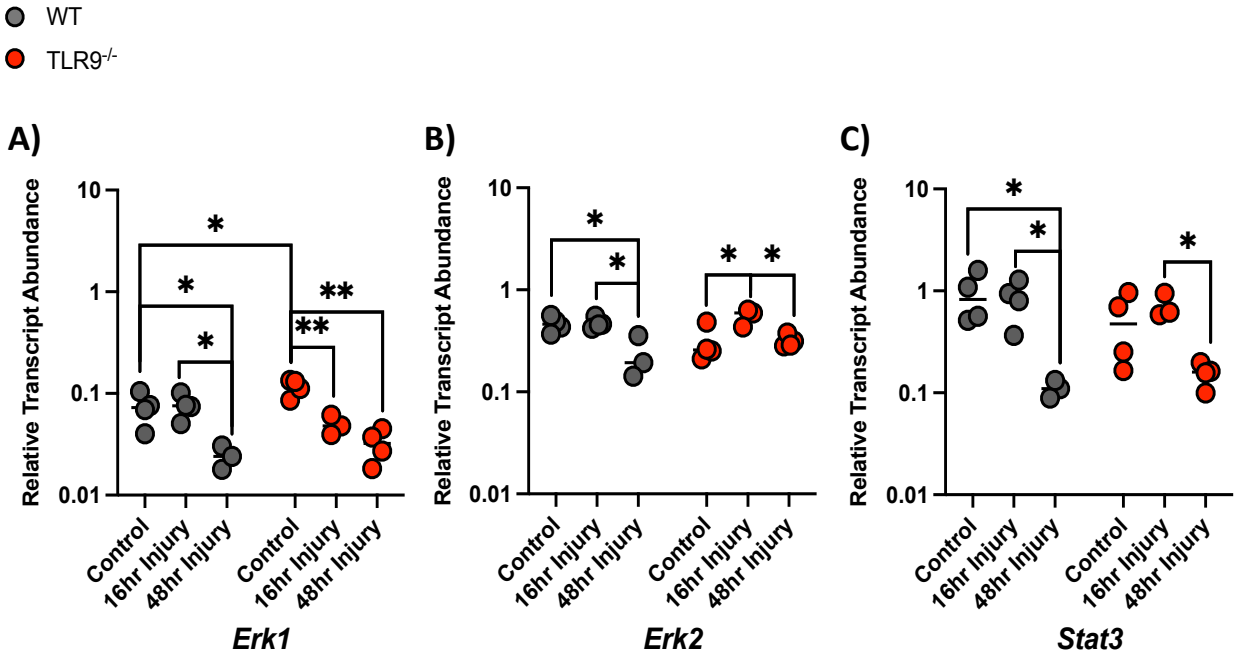

Fig 10 TLR9$^{-/-}$ and WT hepatocytes exhibit similar changes in *Erk1*, *Erk2,* and *Stat3* gene expression during DT-induced liver injury. WT and TLR9$^{-/-}$ mice were injected (r.o.) with 5 x 10^{9} viral genomes of rAAV.mCherry.hDTR or PBS (control mice). After two weeks, mice were injected (i.p.) with 20ng DT and were sacrificed 16 hours or 48 hours later. RNA was extracted from purified hepatocytes and gene expression of A) *Erk1 (Mapk3),* B) *Erk2 (Mapk1)*, and C) *Stat3* relative to *Hprt* and *Gapdh* was assessed for each group. The data is representative of two experiments (n = 3-5 per group in each experiment). Significance determined by unpaired Welch t-test for the following comparisons: Control vs 16hr Injury, Control vs 48hr Injury, 16hr Injury vs 48hr Injury in WT or TLR9$^{-/-}$ mice; WT vs TLR9$^{-/-}$ in the Control, 16hr Injury, or 48hr Injury conditions. * = $p < 0.05$, ** = $p < 0.01$, *** = $p < 0.001$.

A non-canonical TLR9 pathway that protects cardiomyocytes and neurons from pro-inflammatory damage was described by Shintani, et al(22, 23). While pro-inflammatory TLR9 signaling is activated in endosomes and mediated by MyD88, non-canonical TLR9 signaling is activated in the ER and promotes AMP-activated kinase (AMPK) inhibition of non-essential ATP-consuming metabolism to facilitate cell survival during hypoxia(22). This alternative TLR9 signaling requires low levels of Unc93b1, a TLR9 chaperone that is required for transport from the ER to endosomes(22). Our previous work showed that MyD88 deletion reduced liver injury ~50% compared to WT mice 48 hours post-DT administration(7), which suggests that TLR9-dependent protection was still intact. We therefore hypothesized that WT hepatocytes would utilize the alternative TLR9 signaling pathway to increase survival during DT-induced liver injury. To test this, we first evaluated *Prkaa1* and *Unc93b1* gene expression in total liver, hepatocytes, and KCs of uninjured WT and TLR9$^{-/-}$ mice. We predicted that if the alternative TLR9 pathway was being utilized in hepatocytes, *Unc93b1* gene expression would be decreased in WT hepatocytes compared to expression in total liver and KCs. We observed *Unc93b1* relative transcript abundance in hepatocytes to be increased compared to total liver but decreased compared to KCs from both WT and TLR9$^{-/-}$ mice (Fig. 11A). Because hepatocyte-specific *Unc93b1* relative transcript abundance was between that of whole liver and KCs, it was unclear whether sufficient TLR9 would remain at the ER in hepatocytes to activate the alternative signaling pathway. To determine if TLR9 was promoting AMPK activation in WT hepatocytes in response to liver inflammation, we quantified *Prkaa1* (aka AMPK) gene expression at 16 hours and 48 hours post-DT administration. In both WT and TLR9$^{-/-}$ hepatocytes however, *Prkaa1* gene expression did not increase at either timepoint of liver injury. In fact, *Prkaa1* gene expression was significantly decreased by 48 hours post-DT administration in both WT and TLR9$^{-/-}$ hepatocytes (Fig. 11B). These results suggest that the hepatoprotective effects of TLR9 in hepatocytes is not due to the alternative signaling pathway.

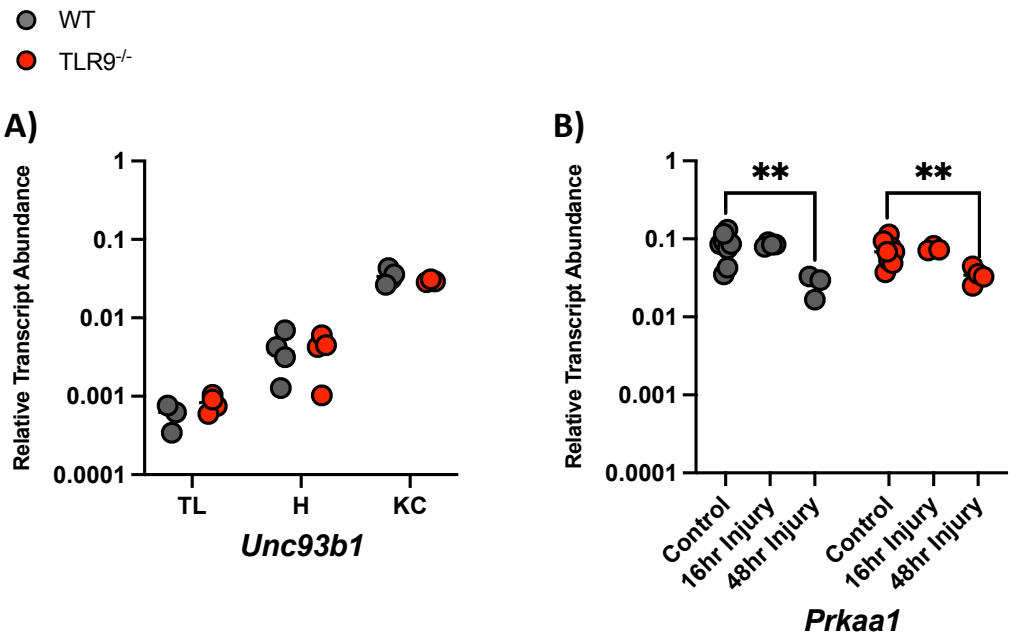

Fig 11 Liver injury does not induce the alternative TLR9 pathway in hepatocytes. (A) WT and TLR9$^{-/-}$ mouse livers were perfused and RNA was extracted from total liver (TL), purified hepatocytes (H), and purified Kupffer cells (KC). Gene expression of *Unc93b1* relative to Hprt and Gapdh was assessed for each group. (B) WT and TLR9$^{-/-}$ mice were injected (r.o.) with 5 x 10^{9} viral genomes of rAAV.mCherry.hDTR or PBS (control mice). After two weeks, mice were injected (i.p.) with 20ng DT and were sacrificed 16 hours or 48 hours later. RNA was extracted from purified hepatocytes and gene expression of *Prkaa1* relative to *Hprt* and *Gapdh* was assessed for each group. The data is representative of two experiments (n = 3-5 per group in each experiment). Significance determined by unpaired Welch t-test. * = $p < 0.05$, ** = $p < 0.01$, *** = $p < 0.001$.

The increased in cell death of ODN 2088-treated Hepa1-6 cells and swifter decrease in *Erk1* gene expression both suggest that TLR9 deletion reduces hepatocyte tolerance of stress during DT-induced liver injury (Fig. 8B and Fig. 10A). One potential explanation is that deletion of TLR9 increases hepatocyte sensitivity to cell death stimuli. This could prime the TLR9$^{-/-}$ mouse liver for uncontrolled secondary hepatocyte death in addition to DT-induced hepatocyte death. Thus, we hypothesized that in uninjured livers, TLR9 deletion would lead to hepatocyte-specific changes in expression of genes associated with programmed cell death. To determine if lack of TLR9 impacted cell-type specific gene expression, RNA was extracted from healthy WT and TLR9$^{-/-}$ male mice (8-10 weeks). Expression of essential genes associated with necroptosis (Fig. 12), intrinsic apoptosis (Fig. 13), and inflammasome activation and pyroptosis (Fig. 14) were then quantified in both WT and TLR9$^{-/-}$ total liver, hepatocytes and KCs. We assessed gene expression of *Ripk3*, *Ripk1*, *Tnfr1*, and *Tnfr2* to determine the impact of TLR9 deletion on necroptosis. TLR9$^{-/-}$ hepatocytes, but not total liver or KCs, showed significantly decreased *Ripk3* gene expression compared to WT, suggesting hepatocyte-specific necroptosis inhibition in TLR9$^{-/-}$ mice (Fig. 12A). To determine the impact of TLR9 deletion on intrinsic, or mitochondrial-mediated, apoptosis we assessed gene expression of pro-apoptotic *Bak*, *Bid*, and *Bax*, as well as pro-survival *Bcl2* BH3-only proteins. We observed a hepatocyte-specific decrease in pro-apoptotic *Bak* gene expression in the absence of TLR9 (Fig. 13A). There was also a decrease in pro-survival *Bcl2* gene expression in TLR9$^{-/-}$ hepatocytes, however the difference was not statistically significant (Fig. 13B, $p = 0.19$). While a change in more than one BH3-only protein level would be required to activate intrinsic apoptosis due to functional redundancy, these data suggest that TLR9 deletion decreases the ability of hepatocytes to induce mitochondrial-induced apoptosis.

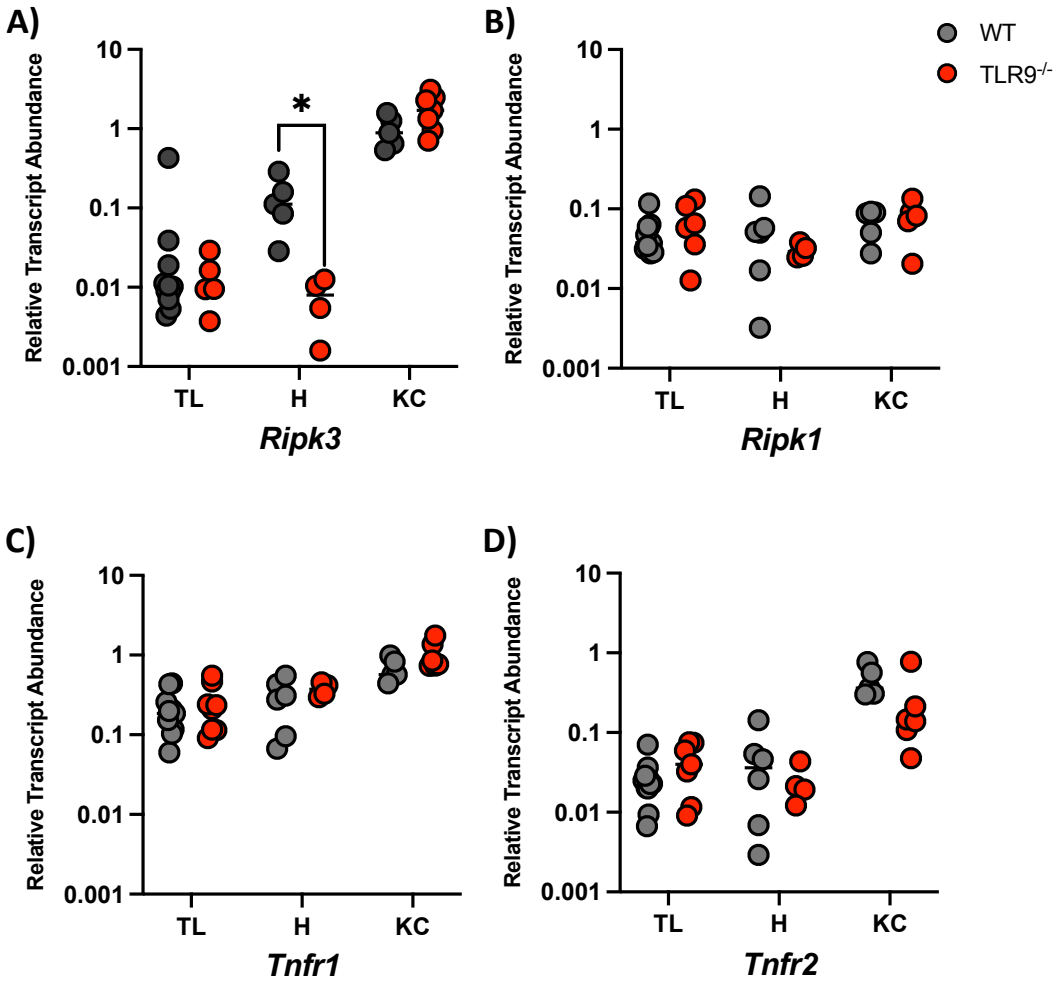

Fig 12 TLR9 deletion decreases hepatocyte-specific gene expression of necroptosis in the uninjured liver. WT or TLR9$^{-/-}$ mouse livers were perfused, and RNA was extracted from whole liver tissue (TL), purified hepatocytes (H), and purified Kupffer cells (KC). mRNA gene expression relative to *Hprt* and *Gapdh* was determined for genes involved in necroptosis: A) *Ripk3,* B) *Ripk1,* C) *Tnfr1,* and D) *Tnfr2*. Data was pooled from 2 experiments (n = 3-5 mice per group). Significance was determined with unpaired Welch t-test, * = $p < 0.05$, ** = $p < 0.01$, *** = $p < 0.001$.

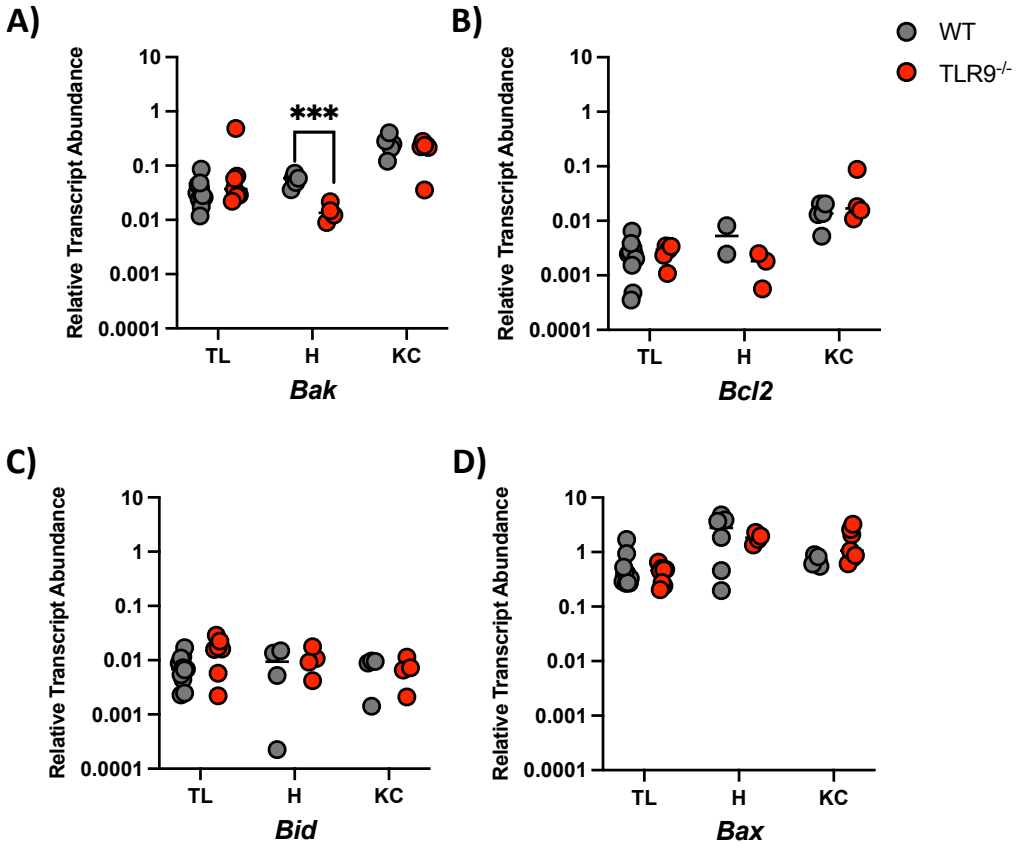

Fig 13 TLR9 deletion decreases hepatocyte-specific gene expression of intrinsic apoptosis in the absence of liver injury. WT or TLR9$^{-/-}$ mouse livers were perfused, and RNA was extracted from whole liver tissue (TL), purified hepatocytes (H), and purified Kupffer cells (KC). mRNA gene expression relative to *Hprt* and *Gapdh* was determined for genes involved in intrinsic apoptosis: A) *Bak,* B) *Bcl2,* C) *Bid,* and D) *Bax*. Data was pooled from 2 experiments (n = 3-5 mice per group). Significance was determined with unpaired Welch t-test, * = $p < 0.05$, ** = $p < 0.01$, *** = $p < 0.001$.

In APAP, I/R, and NASH mouse models, TLR9 deletion was shown to ameliorate liver injury by inhibiting inflammasome activation (27, 29, 35). While we have shown here that TLR9 deletion in DT-induced liver inflammation exacerbates injury, we predicted that TLR9$^{-/-}$ mice would also exhibit reduced expression of genes associated with the inflammasome and pyroptosis in uninjured liver cell populations. To test this hypothesis, we perfused WT and TLR9$^{-/-}$ livers and isolated RNA from total liver, hepatocytes, and KCs to assess the gene expression of *Asc*, *Aim2*, *Caspase 1*, *Scaf11 (Caspase 11)*, *Nfkb1*, *Il1beta*, and *Il18*. TLR9$^{-/-}$ hepatocytes exhibited decreased expression of *Asc*, *Caspase 1*, and *Nfkb1* compared to WT hepatocytes (Fig 14A-C). Additionally, *Il1beta* and *Aim2* gene expression in TLR9$^{-/-}$ hepatocytes were also decreased compared to WT, albeit not statistically significant (Fig. 14D and E, $p = 0.021$ and $p = 0.018$ respectively). Unexpectedly, the only change in inflammasome gene expression in TLR9$^{-/-}$ KCs compared to WT was an increase in *Il18* (Fig. 14G). The NASH and I/R studies showed that TLR9 deletion and subsequent inflammasome inhibition specifically in myeloid cells was sufficient to reduce liver injury (27, 35). We had therefore expected decreased inflammasome gene expression in TLR9$^{-/-}$ KCs isolated from uninjured livers, however there could still be post-translational inflammasome inhibition that we did not detect. These data taken together suggest that TLR9-dependent inflammasome and gene expression occurs specifically in hepatocytes of the uninjured liver. Whether the inflammasome activation in hepatocytes leads to pro-inflammatory signaling or pyroptosis is still unclear.

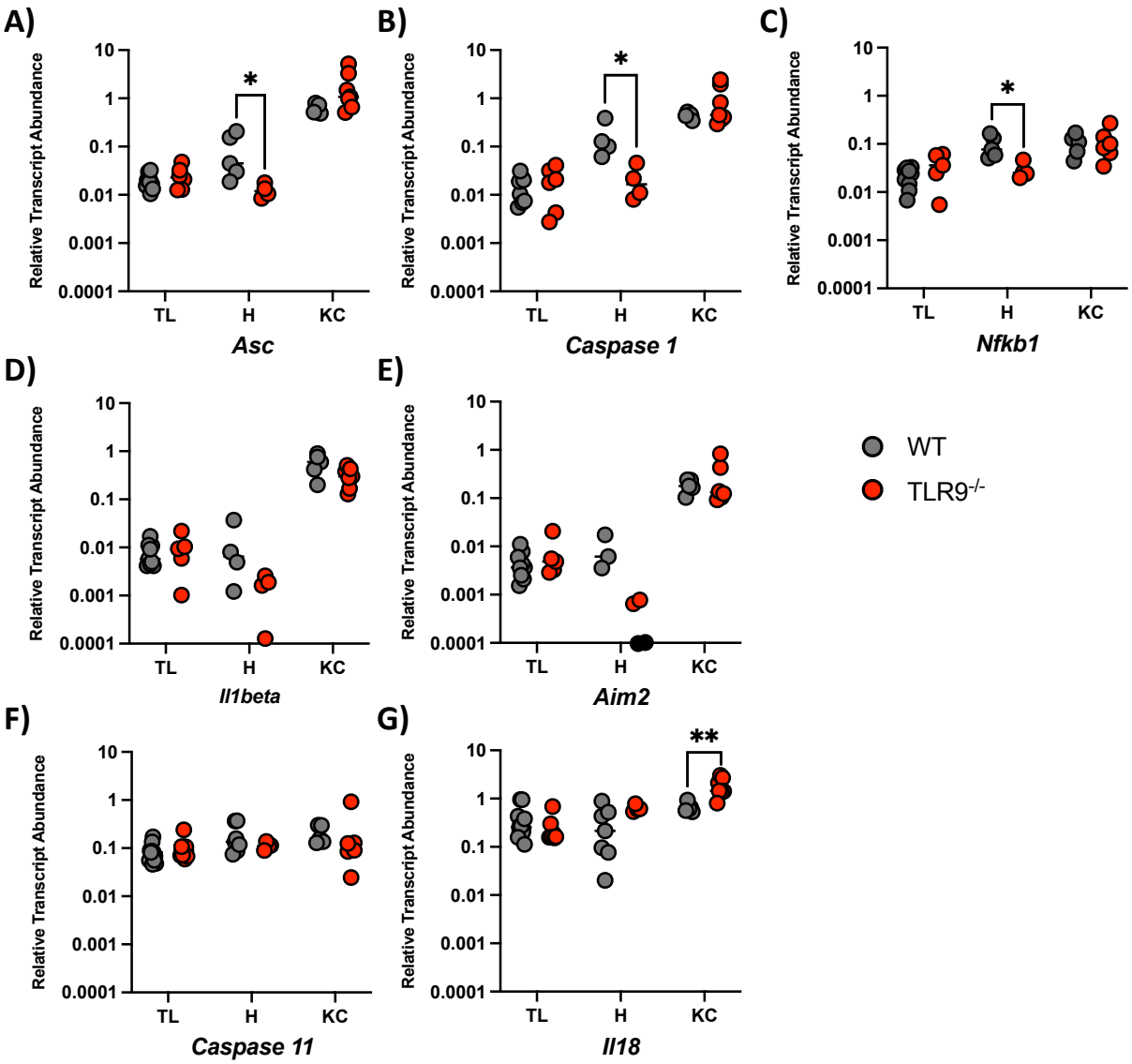

Fig 14 TLR9 deletion decreases hepatocyte-specific inflammasome and pyroptosis gene expression in the uninjured liver. WT or TLR9$^{-/-}$ mouse livers were perfused, and RNA was extracted from whole liver tissue (TL), purified hepatocytes (H), and purified Kupffer cells (KC). mRNA gene expression relative to *Hprt* and *Gapdh* was determined for genes involved in the inflammasome and pyroptosis: A) *Asc*, B) *Caspase 1*, C) *Nfkb1*, D) *Il1β,* E) *Aim2,* F) *Caspase 11,* and G) *Il18*. Data was pooled from 2 experiments (n = 3-5 mice per group). When gene expression was below the limit of detection for the assay, it is represented with a black circle. Significance was determined with unpaired Welch t-test, * = $p < 0.05$, ** = $p < 0.01$, *** = $p < 0.001$.

In TLR9$^{-/-}$ hepatocytes from uninjured livers, we found decreased expression of genes associated with necroptosis, intrinsic apoptosis, and pyroptosis (Figs. 12-14). However, in the case of one cell death pathway, we found evidence for increased expression in hepatocytes lacking TLR9. *Fas* gene expression was significantly increased specifically in TLR9$^{-/-}$ hepatocytes (Fig. 15A), and gene expression of *Caspases 3*, *7*, and *8* was preserved (Fig. 15B-D). The maintenance in caspase gene expression and increase in *Fas* gene expression indicates that Fas-mediated apoptosis is favored in hepatocytes in the absence of TLR9. We next quantified Fas and FasL surface expression in mouse hepatoma Hepa1-6 cells treated with ODN2088 for 24, 48, and 72 hours. The Fas+ cell population was increased in Hepa1-6 cells after 48 hour and 72 hour treatments with the TLR9 inhibitor (Fig 16A). The Fas MFI was increased in ODN 2088-treated cells at 48 and 72 hours, indicating that TLR9 inhibition also increases the amount of Fas expressed on each Fas+ hepatoma cell (Fig. 16A). FasL expression showed an initial spike in expression of 2 out of 3 replicates 24 hours post-TLR9 inhibition and was still elevated after 72 hours (Fig. 16B). In addition, ~60% of the FasL+ Hepa1-6 cells were also Fas+ in the 24 hour treatment group (Fig. 16C). Taken together with the decreased gene expression of other programmed cell death components, our data show that TLR9 deletion promotes the availability of the Fas-mediated apoptotic cell death pathway specifically in hepatocytes.

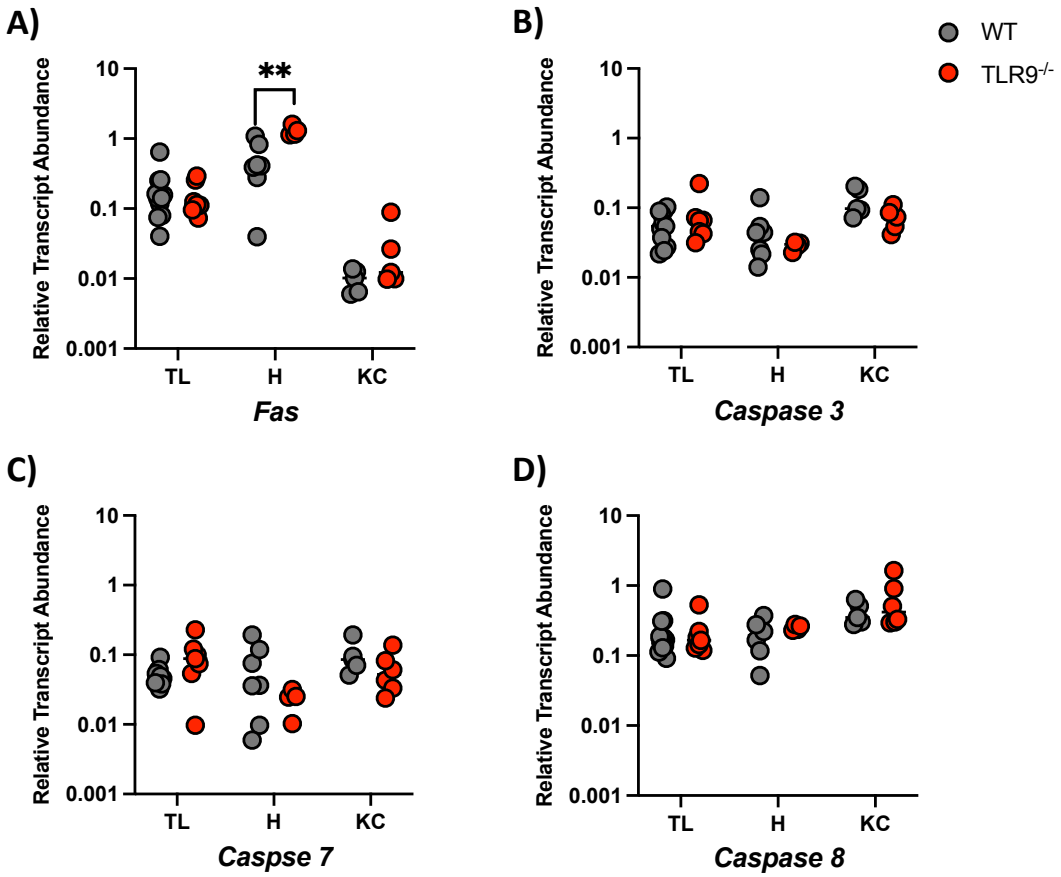

Fig 15 TLR9 deletion increases *Fas* gene expression and conserves apoptosis caspase gene expression in purified hepatocytes from uninjured livers. WT or TLR9$^{-/-}$ mouse livers were perfused, and RNA was extracted from whole liver tissue (TL), purified hepatocytes (H), and purified Kupffer cells (KC). mRNA gene expression relative to *Hprt* and *Gapdh* was quantified for A) *Fas*, B) *Caspase 3*, C) *Caspase 7*, and D) *Caspase 8*. (A-D) Data was pooled from 2 experiments (n = 3-5 mice per group). Significance between WT and TLR9$^{-/-}$ conditions for each cell population was determined by unpaired Welch t-test, ** = $p < 0.01$.

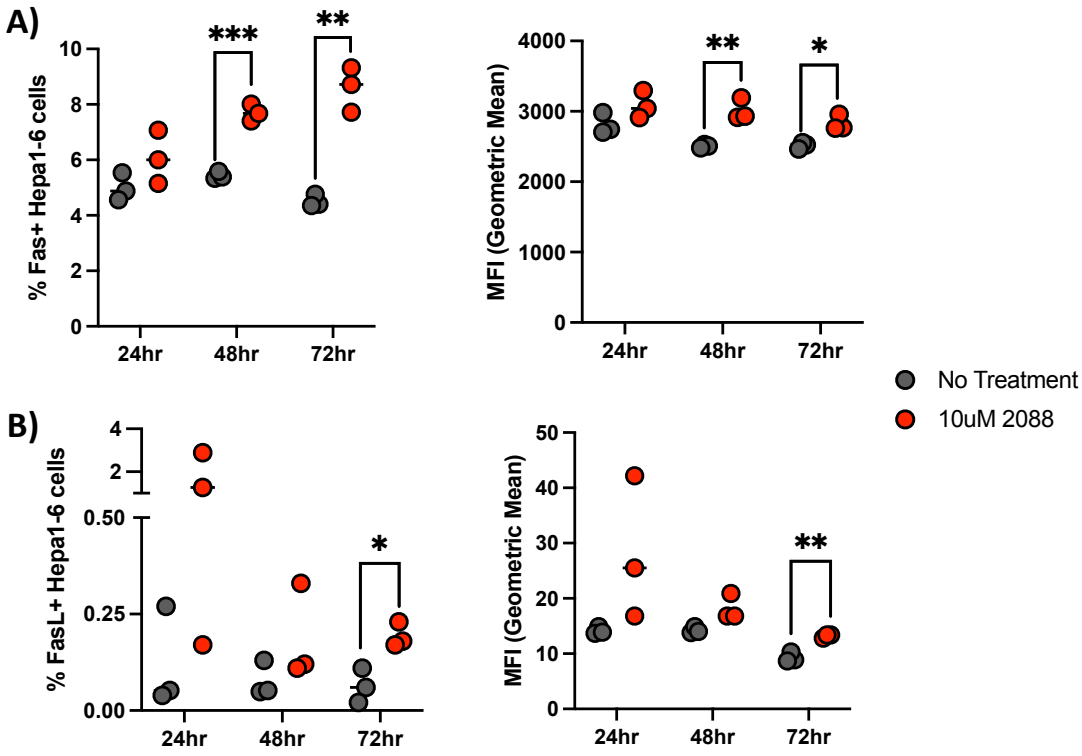

Fig 16 TLR9 inhibition increases surface expression of Fas and FasL over time in Hepa1-6 cells. 24-well plates were seeded with Hepa1-6 cells and then treated with vehicle (1X PBS) or 10uM TLR9 inhibitor (ODN 2088) the next day. At 24, 48, and 72 hours post-treatment, control and treated cells were trysponized, stained for Fas (A) or FasL (B), fixed, and analyzed by flow cytometry. Fas (A) and FasL (B) expression was characterized by both percent positively stained cells and fluorescence intensity within the positive cell populations for each condition. C) ***Next Page*** Dot plots representative of each condition show the proportion of Hepa1-6 cells that express FasL only (Q1), both FasL and Fas (Q2), Fas only (Q3), or do not express either Fas or FasL (Q4). (A-C) Data is from one pilot experiment (n = 3 per condition). Significance was determined with unpaired Welch t-test, * = $p < 0.05$, ** = $p < 0.01$, *** = $p < 0.001$.

C)

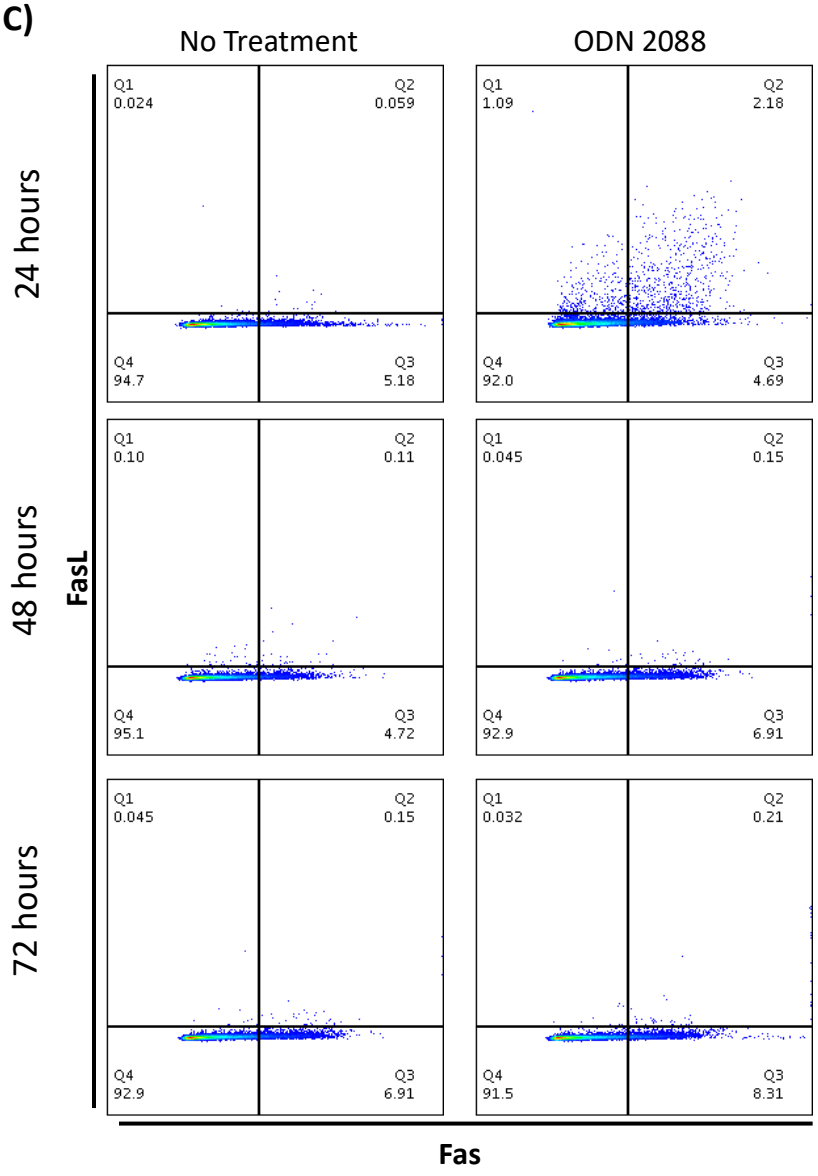
No Treatment
ODN 2088
24 hours
48 hours
72 hours
FasL
Fas
Q1 0.024
Q2 0.059
Q4 94.7
Q3 5.18
Q1 1.09
Q2 2.18
Q4 92.0
Q3 4.69
Q1 0.10
Q2 0.11
Q4 95.1
Q3 4.72
Q1 0.045
Q2 0.15
Q4 92.9
Q3 6.91
Q1 0.045
Q2 0.15
Q4 92.9
Q3 6.91
Q1 0.032
Q2 0.21
Q4 91.5
Q3 8.31

Discussion

Our data indicate that TLR9 is crucial for controlling liver injury following hepatocyte-specific killing with DT (Fig. 5), and that hepatocyte-specific TLR9 inhibition is sufficient to cause increased liver injury and cell death (Fig. 8). The increased hepatocyte death and injury at 48 hours post-DT did not correlate with increased inflammatory gene expression in the liver (Fig. 9). In fact, we observed suppression of inflammasome gene expression in $TLR9^{-/-}$ mice that was also described in a mouse model of APAP toxicity (Fig. 14)(29). Following a lethal dose of acetaminophen, mice lacking TLR9 were unable to activate the NLRP3 inflammasome and exhibited reduced liver injury which prolonged survival by several days(29). Even though TLR9 deletion led to similar impacts on the inflammasome in both models of liver injury, $TLR9^{-/-}$ mice experienced opposite pathological outcomes. The dose of APAP used was still able to cause liver failure in at least a portion of mice even when the inflammatory response is suppressed. On the other hand, DT-induced liver injury is non-lethal even with TLR9-dependent enhanced hepatotoxicity(29).

The opposing outcomes of TLR9 signaling in different sterile liver injury models could be influenced by cell-type specific TLR9 responses or acute vs. chronic TLR9 stimulation. In this study, purified hepatocytes from $TLR9^{-/-}$ untreated livers exhibited altered gene expression compared to WT hepatocytes amongst components of different cell death mechanisms (Figs. 11-15). TLR9 deletion in KCs, however, did not alter gene expression in these pathways when compared to WT KCs. This indicates that within the liver, TLR9 specifically regulates programmed cell death gene expression in hepatocytes. Previous work showed that liver injury was almost completely ablated in $TRIF^{-/-}$ mice at 48 hours post-DT administration, but only decreased by ~50% in $MyD88^{-/-}$ mice(7). MyD88 and TRIF are TIR-domain adapters that bind to TLRs, where TRIF interacts with TLR3 and TLR4 and MyD88 interacts with all TLRs

except for TLR3. It was therefore surprising that MyD88$^{-/-}$ only had a partial reduction in injury when the majority of TLR signaling was inhibited. When we consider the data from this study however, it is possible that loss of protective TLR9 signaling in hepatocytes promoted some of the liver injury in MyD88$^{-/-}$ mice even though the response to other TLR-specific DAMPs was restricted. In the chronic liver injury model NASH however, TLR9 promotes inflammation and tissue damage via IL-1β in nonparenchymal cell populations such as KCs and hepatic stellate cells(26, 27). This indicates that certain cell-type specific responses may predominate over others depending on acute versus chronic TLR9 stimulation.

Even in the absence of injury, we found that TLR9 controls Fas expression in hepatocytes. Purified hepatocytes from untreated TLR9$^{-/-}$ mice had a 2.5-fold increase in Fas gene expression compared to WT hepatocytes (Fig. 10B). TLR9 inhibition also induced increased surface Fas expression and cell death in Hepa1-6 cells over time (Fig 16). These results suggest that TLR9 prevents secondary hepatocyte death during acute, sterile liver injury by regulating Fas expression in hepatocytes. This is not the first observation of TLR9-dependent Fas regulation – TLR9 inhibition promotes sensitivity to Fas-mediated apoptosis in both human cervical cancer cells and B cells(36, 37). While further functional studies are required to determine if TLR9 deletion does increase Fas-dependent secondary hepatocyte death during DT-induced injury, our findings have several implications. First, the addition of TLR9 inhibitors to immunotherapies for hepatocellular carcinoma (HCC) may improve therapy efficacy by increasing sensitivity to Fas-mediated T cell killing and preventing immune escape(38). Conversely, the administration route for TLR9 inhibitors used to treat autoimmune diseases needs to be carefully considered. TLR9 inactivation drastically improves disease pathogenesis in psoriasis and Sjogren's syndrome, and several recent clinical trials target TLR9 to treat these diseases via daily oral medication(39). The oral administration route could result in active drug in the liver with the potential to

inhibit TLR9 in a large portion of hepatocytes. While this may not cause a problem when in an uninjured liver, even mild insults such as imbibing alcohol or acetaminophen may progress to severe liver injury if hepatocytes are sensitized to Fas-mediated apoptosis. For medications that are meant to be taken long-term therefore, emphasis should be placed on preventing TLR9 inhibition in hepatocytes.

In this study, we found a protective role for TLR9 during self-limiting sterile liver injury via hepatocyte-specific regulation of Fas-mediated apoptosis. These results show how hepatocytes influence the innate immune response to acute, moderate liver injury and create support for evaluating the immunological role of hepatocyte-specific TLR9 signaling in other liver diseases.

Chapter 3 References

1. Heymann F, Tacke F. Immunology in the liver--from homeostasis to disease. Nat Rev Gastroenterol Hepatol. 2016;13(2):88-110.
2. Zhou Z, Xu MJ, Gao B. Hepatocytes: a key cell type for innate immunity. Cell Mol Immunol. 2016;13(3):301-15.
3. Kubes P, Jenne C. Immune Responses in the Liver. Annu Rev Immunol. 2018;36:247-77.
4. Ju C, Tacke F. Hepatic macrophages in homeostasis and liver diseases: from pathogenesis to novel therapeutic strategies. Cell Mol Immunol. 2016;13(3):316-27.
5. Krenkel O, Tacke F. Liver macrophages in tissue homeostasis and disease. Nat Rev Immunol. 2017;17(5):306-21.
6. Crispe IN. Immune tolerance in liver disease. Hepatology. 2014;60(6):2109-17.
7. Brempelis KJ, Yuen SY, Schwarz N, Mohar I, Crispe IN. Central role of the TIR-domain-containing adaptor-inducing interferon-β (TRIF) adaptor protein in murine sterile liver injury. Hepatology. 2017;65(4):1336-51.
8. Crispe IN. Hepatocytes as Immunological Agents. J Immunol. 2016;196(1):17-21.
9. Brenner C, Galluzzi L, Kepp O, Kroemer G. Decoding cell death signals in liver inflammation. J Hepatol. 2013;59(3):583-94.
10. Yatim N, Jusforgues-Saklani H, Orozco S, Schulz O, Barreira da Silva R, Reis e Sousa C, et al. RIPK1 and NF-kappaB signaling in dying cells determines cross-priming of CD8(+) T cells. Science. 2015;350(6258):328-34.
11. Brempelis KJ, Crispe IN. Infiltrating monocytes in liver injury and repair. Clin Transl Immunology. 2016;5(11):e113.
12. Davies SP, Reynolds GM, Stamataki Z. Clearance of Apoptotic Cells by Tissue Epithelia: A Putative Role for Hepatocytes in Liver Efferocytosis. Front Immunol. 2018;9:44.
13. Davies SP, Terry LV, Wilkinson AL, Stamataki Z. Cell-in-Cell Structures in the Liver: A Tale of Four E's. Front Immunol. 2020;11:650.
14. Blander JM. A long-awaited merger of the pathways mediating host defence and programmed cell death. Nat Rev Immunol. 2014;14(9):601-18.
15. Crișan TO, Netea MG, Joosten LA. Innate immune memory: Implications for host responses to damage-associated molecular patterns. Eur J Immunol. 2016;46(4):817-28.
16. Gong T, Liu L, Jiang W, Zhou R. DAMP-sensing receptors in sterile inflammation and inflammatory diseases. Nat Rev Immunol. 2020;20(2):95-112.
17. Lamphier MS, Sirois CM, Verma A, Golenbock DT, Latz E. TLR9 and the recognition of self and non-self nucleic acids. Ann N Y Acad Sci. 2006;1082:31-43.
18. Akira S, Takeda K. Toll-like receptor signalling. Nat Rev Immunol. 2004;4(7):499-511.
19. Riley JS, Tait SW. Mitochondrial DNA in inflammation and immunity. EMBO Rep. 2020;21(4):e49799.
20. Ivanov S, Dragoi AM, Wang X, Dallacosta C, Louten J, Musco G, et al. A novel role for HMGB1 in TLR9-mediated inflammatory responses to CpG-DNA. Blood. 2007;110(6):1970-81.
21. Szabo G, Iracheta-Vellve A. Inflammasome activation in the liver: Focus on alcoholic and non-alcoholic steatohepatitis. Clin Res Hepatol Gastroenterol. 2015;39 Suppl 1:S18-23.
22. Shintani Y, Kapoor A, Kaneko M, Smolenski RT, D'Acquisto F, Coppen SR, et al. TLR9 mediates cellular protection by modulating energy metabolism in cardiomyocytes and neurons. Proc Natl Acad Sci U S A. 2013;110(13):5109-14.
23. Shintani Y, Drexler H, Kioka H, Terracciano C, Coppen S, Imamura H, et al. Toll-like receptor 9 protects non-immune cells from stress by modulating mitochondrial ATP synthesis through the inhibition of SERCA2. EMBO Reports. 2014;15(4):8.

Chapter 3 References, continued

24. Volpi C, Fallarino F, Pallotta MT, Bianchi R, Vacca C, Belladonna ML, et al. High doses of CpG oligodeoxynucleotides stimulate a tolerogenic TLR9-TRIF pathway. Nat Commun. 2013;4:1852.
25. Tilstra JS, John S, Gordon RA, Leibler C, Kashgarian M, Bastacky S, et al. B cell-intrinsic TLR9 expression is protective in murine lupus. J Clin Invest. 2020;130(6):3172-87.
26. Garcia-Martinez I, Santoro N, Chen Y, Hoque R, Ouyang X, Caprio S, et al. Hepatocyte mitochondrial DNA drives nonalcoholic steatohepatitis by activation of TLR9. J Clin Invest. 2016;126(3):859-64.
27. Miura K, Kodama Y, Inokuchi S, Schnabl B, Aoyama T, Ohnishi H, et al. Toll-like receptor 9 promotes steatohepatitis by induction of interleukin-1beta in mice. Gastroenterology. 2010;139(1):323-34.e7.
28. Mridha AR, Haczeyni F, Yeh MM, Haigh WG, Ioannou GN, Barn V, et al. TLR9 is up-regulated in human and murine NASH: pivotal role in inflammatory recruitment and cell survival. Clin Sci (Lond). 2017;131(16):2145-59.
29. Imaeda AB, Watanabe A, Sohail MA, Mahmood S, Mohamadnejad M, Sutterwala FS, et al. Acetaminophen-induced hepatotoxicity in mice is dependent on Tlr9 and the Nalp3 inflammasome. J Clin Invest. 2009;119(2):305-14.
30. Hao L, Zhong W, Sun X, Zhou Z. TLR9 Signaling Protects Alcohol-Induced Hepatic Oxidative Stress but Worsens Liver Inflammation in Mice. Front Pharmacol. 2021;12:709002.
31. Jeng KS, Lu SJ, Wang CH, Chang CF. Liver Fibrosis and Inflammation under the Control of ERK2. Int J Mol Sci. 2020;21(11).
32. Hu Z, Han Y, Liu Y, Zhao Z, Ma F, Cui A, et al. CREBZF as a Key Regulator of STAT3 Pathway in the Control of Liver Regeneration in Mice. Hepatology. 2020;71(4):1421-36.
33. Aroor AR, Jackson DE, Shukla SD. Elevated activation of ERK1 and ERK2 accompany enhanced liver injury following alcohol binge in chronically ethanol-fed rats. Alcohol Clin Exp Res. 2011;35(12):2128-38.
34. Klampfer L. Signal transducers and activators of transcription (STATs): Novel targets of chemopreventive and chemotherapeutic drugs. Curr Cancer Drug Targets. 2006;6(2):107-21.
35. Huang H, Chen HW, Evankovich J, Yan W, Rosborough BR, Nace GW, et al. Histones activate the NLRP3 inflammasome in Kupffer cells during sterile inflammatory liver injury. J Immunol. 2013;191(5):2665-79.
36. Wang L, Zhang S, Cai H, Qi Q, Zhang C, Qi Z, et al. Inhibition of TLR9 signaling stimulates apoptosis and cell cycle arrest and alleviates angiogenic property in human cervical cancer cells. Endocr Metab Immune Disord Drug Targets. 2021.
37. Hancz A, Koncz G, Szili D, Sármay G. TLR9-mediated signals rescue B-cells from Fas-induced apoptosis via inactivation of caspases. Immunol Lett. 2012;143(1):77-84.
38. Zhou B, Yan J, Guo L, Zhang B, Liu S, Yu M, et al. Hepatoma cell-intrinsic TLR9 activation induces immune escape through PD-L1 upregulation in hepatocellular carcinoma. Theranostics. 2020;10(14):6530-43.
39. Anwar MA, Shah M, Kim J, Choi S. Recent clinical trends in Toll-like receptor targeting therapeutics. Med Res Rev. 2019;39(3):1053-90.

Chapter 4 – Discussion of the caveats, challenges, alternate approaches, and future directions

Differentiating between DT-killed and neighboring hepatocyte contributions to liver inflammation

Challenges and Caveats

Our primary analysis of hepatocyte-specific responses for this model is gene expression. DT inhibits translation, not transcription – at earlier timepoints when DT-targeted hepatocytes are still alive, gene expression analysis is capturing their response as well as the neighboring hepatocyte response. This can confound our efforts to identify hepatocyte signaling pathways that contribute to the initial inflammatory response to hepatocyte death. Fortunately, TLR9 deletion has profound impacts on hepatocytes in uninjured livers, and this allowed us to use gene expression analysis to identify Fas-mediated apoptosis as a potential mechanism for exacerbated DT-induced injury in TLR9$^{-/-}$ mice. However, determining the distinct roles that DT-targeted hepatocytes and neighboring hepatocytes contribute to inflammation will require more than just gene expression analysis as we will need to compare their responses shortly after liver injury is initiated.

Multiple attempts were made to culture C57Bl/6J and TLR9$^{-/-}$ primary hepatocytes transduced with rAAV.hDTR.mCherry in order to distinguish between DT-killed and neighboring hepatocytes, however the hepatocytes did not survive past 36 hours post-perfusion in all cases. Additionally, even had *ex vivo* cultures been successful in our hands, proteomic analysis of primary hepatocyte cultures over time shows that they lose the ability to clarify surrounding cell debris via loss of Asialoglycoprotein receptor protein 2 (ASGR-2) and several complement system proteins (CFH, C3, and C4-B)(1). We think that hepatocyte clearance of cellular debris in the microenvironment is a crucial step in the hepatocyte contribution to inflammation caused by DT-killed hepatocytes. It is that inhibition of this process in primary hepatocyte cultures would yield inaccurate results.

Alternate Approaches and Future Direction

While there are many caveats associated with using transformed cell lines to characterize mechanisms identified in complex *in vivo* models of liver injury, there are also distinct advantages to *in vitro* hepatoma cell line experiments. For our purposes, utilizing hepatoma cell lines will allow us to distinguish between the responses of DT-targeted and neighboring cells more easily than in mice. While primary mouse hepatocytes lose essential characteristic shortly after culturing, the hepatoma cell line Hepa1-6 retains some aspects of *in vivo* mouse hepatocytes. The Hepa1-6 cell line originated from a C57Bl/6J mouse hepatocellular hepatoma, and maintains ASGR-2, CFH, and C3 expression in culture, albeit to a lesser extent than primary hepatocytes(1). Going forward we would utilize this cell line to screen for differences between DT-targeted and neighboring populations at the protein level to inform the experimental design of the more complicated and time-consuming mouse model. This includes probing the effects of increased Fas expression, inflammasome inhibition, and potential changes in stress tolerance we observed in $TLR9^{-/-}$ hepatocytes (Ch 3).

Previous work found that TRIF and MyD88 are required for the liver to mount an inflammatory response to DT-killed hepatocytes, yet the current data indicates that TLR3 and TLR4 are not required to initiate acute liver inflammation, and TLR9 restricts liver injury (Ch. 3)(2). To really understand how neighboring hepatocytes and nonparenchymal cells are initiating inflammation in response to hepatocyte death, we need to characterize the potential DAMPs that are released from DT-targeted hepatocytes. This is another way that *in vitro* experiments with hepatoma cell lines will prove useful. We have already optimized DT killing in the human hepatoma cell line Huh7 and could probe for specific DAMPs released into the supernatant. Then we can determine whether any of these DAMPs stimulate TLR2, TLR5, or TLR7 signaling in neighboring hepatocytes and/or nonparenchymal cell populations and. However, if none of these TLRs are responsible for initiating TRIF- and MyD88-dependent responses, we will need to

examine other potential mechanisms by which TRIF and MyD88 are mediating liver inflammation and injury.

The hepatoprotective mechanism of TLR9 signaling

Challenges and Caveats

While we were able to run a pilot experiment in mice that had hepatocyte-specific TLR9 deletion, the time involved in generating these mice was a multi-year process and thus precluded them from being utilized to their intended extent in this project. Additionally, the global impact on gene expression in uninjured TLR9$^{-/-}$ hepatocytes, particularly in genes associated with the inflammasome, generated multiple hypotheses for potential hepatoprotective mechanisms that masked significance of the moderate increase in *Fas* gene expression.

Once we did form the hypothesis that TLR9 deletion increased hepatocyte susceptibility to Fas-mediated cell death, we aimed to test this mechanism in mice and cell culture. We had planned a pilot experiment to treat WT and TLR9$^{-/-}$ mice with a sub-lethal dose of Jo2 and determine whether TLR9$^{-/-}$ livers exhibited greater injury. Unfortunately, project time constraints clashed with the time required for IACUC protocol approval and this experiment was not performed. *In vitro* attempts to determine whether hepatocyte-specific increased *Fas* gene expression in TLR9$^{-/-}$ mice was the cause of increased *in vivo* liver injury gave mixed results. In hepatocytes, Fas predominantly localizes at the Golgi complex with low levels on the plasma membrane. However different stimuli, such as bile acid or increased FasL, can induce transport of Fas to the cell surface(3). TLR9 inhibitor treatment, but not control ODN, led to increased Fas and FasL surface expression in Hepa1-6 cells. This suggests that TLR9 inhibition is one such stimuli that induces transport of Fas to the cell surface in hepatocytes.

Despite the increase in Fas surface expression, attempts to induce Fas-mediated apoptosis using either Jo2 or FasL with cross-linking antibodies were unsuccessful. This may be due to cell line resistance to apoptosis from Fas activation alone(4). Strategies employed by other groups to induce Fas-mediated apoptosis in hepatoma cell lines include the addition of gene or protein synthesis inhibitors or co-cultures with cells overexpressing FasL(4). Both options produce additional variables that may prevent accurate interpretation of TLR9-depenedent Fas regulation. In a pilot experiment, we showed that treating Hepa1-6 cells with the TLR9 inhibitor ODN 2088 for 72 hours increased spontaneous cell death compared to cells treated with the ODN 2088 negative control. Our marker of cell death in this experiment was a permeability dye rather than quantification of apoptosis caspase activation. This meant that we could not definitively show TLR9 inhibition caused Fas-mediated apoptosis, although the increased Fas and FasL surface expression in ODN 2088-treated Hepa1-6 cells does strongly suggest this is the mechanism (Ch. 3).

Alternate Approaches and Future Directions

While the challenges with specifically activating extrinsic apoptosis in cell lines discussed above still apply, our observation that TLR9 inhibition results in increased cell death does provide a few options to probe the relationship between TLR9 and Fas in Hepa1-6 cells. The first option would be to determine if TLR9 inhibition induces Caspase 3 and/or Caspase 8 cleavage, as this would be indicative of the apoptotic pathway being activated even if the cells themselves have not yet died. An alternative strategy would be to determine if the addition of a pan-caspase inhibitor reverses cell death induced by TLR9-inhibition.

It will also be important to proceed with the previously planned Jo2 mouse experiment described earlier in this section. We would expect sub-lethal or even sub-clinical doses of Jo2 will result in significantly

increased liver injury in TLR9$^{-/-}$ mice. If this hypothesis is supported, we would then proceed to reverse the increased hepatocyte death in TLR9$^{-/-}$ or Hep$^{\Delta TLR9}$ mice during DT-induced liver injury with either a Fas inhibitor or pan-caspase inhibitor.

Discussion and Future Directions

In several mouse models discussed in Chapter 1, TLR9 promotes neutrophil-mediated immune aggravation of the initial hepatotoxic insult (Table 3) (5-10). Neutrophils do not contribute to liver injury in the DTR model and may be why TLR9 signaling exerts protective effects during the inflammatory response to hepatocyte death(2). The different mechanisms of acute liver injury between these models could also dictate whether TLR9 promotes hepatocyte survival or aggravates leukocyte inflammatory immune responses (Table 3). Hepatotoxicity is ROS-mediated in APAP and IRI liver injury, whereas DT-induced hepatotoxicity is due to protein synthesis inhibition(4, 8, 11-13). APAP treatment often results in liver failure and animal death while DT-induced liver injury is self-limited. APAP induces ~30% hepatocyte necrosis in C57Bl/6J mice, and DT-induced liver injury induces 10-20% hepatocyte death in mice with a C57Bl/6J background(2, 14). Taken together with different hepatotoxicity mechanisms for each model, this suggests that the outcome of hepatotoxic liver injury in mice is heavily influenced by different types of hepatocyte death. Each mechanism of cell death releases a different milieu of DAMPs into the liver which would then influence the innate immune inflammatory response due to different combinations of DAMP-PRR interactions.

Table 3 – The Alternate Roles of TLR9 in Liver Injury Animal Models

	Acetaminophen (APAP)	Ischemia Reperfusion Injury	Con A	Chronic + Binge Ethanol (NIAAA)	DTR
Model Purpose	Tylenol Overdose	Liver injury from surgeries and transplant donor grafts	Autoimmune hepatitis	Alcohol-induced liver injury	Hepatocyte DAMP-induced liver inflammation
DAMP Source	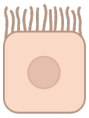 Hepatocytes	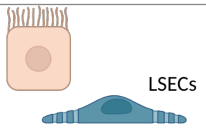 LSECs	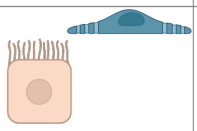	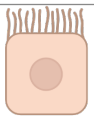	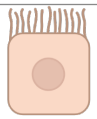
Injury Outcome	Liver failure caused by hemorrhage-induced hypovolemic shock	Injury in 70% of the liver, euthanized shortly after reperfusion stage	Liver failure caused by hemorrhage-induced hypovolemic shock	Steatosis, non-lethal	20% hepatocyte death, Injury resolves by 96 hours post-DT
Injury Mechanism	**Direct Damage:** NAPQI-induced protein adducts damage mitochondria and induce necrosis **Immune Damage:** Neutrophils, NKT, and NK cells	**Direct Damage:** Ischemia depletes ATP, reperfusion induces ROS production **Immune Damage:** Neutrophils, TNFα, IL1β, IL12	**Direct Damage:** LSEC membrane breakdown and detachment **Immune Damage:** TNFα and IFNγ produced by CD4+ T cells	**Direct Damage:** acetaldehyde-induced protein adducts damage DNA and cause ER stress **Immune Damage:** BM-macrophage IL1β secretion and TLR4 pro-inflammatory response	**Direct Damage:** DT-induced protein synthesis inhibition **Immune Damage:** Mediated by TRIF and MyD88
Effects of TLR9 Inhibition	**Increased** Mouse survival **Decreased** Liver injury, inflammasome activation and secretion of IL1β by LSECs	**Decreased** Liver injury, IL6, TNFα, CCL2 serum levels, neutrophil ROS production	**Increased** Mouse survival **Decreased** Liver injury, neutrophil infiltration, MMP8 secretion, p38 pathway	**Increased** Liver injury, cl-caspase-3, Bim, ROS production, steatosis **Decreased** STAT3-mediated neutrophil recruitment	**Increased** Liver injury, steatosis, Hepatocyte Fas and FasL **Decreased** Hepatocyte inflammasome, necroptosis, and BH3 genes

DAMPs released by simultaneous necrosis and apoptosis may alter the inflammatory response such that live failure is prevented in TLR9$^{-/-}$ mice for several ROS-mediated hepatotoxicity models. In particular, the protective effects of TLR9 deletion in APAP-induced liver injury would be due, in part, to a change in the DAMP-induced innate immune response with the addition of Fas-mediated hepatocyte death. I would test this hypothesis in two ways. First, I would compare APAP-induced liver injury in TLR9$^{-/-}$ mice with and without the addition of a Caspase 3 inhibitor. Caspase inhibitors do not impact hepatotoxicity in the APAP model, and the use of a Caspase 3-specific inhibitor should not interfere with inflammasome activation. If my hypothesis is supported, I would expect that APAP-induced liver injury in TLR9$^{-/-}$ mice treated with the Caspase 3 inhibitor would be restored to WT (C57Bl/6J) pathology. Another approach would be to simultaneously treat WT mice with APAP and Jo2, which would result in decreased liver injury if my hypothesis were supported.

Clinically, the inflammatory response in patients presenting with APAP-induced liver injury would likely be too far progressed to benefit from apoptosis-derived DAMPs induced by TLR9 inhibitor treatment. However, not all causes of acute liver injury and failure in humans are due to ROS-mediated hepatotoxicity. It is critical to understand how each cell death mechanism influences liver pathology because these differences may determine whether a patient is able to resolve acute liver injury or progresses to acute liver failure. To that end, we need to determine whether the level of hepatocyte death in TLR9$^{-/-}$ mice during DT-induced injury surpasses the regeneration threshold of the mouse liver. We will need to monitor DT-induced liver pathology in TLR9$^{-/-}$ mice over time until injury is resolved. It is also possible that the exacerbated hepatotoxicity is irreversible in TLR9$^{-/-}$ mice and leads to liver failure due to hypovolemic shock and hemorrhage like the Fas mouse model of liver injury(4).

The data presented in this thesis suggests that TLR9 promotes hepatocyte survival during DT-induced liver injury by suppressing Fas-mediated apoptosis. TLR9 signaling is predominantly considered to exclusively promote a pro-inflammatory response during sterile or pathogenic tissue damage(5, 15-19). Recent studies have described protective functions of TLR9, including promoting cell survival and regulating Fas expression(20-23). In non-immune cells, TLR9 pro-survival effects have previously been described in terminally differentiated cell populations, prompting the hypothesis that TLR9 protects against stressors only in cells that cannot regenerate(21). However, the hepatocyte-specific TLR9 function described in this thesis expands the reach of cell types protected by TLR9 signaling to include non-immune cells that frequently regenerate.

Chapter 4 References

1. Azimifar SB, Nagaraj N, Cox J, Mann M. Cell-type-resolved quantitative proteomics of murine liver. Cell Metab. 2014;20(6):1076-87.
2. Brempelis KJ, Yuen SY, Schwarz N, Mohar I, Crispe IN. Central role of the TIR-domain-containing adaptor-inducing interferon-β (TRIF) adaptor protein in murine sterile liver injury. Hepatology. 2017;65(4):1336-51.
3. Malhi H, Gores GJ, Lemasters JJ. Apoptosis and necrosis in the liver: a tale of two deaths? Hepatology. 2006;43(2 Suppl 1):S31-44.
4. Maes M, Vinken M, Jaeschke H. Experimental models of hepatotoxicity related to acute liver failure. Toxicol Appl Pharmacol. 2016;290:86-97.
5. He Y, Feng D, Li M, Gao Y, Ramirez T, Cao H, et al. Hepatic mitochondrial DNA/Toll-like receptor 9/MicroRNA-223 forms a negative feedback loop to limit neutrophil overactivation and acetaminophen hepatotoxicity in mice. Hepatology. 2017;66(1):220-34.
6. Imaeda AB, Watanabe A, Sohail MA, Mahmood S, Mohamadnejad M, Sutterwala FS, et al. Acetaminophen-induced hepatotoxicity in mice is dependent on Tlr9 and the Nalp3 inflammasome. J Clin Invest. 2009;119(2):305-14.
7. Kiziltas S. Toll-like receptors in pathophysiology of liver diseases. World J Hepatol. 2016;8(32):1354-69.
8. Datta G, Fuller BJ, Davidson BR. Molecular mechanisms of liver ischemia reperfusion injury: insights from transgenic knockout models. World J Gastroenterol. 2013;19(11):1683-98.
9. Chang WJ, Toledo-Pereyra LH. Toll-like receptor signaling in liver ischemia and reperfusion. J Invest Surg. 2012;25(4):271-7.
10. Liu X, Yu T, Hu Y, Zhang L, Zheng J, Wei X. The molecular mechanism of acute liver injury and inflammatory response induced by Concanavalin A. Mol Biomed. 2021;2(1):24.
11. Mateyak MK, Kinzy TG. ADP-ribosylation of translation elongation factor 2 by diphtheria toxin in yeast inhibits translation and cell separation. J Biol Chem. 2013;288(34):24647-55.
12. Murphy JR. Mechanism of diphtheria toxin catalytic domain delivery to the eukaryotic cell cytosol and the cellular factors that directly participate in the process. Toxins (Basel). 2011;3(3):294-308.
13. Morimoto H, Bonavida B. Diphtheria toxin- and Pseudomonas A toxin-mediated apoptosis. ADP ribosylation of elongation factor-2 is required for DNA fragmentation and cell lysis and synergy with tumor necrosis factor-alpha. J Immunol. 1992;149(6):2089-94.
14. Harrill AH, Ross PK, Gatti DM, Threadgill DW, Rusyn I. Population-based discovery of toxicogenomics biomarkers for hepatotoxicity using a laboratory strain diversity panel. Toxicol Sci. 2009;110(1):235-43.
15. Alzahrani B, A AMA, Tantawy A. Therapeutic Impact of ODN2088 to Block TLR9 Activity in Induced Liver Fibrosis Mice. Pak J Biol Sci. 2021;24(1):122-31.
16. Garcia-Martinez I, Santoro N, Chen Y, Hoque R, Ouyang X, Caprio S, et al. Hepatocyte mitochondrial DNA drives nonalcoholic steatohepatitis by activation of TLR9. J Clin Invest. 2016;126(3):859-64.
17. Ma C, Ouyang Q, Huang Z, Chen X, Lin Y, Hu W, et al. Toll-Like Receptor 9 Inactivation Alleviated Atherosclerotic Progression and Inhibited Macrophage Polarized to M1 Phenotype in ApoE-/- Mice. Dis Markers. 2015;2015:909572.
18. Huang H, Chen HW, Evankovich J, Yan W, Rosborough BR, Nace GW, et al. Histones activate the NLRP3 inflammasome in Kupffer cells during sterile inflammatory liver injury. J Immunol. 2013;191(5):2665-79.
19. Żeromski J, Kierepa A, Brzezicha B, Kowala-Piaskowska A, Mozer-Lisewska I. Pattern Recognition Receptors: Significance of Expression in the Liver. Arch Immunol Ther Exp (Warsz). 2020;68(5):29.

Chapter 4 References, continued

20. Hancz A, Koncz G, Szili D, Sármay G. TLR9-mediated signals rescue B-cells from Fas-induced apoptosis via inactivation of caspases. Immunol Lett. 2012;143(1):77-84.
21. Shintani Y, Kapoor A, Kaneko M, Smolenski R, D'Acquisto F, Coppen S, et al. TLR9 mediates cellular protection by modulating energy metabolism in cardiomyocytes and neurons. PNAS. 2013;110(13):6.
22. Tilstra JS, John S, Gordon RA, Leibler C, Kashgarian M, Bastacky S, et al. B cell-intrinsic TLR9 expression is protective in murine lupus. J Clin Invest. 2020;130(6):3172-87.
23. Wang L, Zhang S, Cai H, Qi Q, Zhang C, Qi Z, et al. Inhibition of TLR9 signaling stimulates apoptosis and cell cycle arrest and alleviates angiogenic property in human cervical cancer cells. Endocr Metab Immune Disord Drug Targets. 2021.

Appendix 1 – TLR9 deletion and chemokine gene expression in the liver

Introduction

A hallmark of acute liver inflammation is infiltration of neutrophils and monocytes into the liver early in the injury response(1-4). Hepatocytes, KC, LSECs, and other liver cell populations recruit leukocytes to the site of liver injury via chemokine secretion that forms a concentration gradient. Chemokine gene expression is increased upon pro-inflammatory stimuli such as cytokine production induced by DAMP-PRR interactions. In DT-induced liver injury, gene expression of the chemokines *Ccl2*, *Ccl5*, *Ccl7*, *Cxcl1*, *Cxcl2*, and *Cxcl10* increase significantly after DT administration(1). Of these, the C-C chemokines recruit monocytes, and the C-X-C chemokines recruit neutrophils. While monocyte and neutrophil infiltration during DT-induced liver injury does not contribute to pro-inflammatory liver damage, leukocyte infiltration does play a crucial role in other models of acute sterile liver injury(5-8). Therefore, part of our evaluation of the effects of TLR9 deletion on DT-induced liver injury included comparing chemokine gene expression in total liver, KC, and hepatocytes.

Results and Discussion

We quantified gene expression of the C-C chemokines *Ccl2*, *Ccl5*, *Ccl7*, and C-X-C chemokines *Cxcl1*, *Cxcl2*, and *Cxcl10* at 16 hours and 48 hours post-DT administration for total liver, KC, and hepatocytes. *Ccl2* gene expression in WT total liver increased at 48 hours compared to both the control and 16 hour post-DT conditions, however there was no change in *Ccl2* gene expression in TLR9$^{-/-}$ livers at either 16 hours or 48 hours post-DT (Fig. 17A). Additionally, *Ccl2* gene expression was increased in TLR9$^{-/-}$ total liver controls compared to WT controls (biological trend), but this effect was not exhibited by either TLR9$^{-/-}$ KC or hepatocyte controls (Fig. 17B and C). This suggests that in the absence of TLR9, another cell population is responsible for the increased *Ccl2* gene expression we observed in the liver. Despite the

apparent absence of a *Ccl2* gradient induced in response to liver injury in the whole liver, myeloid infiltration was not impaired in TLR9$^{-/-}$ mice at either 16 hours or 48 hours post-DT (Fig. 9). Purified TLR9$^{-/-}$ hepatocytes did increase *Ccl2* gene expression at both times post-DT, however (Fig. 17C). This suggests that hepatocyte *Ccl2* gene expression dictates myeloid cell infiltration during DT-induced liver injury.

On the other hand, *Ccl5* gene expression was increased in TLR9$^{-/-}$ hepatocyte controls compared to WT hepatocytes (Fig. 17F). The difference in *Ccl5* gene expression between TLR9$^{-/-}$ and WT hepatocytes remained significant until 48 hours post-DT. We were unable to determine whether *Ccl5* gene expression was also increased in TLR9$^{-/-}$ total liver controls compared to WT because the gene expression in the TLR9$^{-/-}$ samples splits into two groups of relative transcript abundance (Fig. 17D). While the data represented in these graphs are pooled from two experiments, each grouping of *Ccl5* relative transcript abundance in the TLR9$^{-/-}$ total liver control condition includes samples from both experiments. CCL5 recruits several different immune cell populations including monocytes, however the absence of a gradient induced by liver injury in TLR9$^{-/-}$ hepatocytes did not prevent monocyte recruitment to the liver (Fig. 17F and Fig 9).

Similar to *Ccl2* gene expression, *Ccl7* was increased in the TLR9$^{-/-}$ total liver controls compared to WT, although this was a biological trend and not statistically significant (Fig. 17G). TLR9 deletion in hepatocytes did not increase *Ccl7* expression in controls compared to WT, and both WT and TLR9$^{-/-}$ hepatocytes induced *Ccl7* gene expression in response to liver injury at both 16 hours and 48 hours post-DT (Fig. 17I). Surprisingly, TLR9 deletion completely altered *Ccl7* gene expression in KCs. WT KCs decrease *Ccl7* gene expression almost 100-fold by 48 hours post-DT, whereas TLR9$^{-/-}$ KCs increase *Ccl7* gene expression 16 hours post-DT and maintain this increase 48 hours post-DT (Fig. 17H).

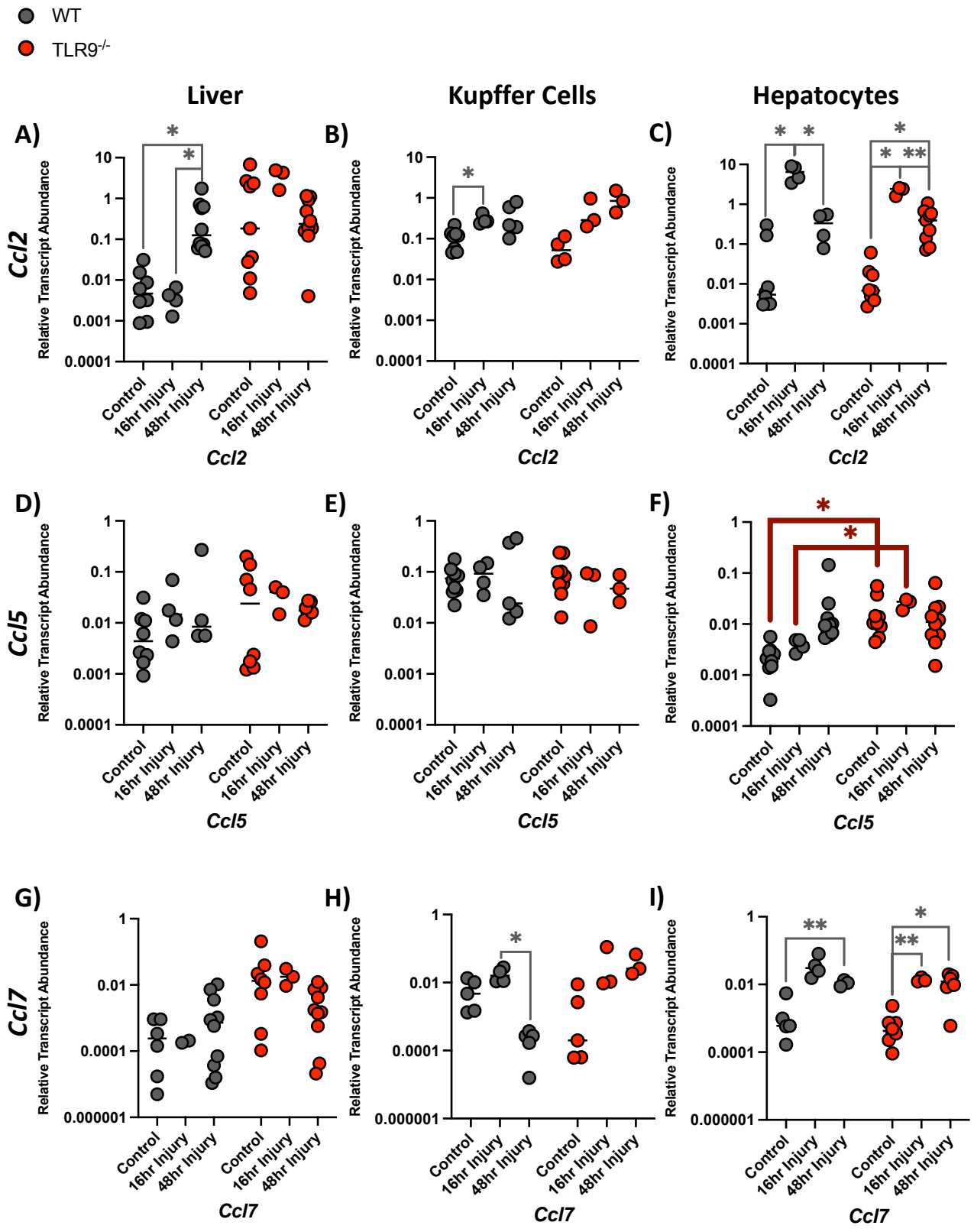
WT
TLR9-/-
Liver
Kupffer Cells
Hepatocytes
A)
B)
C)
D)
E)
F)
G)
H)
I)
Ccl2
Ccl5
Ccl7
Relative Transcript Abundance
Control
16hr Injury
48hr Injury

Fig 17. Cell population-specific C-C chemokine gene expression with and without TLR9 at 16 hours and 48 hours post-DT. WT and TLR9$^{-/-}$ mice were injected (r.o.) with 5 x 10^{9} viral genomes of rAAV.mCherry.hDTR or PBS (control mice). After two weeks, mice were injected (i.p.) with 20ng DT and were sacrificed 16 hours or 48 hours later. RNA was extracted from whole liver, purified hepatocytes, and purified Kupffer cells and gene expression of A-C) *Ccl2*, D-F) *Ccl5, G-I*) *Ccl7* relative to *Hprt* and *Gapdh* was assessed for each group. The data is pooled from two experiments (n = 3-5 per group in each experiment). Significance determined by unpaired Welch t-test for the following comparisons: Control vs 16hr Injury, Control vs 48hr Injury, 16hr Injury vs 48hr Injury in WT or TLR9$^{-/-}$ mice (gray statistics); WT vs TLR9$^{-/-}$ in the Control, 16hr Injury, or 48hr Injury conditions (red statistics). * = p <0.05, ** = p < 0.01, *** = p < 0.001. *Note: Hepatocyte C-C chemokine gene expression at 16hr and 48hr post-DT was first discussed in Chapter 3 Fi. 3. These graphs are also displayed here for ease of interpreting data only and are not being presented as new data.*

Cxcl1 and *Cxcl2* gene expression was increased in TLR9$^{-/-}$ livers compared to WT, either 16 hours post-DT or in the control groups (Fig. 18A and 18D, respectively). In WT livers DT-induced liver injury promoted an increase in *Cxcl1* and *Cxcl2* gene expression by 48 hours post-DT compared to the control condition, however neither of these genes increased following DT administration in TLR9$^{-/-}$ livers (Fig. 18A and D). TLR9 deletion in hepatocytes did not prevent increased *Cxcl1* and *Cxcl2* gene expression in response to DT-induced liver injury (Fig. 18C). WT KC decreased *Cxcl2* gene expression by 48 hours post-DT, however TLR9 deletion in KC results in increased *Cxcl2* gene expression 48 hours post-DT (Fig. 18E, biological trend only).

TLR9 deletion resulted in increased *Cxcl10* gene expression by both total liver and hepatocytes 16 hours post DT compared to WT (Fig. 18G and I). While *Cxcl10* gene expression in TLR9$^{-/-}$ hepatocyte controls did not differ, it is unclear whether the same is true for total liver due to the wide range in gene expression in the TLR9$^{-/-}$ control group (Fig. 18G and I). WT KCs showed increased *Cxcl10* gene expression 16 hours post-DT that returned to basal levels by 48 hours, however KC lacking TLR9 retained elevated *Cxcl10* gene expression at 48 hours post-DT (Fig. 18H).

TLR9 deletion did not decrease myeloid or neutrophil infiltration into the liver during DT-induced liver injury even though livers lacking TLR9 did not increase gene expression of *Ccl2*, *Ccl7*, *Cxcl1*, or *Cxcl2* compared to controls (Fig. 6 and Figs. 17A, 17G, 18A, and 18G). Conversely, TLR9 deletion did not prevent hepatocytes from increasing gene expression of *Ccl2*, *Ccl7*, *Cxcl1*, and *Cxcl2* following DT administration. (Figs. 17C, 17I, 18C, and 18I). This suggests that hepatocytes dictate myeloid cell and neutrophil recruitment during DT-induced liver injury. Basal levels of *Ccl2*, *Ccl7*, *Cxcl1*, and *Cxcl2* gene expression were increased compared to WT in TLR9$^{-/-}$total liver but not hepatocytes or KC (Figs. 17 and 18). This suggests TLR9 deletion is increasing chemokine expression in other liver cell populations in the

absence of injury, such as LSECs. And finally, hepatocytes are the most abundant cell in the liver, yet the chemokine gene expression changes in total liver tissue did not mimic the hepatocyte response to liver injury even in WT mice. These results caution against exclusively assessing total liver gene expression to fully describe the impact of TLR9 deletion during an inflammatory response.

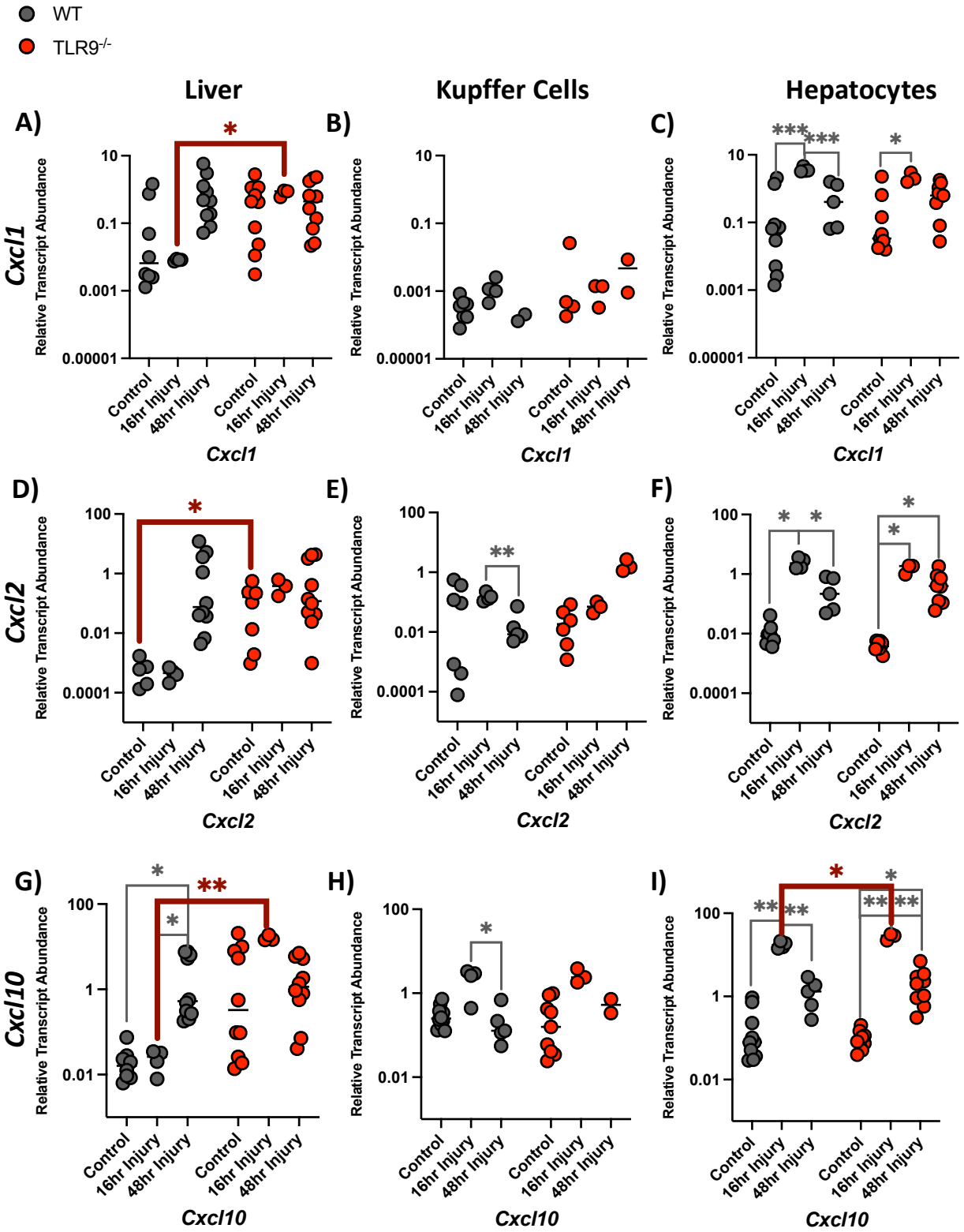
WT
TLR9-/-
Liver
Kupffer Cells
Hepatocytes
A)
B)
C)
D)
E)
F)
G)
H)
I)
Cxcl1
Cxcl2
Cxcl10
Relative Transcript Abundance
Control
16hr Injury
48hr Injury

Fig 18. Cell population-specific C-X-C chemokine gene expression with and without TLR9 at 16 hours and 48 hours post-DT. WT and TLR9$^{-/-}$ mice were injected (r.o.) with 5 x 10^9 viral genomes of rAAV.mCherry.hDTR or PBS (control mice). After two weeks, mice were injected (i.p.) with 20ng DT and were sacrificed 16 hours or 48 hours later. RNA was extracted from whole liver, purified hepatocytes, and purified Kupffer cells and gene expression of A) *Cxcl1*, B) *Cxcl2,* C) *Cxcl10* relative to *Hprt* and *Gapdh* was assessed for each group. The data is representative of two experiments (n = 3-5 per group in each experiment). Significance determined by unpaired Welch t-test for the following comparisons: Control vs 16hr Injury, Control vs 48hr Injury, 16hr Injury vs 48hr Injury in WT or TLR9$^{-/-}$ mice (**gray statistics**); WT vs TLR9$^{-/-}$ in the Control, 16hr Injury, or 48hr Injury conditions (**red statistics**). NS = not significant, * = p <0.05, ** = p < 0.01, *** = p < 0.001. *Note: Hepatocyte C-X-C chemokine gene expression was first discussed in Chapter 3 Fi. 3. These graphs are also displayed here for ease of interpreting data and are not being presented as new data.*

Appendix 1 References

1. Brempelis KJ, Yuen SY, Schwarz N, Mohar I, Crispe IN. Central role of the TIR-domain-containing adaptor-inducing interferon-β (TRIF) adaptor protein in murine sterile liver injury. Hepatology. 2017;65(4):1336-51.
2. Cao S, Liu M, Sehrawat TS, Shah VH. Regulation and functional roles of chemokines in liver diseases. Nat Rev Gastroenterol Hepatol. 2021;18(9):630-47.
3. Marra F, Tacke F. Roles for chemokines in liver disease. Gastroenterology. 2014;147(3):577-94.e1.
4. Marques PE, Amaral SS, Pires DA, Nogueira LL, Soriani FM, Lima BH, et al. Chemokines and mitochondrial products activate neutrophils to amplify organ injury during mouse acute liver failure. Hepatology. 2012;56(5):1971-82.
5. Imaeda AB, Watanabe A, Sohail MA, Mahmood S, Mohamadnejad M, Sutterwala FS, et al. Acetaminophen-induced hepatotoxicity in mice is dependent on Tlr9 and the Nalp3 inflammasome. J Clin Invest. 2009;119(2):305-14.
6. Maes M, Vinken M, Jaeschke H. Experimental models of hepatotoxicity related to acute liver failure. Toxicol Appl Pharmacol. 2016;290:86-97.
7. McGill MR, Jaeschke H. Animal models of drug-induced liver injury. Biochim Biophys Acta Mol Basis Dis. 2019;1865(5):1031-9.
8. McGill MR, Jaeschke H. Mechanistic biomarkers in acetaminophen-induced hepatotoxicity and acute liver failure: from preclinical models to patients. Expert Opin Drug Metab Toxicol. 2014;10(7):1005-17.

Appendix 2 – The effects of Silymarin treatment on DT-induced liver injury and inflammation

Introduction

Silymarin is an extract from *Silybum marianum*, commonly known as milk thistle, and is one of the oldest plants used to treat various liver diseases ranging from acute *Amanita* mushroom poisoning to cirrhosis(1-3). The active component of silymarin is the flavonolignan silybin, which exerts a wide range of anti-inflammatory, anti-oxidant, and cell regeneration effects in the liver(2, 4, 5). Pre-treatment with Silymarin protects against APAP-mediated liver injury in mice, without preventing NAPQI metabolism, due to both its ROS scavenging ability and inhibition of JNK phosphorylation(5). Additionally, Silymarin inhibits pro-inflammatory cytokine and chemokine production in the human hepatoma cell line Huh7(4). We therefore hypothesized that Silymarin would ameliorate injury and inflammation in our model of DT-induced liver injury.

Results and Discussion

To determine if Silymarin treatment would decrease injury or inflammation following hepatocyte-specific death, we tested two different doses of oral Silymarin treatment in our DT-induced liver injury model. C57Bl/6J mice were injected with rAAV.mCherry.hDTR two weeks prior to initiation of liver injury with DT. Mice received two oral gavage treatments of either vehicle, 100mg/kg Silymarin, or 300mg/kg Silymarin on the same day as DT injection and 24 hours post-DT. There was no difference in liver injury Serum ALT activity was quantified 48 hours post-DT and showed no difference in liver injury with either dose of Silymarin (Fig. 19A). However, serum ALT activity was decreased in the control mice (1X PBS + DT) treated with 300mg/kg Silymarin (Fig. 19B). We find that control mice who receive DT without the DTR vector experience mild, non-DTR-specific liver injury with ALT activity usually between 100-300 IU/L (empirical observation). The mechanism of DTR-independent mild liver injury induced by DT is unknown

but could be due to either hepatotoxic effects from ASGR2-mediated endocytosis, or DT recognition by a PRR resulting in mild inflammation. These results show that the highest dose of Silymarin reduces minor DTR-independent liver injury caused by DT, but not the greater injury due to DTR-dependent hepatocyte death.

We also quantified whole liver gene expression from mice treated with vehicle only, 100mg/kg Silymarin, and 300mg/kg Silymarin injured mice and no injury vehicle-treated mice. Due to experiment size and initial goals of the experiment, we did not assess gene expression in control mice receiving either dose of Silymarin treatment. Silymarin treatment moderately reduced *Ccl25*, *Cxcl1*, and *Cxcl2* chemokine gene expression in the liver (Fig. 20F, G, and H). Decreased *Cxcl1* and *Cxcl2* gene expression may impair neutrophil recruitment to the liver, suggesting that Silymarin treatment would be more effective at reducing injury in neutrophil-dependent acute liver injury models.

In addition to *Cxcl1* and *Cxcl2* gene expression, 100mg/kg Silymarin treatment also reduced *Tlr11* gene expression (Fig. 22F). Mice treated with the 300mg/kg dose exhibited decreased *Caspase 1* (Fig. 21B), *Il1b* (Fig. 21D), *Socs2* (Fig. 21B), and *Vcam1* (Fig. 27B) gene expression, and increased *Atg7* gene expression (Fig. 24B). Both doses of Silymarin decreased *Irf3* gene expression (Fig. 23F). Silymarin treatment did not impact gene expression of pro-apoptotic *Bid* or pro-survival *Bcl2*, in contrast to a previous finding where treatment promoted BH3-mediated apoptosis (Fig. 25)(6).When these effects on gene expression are taken together, the overall impact of Silymarin treatment is anti-inflammatory (Table 4). However, the decrease in these inflammatory genes did not reduce serum ALT levels in either treatment group. There are two potential reasons for this. First, the genes that are targeted by Silymarin treatment may not be involved in the inflammatory response during DT-induced liver injury. Our other

work with the DT-induced liver injury model indicate that neutrophils and inflammasome activation do not play a crucial role in promoting inflammation or injury (Fig. 9)(7).

Alternatively, the moderate impact on gene expression after Silymarin treatment may instead be due to the poor solubility of the oral treatment in solution (empirical observation). Oral Silymarin also has poor bioavailability due to low absorption of only 20-50% in the intestines, and a relatively quick half-life of up to 8 hours prior to excretion via bile and urine(2). In human studies, oral consumption of either Silymarin (clinical trials) or milk thistle supplements (over the counter) has been shown to have little to no effect on liver inflammation(1, 2, 8). Effective treatment of HCV and acute liver failure caused by mushroom poisoning has been achieved using an intravenous formulation of Silymarin, called Legalon® SIL(8, 9). It is therefore important to test the effect of the intravenous Silymarin formulation on DT-induced liver injury. This experiment would either confirm that the drug's targets do not largely contribute to liver injury and inflammation caused by non-ROS-dependent hepatocyte death or provide evidence that oral formulations of Silymarin do not effectively reach the liver. Regardless of whether Legalon® SIL ameliorates DT-induced liver injury, the anti-inflammatory changes in gene expression do agree with some of the effects observed in *in vitro* experiments and provide support for further study of the role Silymarin can play in liver diseases(4).

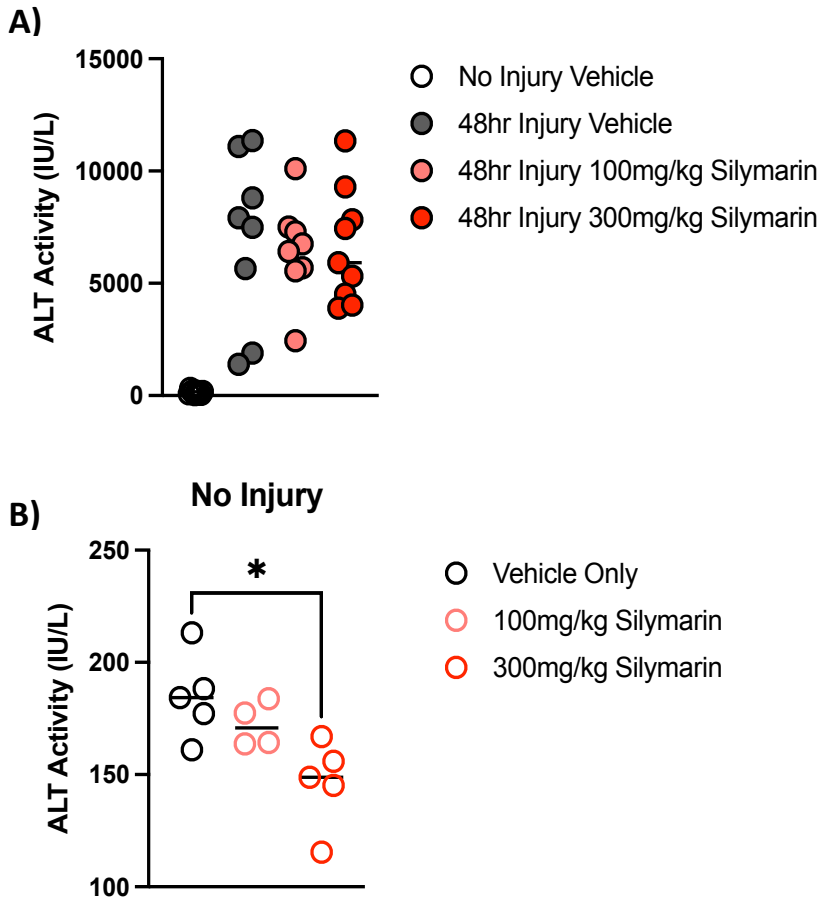

Fig 19. Silymarin treatment does not reduce DT-dependent liver injury. Mice were injected (r.o.) with 5 x 10^9 viral genomes of rAAV.mCherry.hDTR or 1X PBS. After two weeks, mice were injected (i.p.) with 20ng DT and received either vehicle, 100mg/kg Silymarin, or 300mg/kg Silymarin via oral gavage. Mice received a second treatment with vehicle, 100mg/kg Silymarin, or 300mg/kg Silymarin via oral gavage 24 hours later. Mice were sacrificed 48 hours post-DT, and blood was harvested to quantify serum ALT activity. A) Serum ALT activity for 48 hour injury in mice treated with vehicle only, 100mg/kg Silymarin, or 300mg/kg Silymarin, with vehicle no injury control for reference. Data is pooled from 2 experiments with n = 5 per group. B) Serum ALT activity for no injury control mice treated with vehicle, 100mg/kg Silymarin, or 300mg/kg Silymarin. Data is pooled from 2 experiments with n = 5 per group. Significance was determined with unpaired, Welch t-test, * = $p < 0.05$

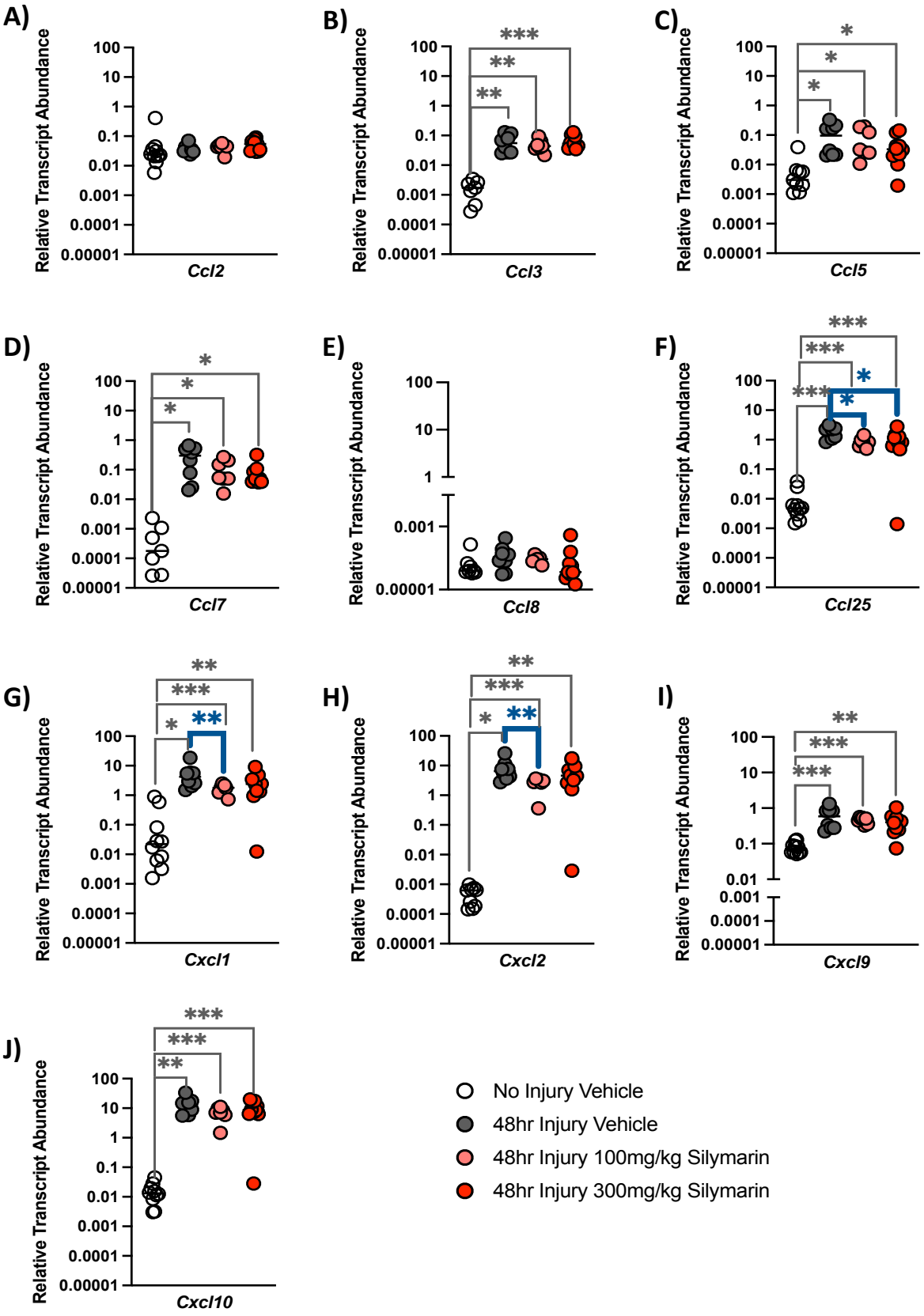
A)
B)
C)
D)
E)
F)
G)
H)
I)
J)
Relative Transcript Abundance
100
10
1
0.1
0.01
0.001
0.0001
0.00001
Ccl2
Ccl3
Ccl5
Ccl7
Ccl8
Ccl25
Cxcl1
Cxcl2
Cxcl9
Cxcl10
No Injury Vehicle
48hr Injury Vehicle
48hr Injury 100mg/kg Silymarin
48hr Injury 300mg/kg Silymarin

Fig 20. Silymarin treatment does reduce chemokine gene expression 48 hours post-DT treatment. Mice were injected (r.o.) with 5 x 10^9 viral genomes of rAAV.mCherry.hDTR or 1X PBS. After two weeks, mice were injected (i.p.) with 20ng DT and received either vehicle, 100mg/kg Silymarin, or 300mg/kg Silymarin via oral gavage. Mice received a second treatment with vehicle, 100mg/kg Silymarin, or 300mg/kg Silymarin via oral gavage 24 hours later. Mice were sacrificed 48 hours post-DT, and liver tissue was harvested for RNA extraction. Gene expression for A) Ccl2, B) Ccl3, C) Ccl5, D) Ccl7, E) Ccl8, F) Ccl25, G) Cxcl1, H) Cxcl2, I) Cxcl9, and J) Cxcl10 relative to Gapdh and Hprt was quantified for all groups. Data is pooled from 2 experiments with n = 5 per group. Significance was determined with unpaired, Welch t-test. * = $p < 0.05$; ** = $p < 0.01$; *** = $p < 0.001$. Statistics represented in gray compared each 48 hour injury group to the No Injury Vehicle group. Statistics represented in blue compared each 48 hour Injury Silymarin treatment to the 48 hour Injury Vehicle group.

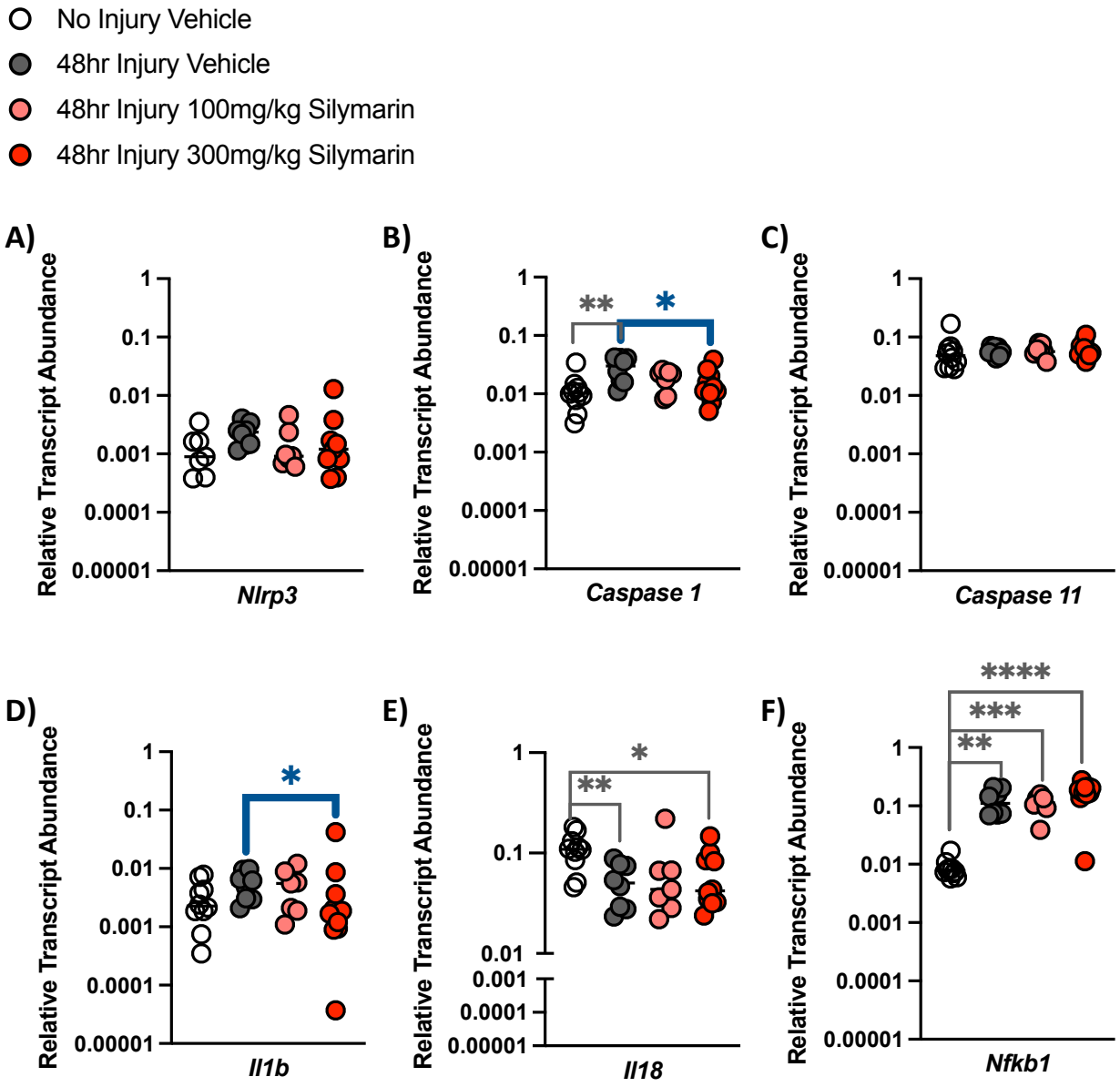
No Injury Vehicle
48hr Injury Vehicle
48hr Injury 100mg/kg Silymarin
48hr Injury 300mg/kg Silymarin
A)
B)
C)
D)
E)
F)
Relative Transcript Abundance
1
0.1
0.01
0.001
0.0001
0.00001
Nlrp3
Caspase 1
Caspase 11
Il1b
Il18
Nfkb1
*
**
***
****

Fig 21. Silymarin treatment does reduce inflammasome gene expression 48 hours post-DT treatment.

Mice were injected (r.o.) with 5 x 10^9 viral genomes of rAAV.mCherry.hDTR or 1X PBS. After two weeks, mice were injected (i.p.) with 20ng DT and received either vehicle, 100mg/kg Silymarin, or 300mg/kg Silymarin via oral gavage. Mice received a second treatment with vehicle, 100mg/kg Silymarin, or 300mg/kg Silymarin via oral gavage 24 hours later. Mice were sacrificed 48 hours post-DT, and liver tissue was harvested for RNA extraction. Gene expression for A) *Nlrp3*, B) *Caspase 1*, C) *Caspase 11*, D) *Il1beta*, E) *Il18*, and F) *Nfkb1* relative to *Gapdh* and *Hprt* was quantified for all groups. Data is pooled from 2 experiments with n = 5 per group. Significance was determined with unpaired, Welch t-test. * = $p < 0.05$; ** = $p < 0.01$; *** = $p < 0.001$. Statistics represented in gray compared each 48 hour injury group to the No Injury Vehicle group. Statistics represented in blue compared each 48 hour Injury Silymarin treatment to the 48 hour Injury Vehicle group.

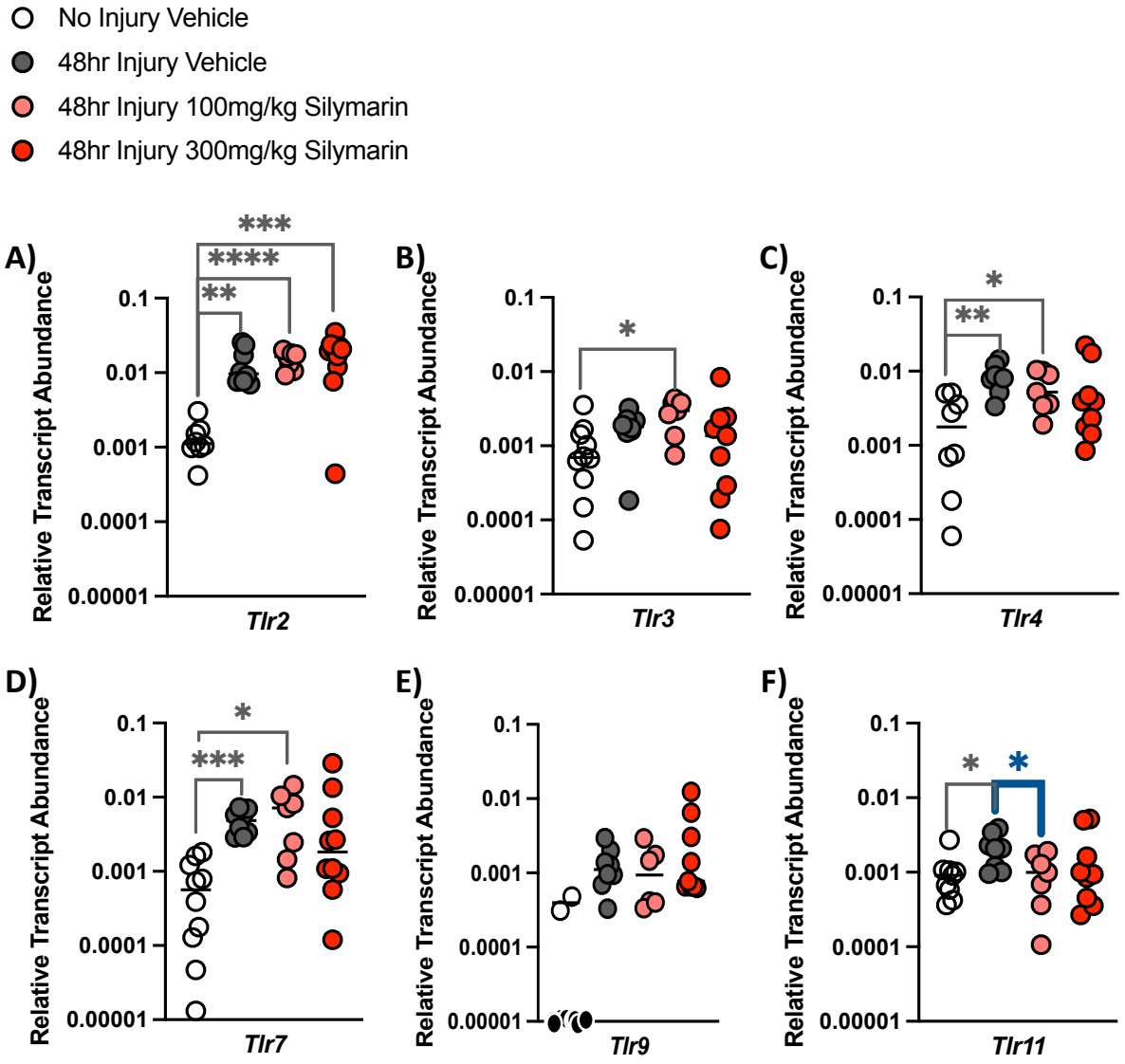
No Injury Vehicle
48hr Injury Vehicle
48hr Injury 100mg/kg Silymarin
48hr Injury 300mg/kg Silymarin
A)
B)
C)
D)
E)
F)
Relative Transcript Abundance
0.1
0.01
0.001
0.0001
0.00001
***
****
**
*
Tlr2
Tlr3
Tlr4
Tlr7
Tlr9
Tlr11

Fig 22. Silymarin treatment reduces *Tlr11* gene expression 48 hours post-DT treatment. Mice were injected (r.o.) with 5 x 10^9 viral genomes of rAAV.mCherry.hDTR or 1X PBS. After two weeks, mice were injected (i.p.) with 20ng DT and received either vehicle, 100mg/kg Silymarin, or 300mg/kg Silymarin via oral gavage. Mice received a second treatment with vehicle, 100mg/kg Silymarin, or 300mg/kg Silymarin via oral gavage 24 hours later. Mice were sacrificed 48 hours post-DT, and liver tissue was harvested for RNA extraction. Gene expression for A) *Tlr2*, B) *Tlr3*, C) *Tlr4*, D) *Tlr7*, E) *Tlr9*, and F) *Tlr11* relative to Gapdh and Hprt was quantified for all groups. Data is pooled from 2 experiments with n = 5 per group. Significance was determined with unpaired, Welch t-test. * = $p < 0.05$; ** = $p < 0.01$; *** = $p < 0.001$. Statistics represented in gray compared each 48 hour injury group to the No Injury Vehicle group. Statistics represented in blue compared each 48 hour Injury Silymarin treatment to the 48 hour Injury Vehicle group. Black circles represent gene expression below the limit of detection.

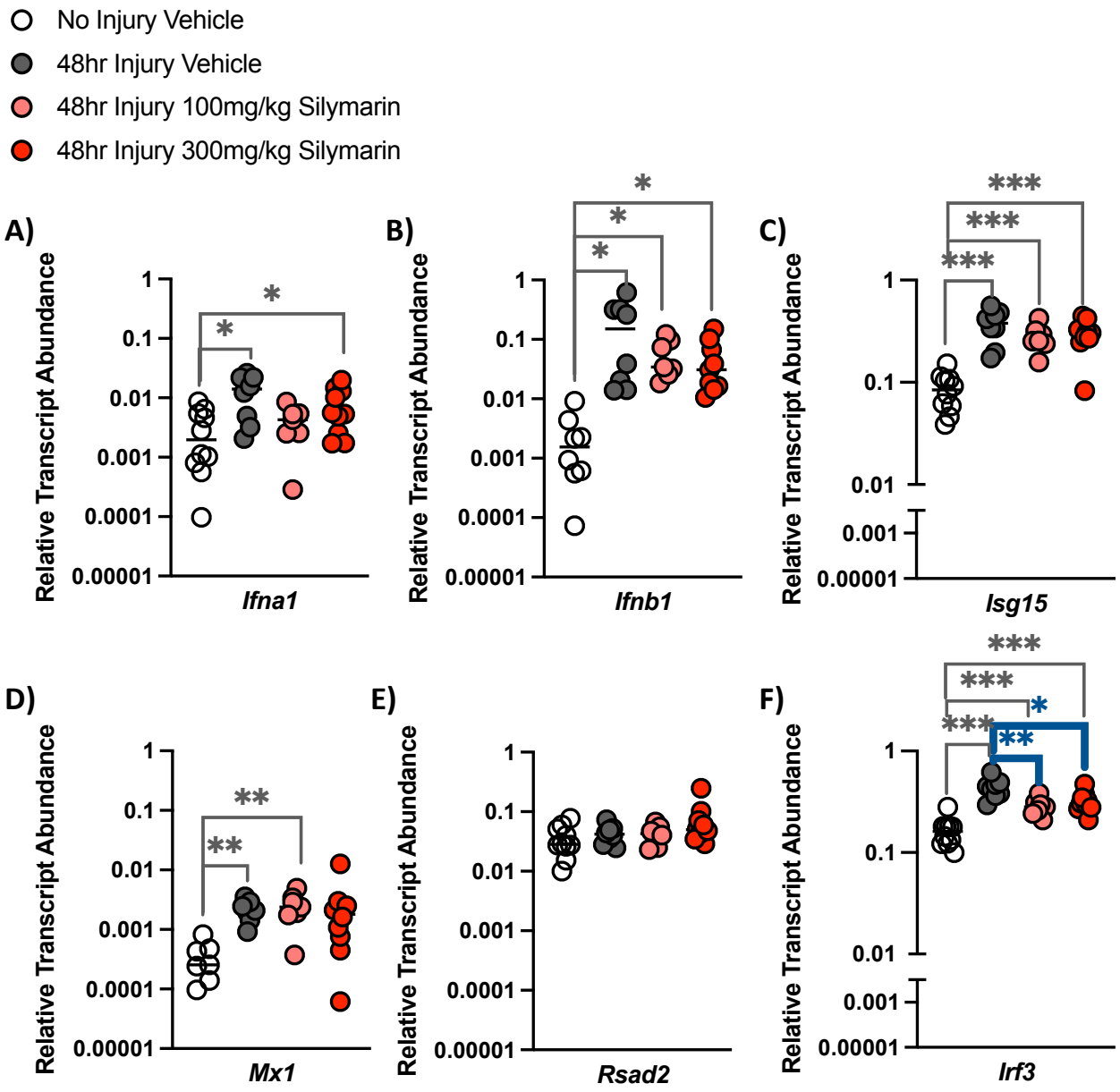
No Injury Vehicle
48hr Injury Vehicle
48hr Injury 100mg/kg Silymarin
48hr Injury 300mg/kg Silymarin
A)
B)
C)
D)
E)
F)
Relative Transcript Abundance
1
0.1
0.01
0.001
0.0001
0.00001
Ifna1
Ifnb1
Isg15
Mx1
Rsad2
Irf3
*
**
***

Fig 23. Silymarin treatment reduces *Irf3* gene expression 48 hours post-DT treatment. Mice were injected (r.o.) with 5 x 10^9 viral genomes of rAAV.mCherry.hDTR or 1X PBS. After two weeks, mice were injected (i.p.) with 20ng DT and received either vehicle, 100mg/kg Silymarin, or 300mg/kg Silymarin via oral gavage. Mice received a second treatment with vehicle, 100mg/kg Silymarin, or 300mg/kg Silymarin via oral gavage 24 hours later. Mice were sacrificed 48 hours post-DT, and liver tissue was harvested for RNA extraction. Gene expression for A) *Tlr2*, B) *Tlr3*, C) *Tlr4*, D) *Tlr7*, E) *Tlr9*, and F) *Tlr11* relative to Gapdh and Hprt was quantified for all groups. Data is pooled from 2 experiments with n = 5 per group. Significance was determined with unpaired, Welch t-test. * = $p < 0.05$; ** = $p < 0.01$; *** = $p < 0.001$. Statistics represented in gray compared each 48 hour injury group to the No Injury Vehicle group. Statistics represented in blue compared each 48 hour Injury Silymarin treatment to the 48 hour Injury Vehicle group.

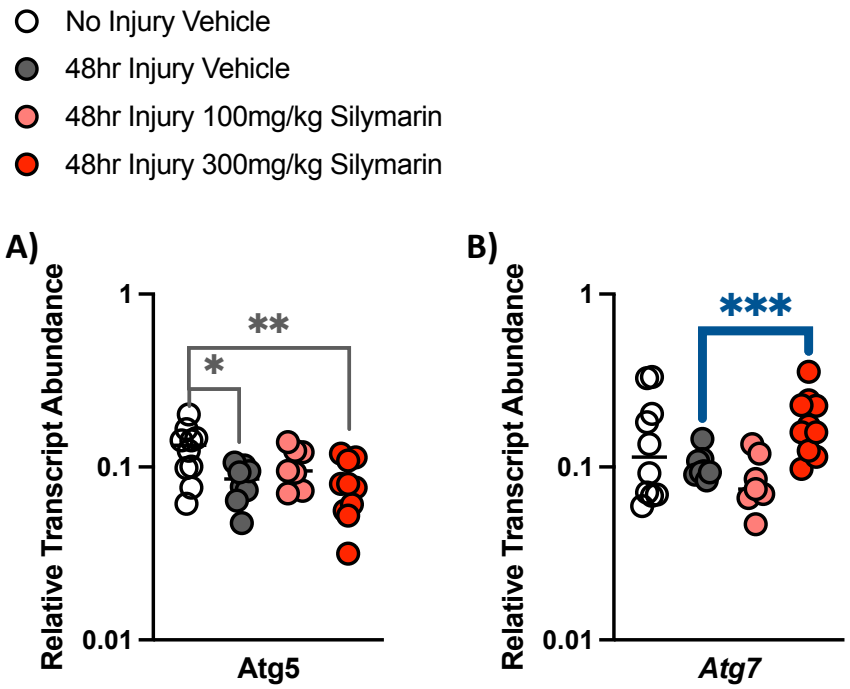

Fig 24. Silymarin treatment increases *Atg7* gene expression 48 hours post-DT treatment. Mice were injected (r.o.) with 5 x 10^9 viral genomes of rAAV.mCherry.hDTR or 1X PBS. After two weeks, mice were injected (i.p.) with 20ng DT and received either vehicle, 100mg/kg Silymarin, or 300mg/kg Silymarin via oral gavage. Mice received a second treatment with vehicle, 100mg/kg Silymarin, or 300mg/kg Silymarin via oral gavage 24 hours later. Mice were sacrificed 48 hours post-DT, and liver tissue was harvested for RNA extraction. Gene expression for A) *Atg5* and B) *Atg7* relative to Gapdh and Hprt was quantified for all groups. Data is pooled from 2 experiments with n = 5 per group. Significance was determined with unpaired, Welch t-test. * = $p < 0.05$; ** = $p < 0.01$; *** = $p < 0.001$. Statistics represented in gray compared each 48 hour injury group to the No Injury Vehicle group. Statistics represented in blue compared each 48 hour Injury Silymarin treatment to the 48 hour Injury Vehicle group.

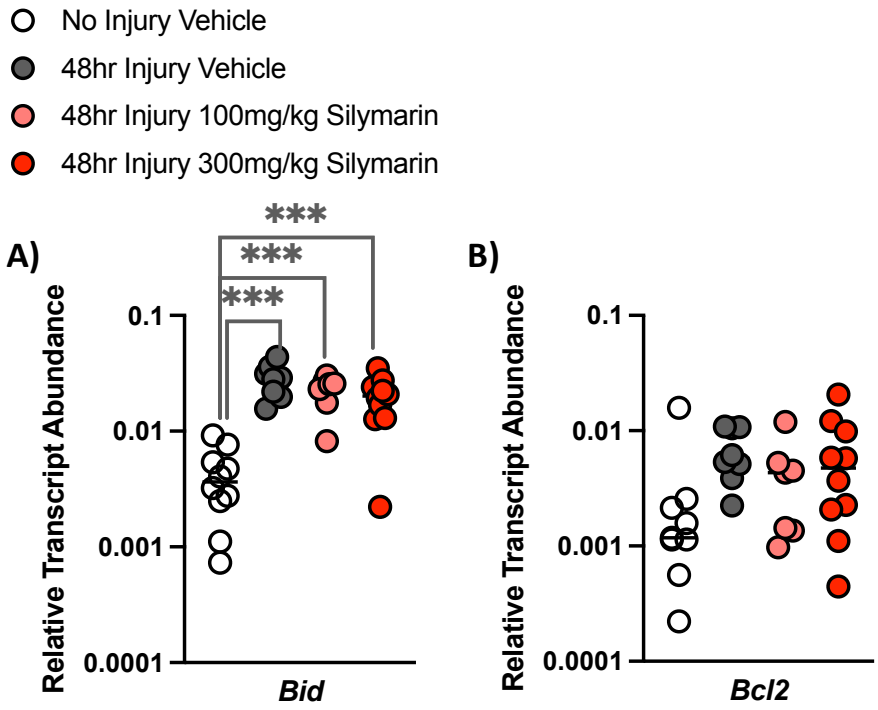

Fig 25. Silymarin treatment does not decrease BH3 gene expression 48 hours post-DT treatment. Mice were injected (r.o.) with 5 x 10^9 viral genomes of rAAV.mCherry.hDTR or 1X PBS. After two weeks, mice were injected (i.p.) with 20ng DT and received either vehicle, 100mg/kg Silymarin, or 300mg/kg Silymarin via oral gavage. Mice received a second treatment with vehicle, 100mg/kg Silymarin, or 300mg/kg Silymarin via oral gavage 24 hours later. Mice were sacrificed 48 hours post-DT, and liver tissue was harvested for RNA extraction. Gene expression for A) *Bid* and B) *Bcl2* relative to Gapdh and Hprt was quantified for all groups. Data is pooled from 2 experiments with n = 5 per group. Significance was determined with unpaired, Welch t-test. * = $p < 0.05$; ** = $p < 0.01$; *** = $p < 0.001$. Statistics represented in gray compared each 48 hour injury group to the No Injury Vehicle group.

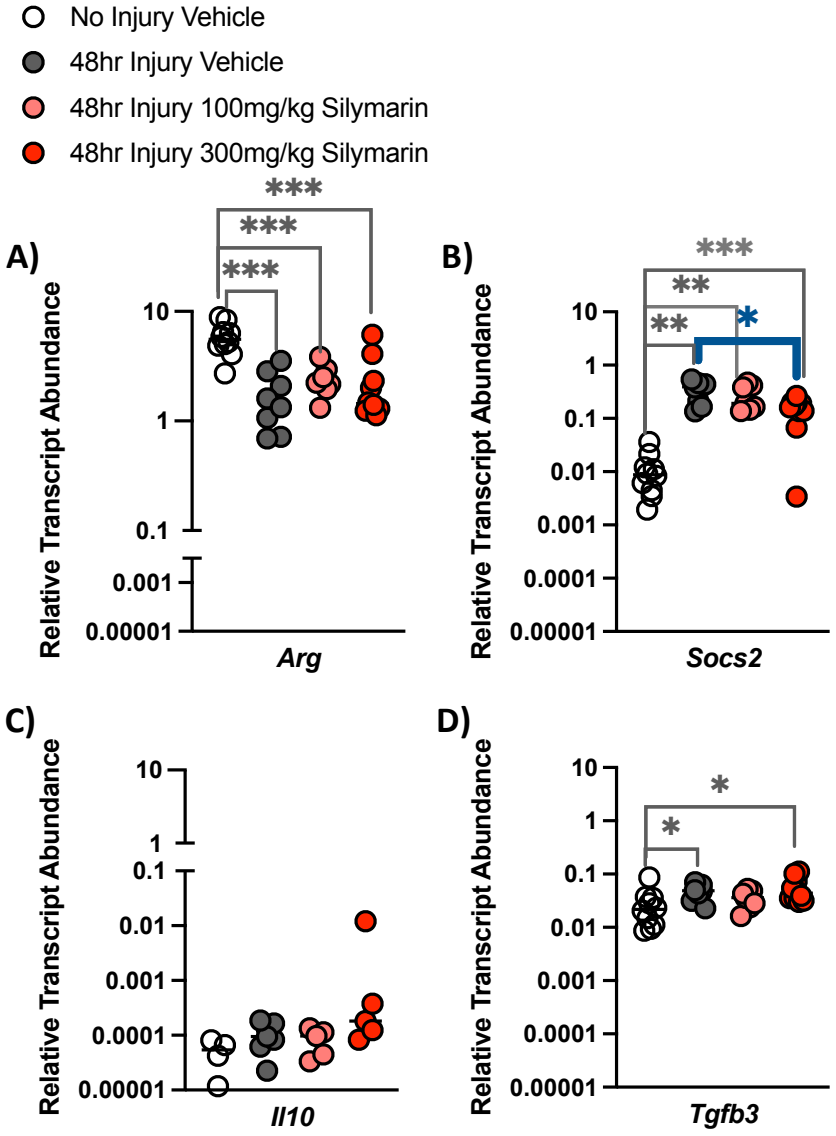
No Injury Vehicle
48hr Injury Vehicle
48hr Injury 100mg/kg Silymarin
48hr Injury 300mg/kg Silymarin
A)
B)
C)
D)
Relative Transcript Abundance
Arg
Socs2
Il10
Tgfb3
10
1
0.1
0.01
0.001
0.0001
0.00001
***
**
*

Fig 26. Silymarin treatment decreases *Socs2* gene expression 48 hours post-DT treatment. Mice were injected (r.o.) with 5 x 10^9 viral genomes of rAAV.mCherry.hDTR or 1X PBS. After two weeks, mice were injected (i.p.) with 20ng DT and received either vehicle, 100mg/kg Silymarin, or 300mg/kg Silymarin via oral gavage. Mice received a second treatment with vehicle, 100mg/kg Silymarin, or 300mg/kg Silymarin via oral gavage 24 hours later. Mice were sacrificed 48 hours post-DT, and liver tissue was harvested for RNA extraction. Gene expression for A) *Arg* and B) *Socs2*, C) *Il10*, D) *Tgfb3* relative to Gapdh and Hprt was quantified for all groups. Data is pooled from 2 experiments with n = 5 per group. Significance was determined with unpaired, Welch t-test. * = $p < 0.05$; ** = $p < 0.01$; *** = $p < 0.001$. Statistics represented in gray compared each 48 hour injury group to the No Injury Vehicle group. Statistics represented in blue compared each 48 hour Injury Silymarin treatment to the 48 hour Injury Vehicle group.

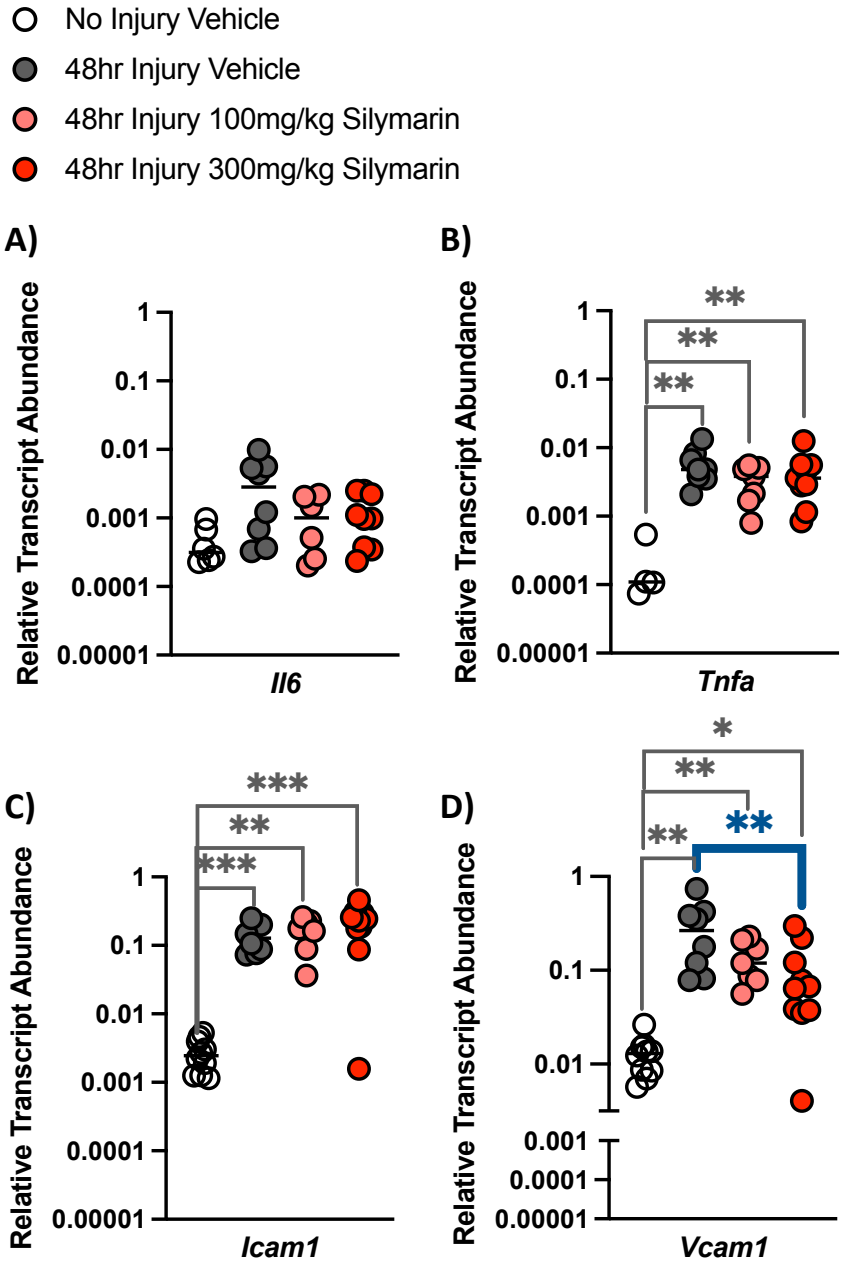
No Injury Vehicle
48hr Injury Vehicle
48hr Injury 100mg/kg Silymarin
48hr Injury 300mg/kg Silymarin
A)
B)
C)
D)
Relative Transcript Abundance
1
0.1
0.01
0.001
0.0001
0.00001
Il6
Tnfa
Icam1
Vcam1
*
**
***

Fig 27. Silymarin treatment decreases *Vcam1* gene expression 48 hours post-DT treatment. Mice were injected (r.o.) with 5 x 10^9 viral genomes of rAAV.mCherry.hDTR or 1X PBS. After two weeks, mice were injected (i.p.) with 20ng DT and received either vehicle, 100mg/kg Silymarin, or 300mg/kg Silymarin via oral gavage. Mice received a second treatment with vehicle, 100mg/kg Silymarin, or 300mg/kg Silymarin via oral gavage 24 hours later. Mice were sacrificed 48 hours post-DT, and liver tissue was harvested for RNA extraction. Gene expression for A) *Il6* and B) *Tnfa*, C) *Icam1*, D) *Vcam1* relative to Gapdh and Hprt was quantified for all groups. Data is pooled from 2 experiments with n = 5 per group. Significance was determined with unpaired, Welch t-test. * = $p < 0.05$; ** = $p < 0.01$; *** = $p < 0.001$. Statistics represented in gray compared each 48 hour injury group to the No Injury Vehicle group. Statistics represented in blue compared each 48 hour Injury Silymarin treatment to the 48 hour Injury Vehicle group.

Table 4 – Gene expression significantly altered by Silymarin treatment

Gene	Function	Immune Response Impact	After Silymarin Treatment
Atg7	Autophagosome assembly(10)	Anti-inflammatory, delivers cargo to lysosomes for digestion(11)	**Increased**
Ccl25	Chemokine, binds to CCR9	Lymphocyte(12) and myeloid(13) trafficking	**Decreased**
Cxcl1	Chemokine, binds to CXCR2	Neutrophil trafficking and activation	**Decreased**
Cxcl2	Chemokine, binds to CXCR2	Neutrophil trafficking and activation	**Decreased**
Caspase 1	Cleaves pro-IL-1β and IL-18 into active forms	Inflammasome activation, pyroptosis	**Decreased**
Il1b	Cytokine, binds IL-1RI and IL-1RII	Prostaglandin synthesis, proinflammatory cytokine production, and neutrophil, T cell, and B cell activation	**Decreased**
Socs2	STAT inhibitor	Negative regulation of cytokine receptor signaling	**Decreased**
Irf3	Transcription factor specific for IFNα, IFNβ, and ISGs	Type I IFN Response, especially in macrophages	**Decreased**
Tlr11	Endosomal PRR, recognizes flagellin(14) and profilin	Induces IL-12 and IFNγ production, promotes NK and CTL activation, DC migration to LN(15)	**Decreased**
Vcam1	Endothelial surface expression, binds VLA-4 integrin	Mediates adhesion of lymphocytes, monocytes, eosinophils, and basophils to vascular endothelium	**Decreased**

Appendix 2 References

1. Federico A, Dallio M, Loguercio C. Silymarin/Silybin and Chronic Liver Disease: A Marriage of Many Years. Molecules. 2017;22(2).
2. Javed S, Kohli K, Ali M. Reassessing bioavailability of silymarin. Altern Med Rev. 2011;16(3):239-49.
3. Crocenzi FA, Roma MG. Silymarin as a new hepatoprotective agent in experimental cholestasis: new possibilities for an ancient medication. Curr Med Chem. 2006;13(9):1055-74.
4. Lovelace ES, Wagoner J, MacDonald J, Bammler T, Bruckner J, Brownell J, et al. Silymarin Suppresses Cellular Inflammation By Inducing Reparative Stress Signaling. J Nat Prod. 2015;78(8):1990-2000.
5. Papackova Z, Heczkova M, Dankova H, Sticova E, Lodererova A, Bartonova L, et al. Silymarin prevents acetaminophen-induced hepatotoxicity in mice. PLoS One. 2018;13(1):e0191353.
6. Yoo HG, Jung SN, Hwang YS, Park JS, Kim MH, Jeong M, et al. Involvement of NF-kappaB and caspases in silibinin-induced apoptosis of endothelial cells. Int J Mol Med. 2004;13(1):81-6.
7. Brempelis KJ, Yuen SY, Schwarz N, Mohar I, Crispe IN. Central role of the TIR-domain-containing adaptor-inducing interferon-β (TRIF) adaptor protein in murine sterile liver injury. Hepatology. 2017;65(4):1336-51.
8. Yang Z, Zhuang L, Lu Y, Xu Q, Chen X. Effects and tolerance of silymarin (milk thistle) in chronic hepatitis C virus infection patients: a meta-analysis of randomized controlled trials. Biomed Res Int. 2014;2014:941085.
9. Mengs U, Pohl RT, Mitchell T. Legalon® SIL: the antidote of choice in patients with acute hepatotoxicity from amatoxin poisoning. Curr Pharm Biotechnol. 2012;13(10):1964-70.
10. Yuan W, Stromhaug PE, Dunn WA, Jr. Glucose-induced autophagy of peroxisomes in Pichia pastoris requires a unique E1-like protein. Mol Biol Cell. 1999;10(5):1353-66.
11. Deretic V. Autophagy in inflammation, infection, and immunometabolism. Immunity. 2021;54(3):437-53.
12. Vicari AP, Figueroa DJ, Hedrick JA, Foster JS, Singh KP, Menon S, et al. TECK: a novel CC chemokine specifically expressed by thymic dendritic cells and potentially involved in T cell development. Immunity. 1997;7(2):291-301.
13. Schmutz C, Cartwright A, Williams H, Haworth O, Williams JH, Filer A, et al. Monocytes/macrophages express chemokine receptor CCR9 in rheumatoid arthritis and CCL25 stimulates their differentiation. Arthritis Res Ther. 2010;12(4):R161.
14. Yarovinsky F, Zhang D, Andersen JF, Bannenberg GL, Serhan CN, Hayden MS, et al. TLR11 activation of dendritic cells by a protozoan profilin-like protein. Science. 2005;308(5728):1626-9.
15. Yarovinsky F, Hieny S, Sher A. Recognition of Toxoplasma gondii by TLR11 prevents parasite-induced immunopathology. J Immunol. 2008;181(12):8478-84.